THE JACOBIAN MAP ON OUTER SPACE

A Dissertation

Presented to the Faculty of the Graduate School

of Cornell University

in Partial Fulfillment of the Requirements for the Degree of

Doctor of Philosophy

by

Owen Baker

August 2011

THE JACOBIAN MAP ON OUTER SPACE

Owen Baker, Ph.D.

Cornell University 2011

The outer automorphism group Out(F_n) of a finite rank free group admits a proper, cocompact action on a contractible space X_n known as Outer space. Likewise, the outer automorphism group GL$(n, \mathbb{Z})$ of a finite rank free abelian group admits such an action on the homogeneous space Y_n of positive definite quadratic forms. Both spaces have been used to study the homology of the respective groups. In this thesis, a Jacobian map J from X_n to Y_n compatible with the two actions is investigated. The image of J is discussed. It is shown that the preimage of Soulé's well-rounded retract of Y_3 is a deformation retract of X_3. The quotient K of this preimage by the kernel of the natural map from Out(F_n) to GL$(n, \mathbb{Z})$ is an Eilenberg-MacLane space for this kernel. A 2-dimensional subspace $\widetilde{A}$ of K is found whose integral homology groups surject onto those of the kernel. The kernel of $H_2(\widetilde{A}; \mathbb{Z}) \to H_2(K; \mathbb{Z})$ is shown to be generated by two elements as a $\mathrm{GL}_3(\mathbb{Z})$-module.

BIOGRAPHICAL SKETCH

Owen Baker graduated from Columbia High School in Maplewood, NJ. He graduated Summa Cum Laude from NCSU with a B.S. in Mathematics, and has an M.S. in Mathematics from Cornell University.

This thesis is dedicated to my parents.

ACKNOWLEDGEMENTS

First, I would like to express my gratitude to Professor Karen Vogtmann for suggesting an interesting thesis topic and for providing a good deal of advice. She has helped me find opportunities to expand my knowledge and has always been supportive.

I would also like to thank Professors Ken Brown and Keith Dennis for serving on my thesis committee. Professor Allen Hatcher also provided useful feedback on my thesis.

I would like to thank everyone associated with the Berstein Seminar, Cornell's graduate student topology seminar, for making it such a good learning experience. I would particularly like to thank Professor Tim Riley for choosing interesting material for the first and last seminars in which I was able to participate; and former and graduating students Brad Forrest, Victor Kostyuk, and Juan Alonso for discussing ideas from my thesis and theirs.

My teachers Carter Kemp, Richard Moss, Chandar Gulati, and Jon Riecke deserve special thanks for stimulating my interest in mathematics.

I am grateful to the Cornell Mathematics Department and the Hausdorff Research Institute for Mathematics (HIM) for their hospitality and financial support, and to the NSF VIGRE program.

Finally, I would like to thank my parents, Carol and Tom Baker, for always appreciating and supporting my interest in mathematics.

TABLE OF CONTENTS

LIST OF TABLES

LIST OF FIGURES

CHAPTER 1

INTRODUCTION

This thesis concerns a Jacobian map J from Culler-Vogtmann Outer space X_n to the homogeneous space Y_n of positive definite quadratic forms. In a sense to be discussed in section 4.1, it is a tropical analogue of the classical map in algebraic geometry that assigns a Jacobian variety to each complex algebraic curve. Since X_n has been used to study the homological properties of Out(F_n), the outer automorphism group of a free group, and Y_n has been used to study the homological properites of GL$(n, \mathbb{Z})$, the outer automorphism group of a free abelian group, one may hope that J can be used to study the homological properties of IO$_n$, the kernel of the natural map Out$(F_n) \to$ GL$(n, \mathbb{Z})$.

Indeed, for the case $n = 3$ it turns out that there are compatible deformation retracts of X_3 and Y_3. This deformation retract of X_3 is a 3-dimensional space distinct from the standard Spine of Outer space, another 3-dimensional deformation retract. Bestvina, Bux and Margalit studied the group homology of IO$_3$ by using Bestvina-Brady Morse Theory to replace the 3-dimensional quotient of the spine by IO$_3$ with a homotopy equivalent 2-dimensional space[4]. They concluded that IO$_3$ has cohomological dimension 2, and they showed that H_2(IO$_3$; $\mathbb{Z}$) is not finitely generated as an abelian group. They leave open the question of its finiteness properties as a GL$(3, \mathbb{Z})$-module.

In place of their 2-dimensional space, an Eilenberg-MacLane space K for IO$_3$ and a 2-dimensional subspace $\widetilde{A} \subset K$ will be produced, for which $H_i(\widetilde{A}; \mathbb{Z}) \twoheadrightarrow H_i$(IO$_3$; $\mathbb{Z}$) is surjective for all i. This approach has two potential advantages over that of Bestvina, Bux and Margalit:

(i) Their infinite recursion is non-canonical. A canonical subspace should be easier to work with in terms of the $\mathrm{GL}(3,\mathbb{Z})$ action than a non-canonical space glued together recursively.

(ii) There is a nice map $J : \widetilde{A} \to A \subset Z_3$ from the 2-dimensional space to a 1-dimensional space. The map can be used to define a space whose third homology group is the kernel of the surjection $H_2(\widetilde{A};\mathbb{Z}) \to H_2(\mathrm{IO}_3,\mathbb{Z})$.

But the approach suffers a drawback that the Bestvina-Bux-Margalit approach does not: $\widetilde{A} \hookrightarrow K$ is not a homotopy equivalence. After all, one could just take the 2-skeleton of the image of the spine in X_3/IO_3 to obtain a space whose homology groups surject to those of IO_3. However, the situation is not too bad. The kernel of $H_2(\widetilde{A};\mathbb{Z}) \to H_2(K;\mathbb{Z})$ is shown to be generated by two elements as a $\mathrm{GL}(3,\mathbb{Z})$-module, so that the finiteness properties of $H_2(\widetilde{A};\mathbb{Z})$ and $H_2(K;\mathbb{Z})$ will be the same.

This thesis is organized as follows. In Chapter 2, the homogeneous space and Culler-Vogtmann Outer space is discussed. Both are described as generalizations of the hyperbolic plane with its classical $\mathrm{PSL}(2,\mathbb{Z})$ action. Background is given for the Identity on Abelianization group and its analogue the Torelli subgroup of a Mapping Class Group, and the classical Jacobian map is reviewed for motivation. Chapter 3 defines the Jacobian of a graph. For the case $n = 3$, the fibers of J are computed using Minkowski reduction. Chapter 4 discusses the Schottky problem: what is the image of J? For $n = 3$, J is surjective. For $n = 4$, the problem is answered explicitly using Conway's theory of vonorms and conorms. Vallentin has given a general answer using Tutte's work with graphical matroids. In Chapter 5, the preimage of Soulé's well-rounded retract Z_3 of Y_3 is shown to be a deformation retract of X_3. This retract is used to pro-

duce a 3-dimensional aspherical space K which is an Eilenberg-MacLane space for IO_3. The CW structure it inherits from J is described. In Chapter 6, K is used to recover Andreadakis's result that $H_1(\mathrm{IO}_3, \mathbb{Z}) = \mathbb{Z}^6$, with a basis given by Magnus's generators for IO_3. Andreadakis's approach is purely algebraic. In Chapter 7, it is shown that every cycle in K is homologous to one in a 2-dimensional subspace $\widetilde{A}$, and that the kernel $H_2(\widetilde{A}; \mathbb{Z}) \to H_2(K; \mathbb{Z})$ is generated by 2 elements as a $\mathrm{GL}(3, \mathbb{Z})$-module so that $H_2(\widetilde{A}; \mathbb{Z})$ and $H_2(K; \mathbb{Z})$ have the same finiteness properties.

CHAPTER 2

BACKGROUND

2.1 The Well-Rounded Retract

There is a prevalent theme of studying groups via their actions on topological spaces. Hurewicz showed that the homotopy type of an aspherical space is determined by its fundamental group G, so that the homology groups of such a space become invariants of G. If a group G acts freely and properly on a contractible space X, then $G\backslash X$ is such an aspherical space, and can be used to study the homology of G.

Sometimes there is a natural action of a group on a space, but the action is not free. In this case, one might use the action to obtain coarser information about the group. For instance, the virtual cohomological dimension of a group is the common cohomological dimension of finite index torsionfree subgroups. Serre proved that this notion is well-defined for virtually torsion-free groups (see e.g. [7]). In the case of $\mathrm{SL}_3(\mathbb{Z})$ acting on the symmetric space of positive definite quadratic forms up to homothety, however, Soulé was able to use this (non-free) action to exactly compute the group cohomology. He did this by first finding an invariant contractible subspace on which the action is proper and cocompact, and then using a spectral sequence to find the group cohomology in terms of the stabilizers of certain points[30]. The subspace consists of those quadratic forms for which there is a basis for $\mathbb{Z}^3$ consisting of systoles (minimal length nonzero integral vectors). See section 5.1 for definitions.

The construction of Soulé was generalized by Ash, who found cocompact

deformation retracts for the action of $\mathrm{GL}(n,\mathbb{Z})$ on the space of real quadratic forms (and even for arithmetic subgroups of general linear groups over finite dimensional division algebras over the rationals on the corresponding symmetric space)[2]. This *well-rounded retract* consists of the quadratic forms for which the systoles in $\mathbb{Z}^n$ generate a finite index subgroup of $\mathbb{Z}^n$. (It may seem more natural to generalize Soulé's construction by requiring $\mathbb{Z}^n$ to contain a basis of systoles, but Pettet and Souto showed that the subspace of such forms is not even contractible, let alone a deformation retract of the symmetric space[27].)

For the case $n = 2$, the symmetric space and its retract have a nice visualization due to Serre (see e.g. Ch. VIII.9 of Brown's textbook [7], which also discusses many of the ideas in this section.) The set of homothety classes of positive definite binary quadratic forms can be identified with the upper half-plane $\mathbb{H} = \mathrm{SO}_2(\mathbb{R})\backslash\mathrm{SL}_2(\mathbb{R})$: given a homomothety class, associate to it the unique $z \in \mathbb{H}$ where $q(ax + by) = |a + bz|^2$ for some q in the homothety class. Another way of thinking about this space is as the space of marked lattices in $\mathbb{C}$ up to homotheties and isometries, where a marking is an ordered basis (any basis can be normalized to be $1, z$ with $z \in \mathbb{H}$). Then the action of $\mathrm{SL}_2(\mathbb{Z})$ on quadratic forms by change-of-basis corresponds to an action by linear fractional transformations on the upper half-plane. (Indeed, there is an action of $\mathrm{GL}_2(\mathbb{Z})$, where conjugates need to be taken after applying the linear fractional transformation corresponding to a matrix of negative determinant.) The *Farey graph* is an ideal triangulation of $\mathbb{H}$ obtained by joining rational numbers p/q to r/s on the real axis by a hyperbolic geodesic in $\mathbb{H}$ if and only $ps - rq = \pm 1$. This graph is invariant under the $\mathrm{GL}_2(\mathbb{Z})$ action. The dual tree to this triangulation is the well-rounded retract.

Note: finding a cocompact deformation retract is not the only way to deduce cohomological information about a group from its action on a space. Borel and Serre showed that the virtual cohomological dimension of $\mathrm{SL}_n(\mathbb{Z})$ is $n(n-1)/2$ by constructing a bordification of the symmetric space[6].

2.2 Outer Space

Outer space, introduced by Culler and Vogtmann[11] in 1986, plays a role for the outer automorphism group of a free group $\mathrm{Out}(F_n)$ analogous to those played by the symmetric space of quadratic forms for $\mathrm{GL}_n(\mathbb{Z})$ and Teichmüller space for the mapping class group of a surface[35]. Survey papers for Outer space include [36][35] (the former focuses on homological results, the later is more general.) For a very brief introduction, see [37]. Section 3.2 provides precise definitions of Outer space and the concepts needed to define it.

Outer space is a contractible space admitting a proper action of $\mathrm{Out}(F_n)$. Although the action is not cocompact, there is a cocompact deformation retract called the *spine*, analogous to the well-rounded retract for $\mathrm{GL}_n(\mathbb{Z})$[11].

Recall that points of Teichmüller space for a fixed surface S are marked surfaces, represented by diffeomorphisms from S to hyperbolic surfaces. The action of the mapping class group on Teichmüller space is by precomposing a marking with a surface automorphism. By the Dehn-Nielsen-Behr Theorem (see e.g. [6]), the mapping class group is isomorphic to a group of outer automorphisms of the fundamental group of S. This motivated the definition of Outer space as the space of marked graphs, since graphs have free fundamental groups. The appropriate notion of marking turned out to be homotopy equiva-

lence (from a fixed graph to a graph) in place of diffeomorphism. (Had homeomorphisms been used instead, then very few automorphisms of the free group would be realized by self-maps of the fixed graph.)

Note that the Teichmüller space for a torus (the space of marked Euclidean metrics on a torus, or equivalently of lattices in $\mathbb{R}^2$ up to isometries and homotheties) can be identified with $\mathbb{H} = \mathrm{SO}_2(\mathbb{R})\backslash\mathrm{SL}_2(\mathbb{R})$, the symmetric space on which $\mathrm{GL}_2(\mathbb{Z})$ acted in the previous section. The group acting on the Teichmüller space is $\mathrm{Out}(\pi_1(T^2)) = \mathrm{Out}(\mathbb{Z}^2) = \mathrm{GL}_2(\mathbb{Z})$ by the Dehn-Nielsen-Behr theorem. Likewise, Teichmüller space of the punctured torus is again the same space, with the action of $\mathrm{Out}(\pi_1(T^2 \setminus \{p\})) = \mathrm{Out}(F_2)\,(= \mathrm{GL}_2(\mathbb{Z}))$, the same group. So Teichmuller space with the action of the mapping class groups generalizes the classical action of $\mathrm{GL}_2(\mathbb{Z})$ on $\mathrm{SO}_2(\mathbb{R})\backslash\mathrm{SL}_2(\mathbb{R})$.

The action of $\mathrm{Out}(F_n)$ on Outer space is yet another generalization of this classical action. In the case $n = 2$, (reduced) Outer space is again the ideally triangulated hyperbolic plane with the familiar $\mathrm{Out}(F_2) = \mathrm{GL}_2(\mathbb{Z})$ action. Points on the geodesics correspond to marked roses with two petals, while the interior points of triangles correspond to marked theta graphs (see Section 3.1 for definitions.)

The spine of (projectivized) Outer space consists of the points represented by marked graphs all of whose edges have length at most 1, and have length exactly 1 outside of some forest. This subspace is naturally a CAT(0) cubical complex, and it is also a subcomplex of the barycentric subdivision of the simplicial description of Outer space (see Section 3.2.) The deformation onto the spine is then achieved by pushing away from the ideal simplices "missing" from Outer space in this model.

Culler and Vogtmann used the spine to determine the virtual cohomological dimension (vcd) of Out(F_n)[11]. The spine has dimension $2n-3$ (the number of edges in a maximal tree contained in a trivalent rank n graph, trivalent graphs having the largest maximal trees), which gives an upper bound for the vcd. They obtained the same value as a lower bound for the vcd by finding a free abelian subgroup of Out(F_n) of that rank. Out(F_n) contains finite index torsion-free subgroups, which act freely on the spine with compact quotient. These subgroups therefore have finitely generated homology groups, and the same is therefore true for Out(F_n).

2.3 The Classical Jacobian Map

The classical Jacobian Map associates to an algebraic curve the period matrix of its Jacobian torus (see below). Thus it is a map from the moduli space of genus g complex algebaic curves to the space of symmetric $g \times g$ complex matrices with positive definite imaginary parts. (Warning: Jacobian varieties are named after Carl Jacobi for his early work on the relation between elliptic and hyper-elliptic elliptic integrals and the curves of the same names. Do not confuse the classical Jacobian Map with the Abel-Jacobi map from an algebraic curve to its Jacbobian variety, or with the Jacobian matrix associated to a differentiable map between Euclidean spaces, though both of these concepts are also named after Carl Jacobi.) For an "impressionistic journey" through complex curve theory focussing on classical Jacobian varieties and the Schottky problem, see [9]. A more rigorous treatment is [15]. All the material in this section can be found in both books.

A Riemann surface is a 1-dimensional complex manifold, and a complex curve is a compact Riemann surface. Such can arise as the solution in the complex projective plane $\mathbb{CP}^2$ to an irreducible homogeneous polynomial equation. If the polynomial is degree 1, the resulting curve is a hyperplane $\mathbb{CP}^1$, the Riemann sphere. Stereographic projection from (any) point on the curve to (any) hyperplane shows that conics, degree 2 curves, are also isomorphic to the Riemann sphere.

Cubic curves E are topologically tori. By integrating a certain holomorphic 1-form ω from a fixed basepoint $p_0 \in E$ to a point $p \in E$, one obtains a complex number. The integral depends on the path taken, but only up to a $\mathbb{Z}$-linear combination of the integrals of ω around a longitude and around a meridian. So integration induces a holomorphic map from E to the quotient of $\mathbb{C}$ by a lattice. By composing with a scaling and rotation of the complex plane, one gets a holomorphic map $E \to \mathbb{C}/(\mathbb{Z} + \mathbb{Z}\tau)$ for some τ in the upper half-plane $\mathbb{H}$, and the map turns out to be an isomorphism. (Using the Weierstrass $\wp$-function, one can show that $\mathbb{C}/(\mathbb{Z}+\tau\mathbb{Z})$ is isomorphic to some cubic curve for any $\tau \in \mathbb{H}$, since $\wp$ and its derivative satisfy a certain cubic identity.)

For curves C of higher genus ($g \geq 1$), some of this nice picture for cubics can be reconstructed. The 2-torus $\mathbb{C}/(\mathbb{Z} + \mathbb{Z}\tau)$ is replaced by a $2g$-dimensional *Jacobian* torus $J(C)$. The isomorphism $E \to \mathbb{C}/(\mathbb{Z} + \mathbb{Z}\tau)$ is replaced by the *Abel-Jacobi* map $C \to J(C)$, which is no longer an isomorphism but is an embedding. There are several equivalent definitions of the Jacobian variety, the complex torus $J(C)$. One is the *Albanese torus* $\mathrm{Alb}(C) = H_1(C;\mathbb{R})/H_1(C;\mathbb{Z})$. The Abel-Jacobi map $\kappa : C \to \mathrm{Alb}(C)$ is defined to send $p \in C$ to a homology element defined as a functional on cohomology, $\kappa(p) = \int_{p_0}^{p} : H^1(C;\mathbb{R}) \to \mathbb{C}$ sending an

$H^1(C;\mathbb{R})$ representative to its integral along any fixed path from p_0 to p. The intersection pairing on $H_1(C;\mathbb{Z})$ induces an isomorphism between $H_1(C;\mathbb{R})$ and $H^1(C;\mathbb{R})$, and therefore an isomorphism between the Albanese torus and the *Jacobian torus* $\mathrm{Jac}(C) := H^1(C;\mathbb{R})/H^1(C;\mathbb{Z})$.

Abel's Theorem says $J(C)$ can also be identified with the *Picard variety* $\mathrm{Pic}^0(C)$ of topologically trivial holomorphic line bundles over C. The Picard variety is a group under the operation of tensor product, and the identification is a group isomorphism sending $\kappa(p)$ to the line bundle associated to the divisor $p - p_0$. Abel's Theorem implies that the Abel-Jacobi map is injective, for if $\kappa(p) = \kappa(q)$, then the divisor $p - q$ represents the trivial holomorphic line bundle. A global meromorphic function cannot have a single simple pole, as $g > 0$, so $p = q$. More generally, Abel's Theorem implies that there is a function with zeros $p_1, \ldots, p_r$ and poles $q_1, \ldots, q_r$ counted with multiplicity if and only if $\int_{p_1}^{q_1} + \cdots + \int_{p_r}^{q_r} = 0$ in $\mathrm{Alb}(C)$. (In the case that C is a cubic, so $C = \mathrm{Alb}(C)$, this condition is equivalent to $p_1 + \cdots + p_r = q_1 + \cdots + q_r$ in C.)

The *period matrix* for C corresponding to a symplectic basis for $H_1(C,\mathbb{Z}) = \mathbb{Z}^{2g}$ is obtained as follows. A *symplectic basis* is a basis $\alpha_1, \ldots, \alpha_g, \beta_1, \ldots, \beta_g$ such that $\alpha_i \cdot \beta_i = -\beta_i \cdot \alpha_i = 1$ for $1 \leq i \leq n$, where $\cdot$ is the algebraic intersection number, and such that the $\cdot$ of any other pair of basis vectors is zero. (Every orientable surface has such a basis, for instance given by meridian and logitude curves.) The space $H^0(C,\Omega^1)$ of global holomorphic 1-forms on C is a complex g-dimensional vector space. It has a unique basis $\omega_1, \ldots, \omega_g$ such that $\int_{\beta_i} \omega_j = \delta_{ij}$, the Kronecker delta. The matrix

$$\Omega := \left(-\int_{\alpha_i} \omega_j \right)_{ij} \tag{2.1}$$

is then called the *period matrix* of C (corresponding to the choice of symplectic

basis). Ω satisfies the *Riemann relations*: it is symmetric and has positive definite imaginary part([9], p.117). In section 3.2, an analogous construction is used to define the Jacobian map associating a positive definite symmetric matrix to a marked graph. (The marking will play a role analogous to the choice of symplectic basis.)

2.4 The IA Group and the Torelli Group

Magnus studied the kernel IA_n of the natural map $\mathrm{Aut}(F_n) \to \mathrm{GL}_n(\mathbb{Z})$, the group of automorphisms that acts as the *identity on the abelianization* $\mathbb{Z}^n = H_1(F_n)$. The notation for this group varies in the literature. Here, IA_n will denote the kernel of $\mathrm{Aut}(F_n) \to \mathrm{GL}_n(\mathbb{Z})$ and IO_n will denote the kernel of $\mathrm{Out}(F_n) \to \mathrm{GL}_n(\mathbb{Z})$.

Nielsen showed that IA_3 is finitely generated. Magnus generalized this result, showing that the following elements generate IA_n[24]:

Magnus Generators There are two kinds of Magnus generators:

- $K_{i,l}$ for $1 \leq i, l \leq n$,$i \neq l$ maps $x_i \mapsto x_l x_i x_l^{-1}$ (and sends $x_j \mapsto x_j$ for $j \neq i$).
- $K_{i,l,s}$ for $1 \leq l < s \leq n$, $i \neq l, s$ maps $x_i \mapsto x_i x_l x_s x_l^{-1} x_s^{-1}$ (and sends $x_j \mapsto x_j$ for $j \neq i$).

There are therefore

$$n(n-1) + n\binom{n-1}{2} = \frac{n^2(n-1)}{2}$$

Magnus generators for IA_n.

In IO_n, one has $K_{1,l}K_{2,l}\cdots K_{n,l} = 1$ for each l. Therefore, one can eliminate one Magnus generator for each $l \in \{1, \ldots, n\}$ to see that IO_n is generated by

$$\frac{n^2(n-1)}{2} - n = \frac{(n+1)n(n-2)}{2}$$

Magnus generators. In fact, Andreadakis showed $H_1(\mathrm{IA}_n; \mathbb{Z}) = \mathbb{Z}^{n^2(n-1)/2}$[1] and Kawazumi showed $H_1(\mathrm{IO}_n; \mathbb{Z}) = Z^{(n+1)n(n-2)/2}$[20], so that these generating sets are minimal.

Magnus asked if the IA group is finitely presented. Krstić and McCool answered this question in the negative for IA_3[22].

Baumslag and Taylor showed that IO_n is torsionfree ([3],[23] p.26), so the spine of Outer space provides an upper bound for the cohomological dimension of IO_n. In fact, Bestvina, Bux and Margalit used an infinite recursion to show that the quotient of the spine by the action of IO_n is homotopy equivalent to a codimension 1 subspace, so that $\mathrm{cd}(\mathrm{IO}_n) \leq 2n - 4$. Indeed, they were able to show that $\mathrm{cd}(\mathrm{IO}_n) = 2n - 4$, obtaining the lower bound in two ways: finding a free abelian subgroup $\mathbb{Z}^{2n-4} \hookrightarrow \mathrm{IO}_n$ and showing that $H_{2n-4}(\mathrm{IO}_n; \mathbb{Z})$ is not finitely generated[4]. In particular, $H_2(\mathrm{IO}_3; \mathbb{Z})$ is not finitely generated, so they recovered the Krstić-McCool result.

Analogous to the IA group is the Torelli subgroup $\mathcal{I}(S_g)$ of the mapping class group of a genus g surface, consisting of the surface automorphisms that act as the identity on the abelianization $\mathbb{Z}^{2g} = H_1(S_g)$ of the fundamental group of the surface. Since orientation-preserving surface automorphisms preserve the algebraic intersection number of curves, there is an invariant symplectic structure. The Torelli group is therefore the kernel of $\mathrm{Mod}(S_g) \to \mathrm{Sp}_{2g}(\mathbb{Z})$. See [14] for an introduction to the Torelli group.

The Torelli group enjoys some analogous properties to the IA group. For instance, $\mathcal{I}(S_g)$ is torsion-free (see e.g. [14] p.192). Johnson showed it is finitely generated (by Dehn twists about certain pairs of bounding curves)[19], but requires at least $(4g^3 - g)/3$ generators[18]. Both IO_n and $\mathcal{I}(S_g)$ have Johnson filtrations: they are the first terms in sequences of groups $\mathrm{Out}(\Gamma) \to \mathrm{Out}(\Gamma/\Gamma_{i+1})$, where Γ_k is the kth term of the lower central series for $\Gamma = F_n$ or $\Gamma = \pi_1(S_g)$. (Recall that the lower central series of a group Γ is defined inductively by $\Gamma_1 = \Gamma$, $\Gamma_{i+1} = [\Gamma, \Gamma_i]$.) This terminology is perhaps a misnomer as Andreadakis studied the filtration for IA_n first, but Johnson introduced homomorphisms[17] embedding the quotients of consecutive terms into certain tensor algebras of $H_1(\Gamma; \mathbb{Z})$. Kawazumi has used these homomorphisms to compute $H_1(\mathrm{IO}_n; \mathbb{Z})$ in [20].

CHAPTER 3

THE JACOBIAN MAP

3.1 The Inner Product on a Graph

Kotani-Sunada and Nagnibeda defined an inner product on a finite graph (a connected 1-dimensional CW complexes with edge lengths 1), and used it to define the *Albanese* and *Jacobian* tori of the graph[21][25]. The author learned about the inner product and its natural generalization to metric graphs from Vogtmann. This generalization has since appeared in (Camporaso and Viviani, [8]). In this section, the definition for metric graphs (which are simply called *graphs* in the sequel) is reviewed, and is shown to be the unique inner product inducing the length function on circuits.

Combinatorial Graphs A *combinatorial graph* is a 1-dimensional finite connected CW complex G with vertex set $V(G)$ and edge set $E(G)$. Each vertex has valence at least 3. There are no *separating edges*: the graph remains connected upon deleting any open 1-cell.

Note that the definition of combinatorial graph is more restrictive than the usual definition.

Graphs A (metric) *graph* (G, l) is a combinatorial graph G together with a function $l : E(G) \to \mathbb{R}_{>0}$, called the length function. The graph gets an induced path-metric by assigning the length $l(e)$ to each edge e. An *isomorphism* of marked graphs is an isometry of the induced metric spaces. The graph (G, l) will usually be abbreviated by G.

Rank of a Graph The *rank* rk (G) of a graph G is its first Betti number. In other words, rk $(G) = \dim_{\mathbb{R}} H_1(G, \mathbb{R}) = 1 - \chi(G)$ where $\chi(G)$ is the Euler characteristic.

Since valence 2 vertices are disallowed, an isomorphism between two graphs establishes bijections between their vertex and edge sets such that corresponding edges have the same length. (Disallowing valence 1 vertices means that no graph deformation retracts onto a proper subgraph.) The following graph-theoretic notions sometimes have slight variations in the literature.

Paths, Cycles, Circuits An *edge-path* τ in a combinatorial or metric graph is a finite sequence $e_1, \ldots, e_n$ of oriented edges such that the terminal vertex of each edge e_i is the initial vertex of e_{i+1}. The same path traversed backwards is denoted $\overline{\tau}$. A *cycle* is an element of $H_1(G; \mathbb{Z})$ represented by a closed edge-path visiting each vertex at most once. It is a *k-cycle* if k edges are used. More generally, a *circuit* is an element of $H_1(G; \mathbb{Z})$ represented by a closed edge-path visiting each edge at most once. The *length* $l(\tau)$ of an edge-path, cycle, or circuit τ in a metric graph is the sum of the lengths of the constituent edges.

Proposition/Definition 3.1.1 (The Inner Product on a Graph)**.** *There is a unique inner product $\langle , \rangle_G$ on the real homology $H_1(G; \mathbb{R})$ of G inducing the length function on circuits, i.e. such that $\langle \sigma, \sigma \rangle_G = l(\sigma)$ for all circuits σ.*

This inner product will sometimes be denoted $\cdot_G$. It may be denoted $\langle , \rangle$ or $\cdot$ if the graph under consideration is clear from context.

Existence follows from the Kotani-Sunada[21] construction for combinatorial graphs. Note that uniqueness cannot be obtained if "circuit" is replaced by "cycle". For instance, if the graph is a *rose* then the length function on cycles yields no information about the dot product of two (oriented) petals.

Roses and Thetas The *rose with n petals* R_n is the combinatorial graph consisting of a single vertex and n edges. A *rose* is a graph with R_n as underlying combinatorial graph. An *n-cage* is a combinatorial or metric graph consisting of two vertices joined by n edges. A *theta graph* is a 3-cage.

Proof of 3.1.1. For existence, first define an inner product on the vector space $C_1(G, \mathbb{R})$ of cellular 1-chains. Choose a basis for $C_1(G, \mathbb{R})$ consisting of arbitrarily oriented edges, and set

$$\langle e, e' \rangle_G = \begin{cases} l(e) & \text{if } e = e' \\ 0 & \text{if } e \neq e' \end{cases}$$

for e, e' in the basis. Extend bilinearly to an inner product on $C_1(G, \mathbb{R})$, then restrict to the vector subspace $H_1(G, \mathbb{R})$ to obtain the desired $\langle , \rangle_G$.

For uniqueness, assume $\langle , \rangle$ is another inner product on $H_1(G, \mathbb{R})$ inducing the length function on circuits. Choose a spanning tree T for G. Let $e_1, \ldots, e_n$ be the edges $E(G) \setminus E(T)$. Take a basis $\sigma_1, \ldots, \sigma_n$ for $H_1(G; \mathbb{R})$ where σ_i is a cycle whose only edge outside T is e_i. It suffices to show $\langle \sigma_i, \sigma_j \rangle = \langle \sigma_i, \sigma_j \rangle_G$ for all $1 \leq i, j \leq n$. We may assume $i \neq j$ since the cycle σ_i is a circuit.

Consider first the case $\sigma_i \cap \sigma_j \neq \emptyset$ (as CW-subcomplexes of G.) $\sigma_i \cap \sigma_j$ is an intersection of segments in the tree T and is therefore a segment or a single vertex. This reduces to the case that G is a rose with two petals or a theta graph. The latter is more general. We may assume σ_i, σ_j cross their common edge e with opposite orientation. $\sigma_i + \sigma_j \in H_1(G, \mathbb{R})$ is represented by a circuit σ, so

$$\begin{aligned} 2\langle \sigma_i, \sigma_j \rangle &= \langle \sigma_i + \sigma_j, \sigma_i + \sigma_j \rangle - \langle \sigma_i, \sigma_i \rangle - \langle \sigma_j, \sigma_j \rangle \\ &= l(\sigma) - l(\sigma_i) - l(\sigma_j) = -2l(e) = 2\langle \sigma_i, \sigma_j \rangle_G. \end{aligned}$$

Next, consider the case $\sigma_i \cap \sigma_j = \emptyset$. By the following lemma, there exist edge-paths τ_1, τ_2 joining the subcomplex σ_i to the subcomplex σ_j with no edges in common with σ_i,σ_j, or each other (see figure 3.1). Reversing orientation on σ_j if necessary, write σ_i (resp. σ_j) as a concatenation of two edge-paths, one of which may be trivial: σ_i^1 (resp. σ_j^1) from the initial (resp. terminal) vertex of τ_1 to the initial (resp. terminal) vertex of τ_2 followed by σ_i^2 (resp. σ_j^2) from the initial (resp. terminal) vertex of τ_2 to the initial (resp. terminal) vertex of τ_1. Let τ denote the circuit obtained as the concatenation $\tau = \tau_1 \cdot \overline{\sigma_j^2} \cdot \overline{\tau_2} \cdot \overline{\sigma_i^1}$. Observe that $\sigma_i + \tau$,$\tau + \sigma_j$,$\sigma_i + \tau + \sigma_j \in H_1(G, \mathbb{R})$ are all represented by circuits. Therefore:

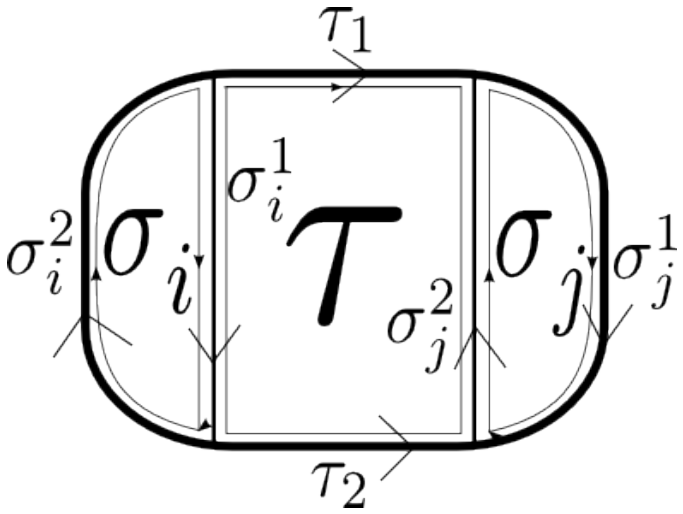

Figure 3.1: Proof of 3.1.1

$$\begin{aligned} 2\langle\sigma_i,\sigma_j\rangle &= \langle\sigma_i+\tau+\sigma_j\rangle - \langle\sigma_i+\tau,\sigma_i+\tau\rangle - \langle\tau+\sigma_j,\tau+\sigma_j\rangle + \langle\tau,\tau\rangle \\ &= [l(\sigma_i^2)+l(\tau_1)+l(\sigma_j^1)+l(\tau_2)] - [l(\sigma_i^2)+l(\tau_1)+l(\sigma_j^2)+l(\tau_2)] \\ &\quad -[l(\sigma_i^1)+l(\tau_1)+l(\sigma_j^1)+l(\tau_2)] + [l(\tau_1)+l(\sigma_j^2)+l(\tau_2)+l(\sigma_i^1)] \\ &= 0 = 2\langle\sigma_i,\sigma_j\rangle_G. \end{aligned}$$

This establishes uniqueness. □

Lemma 3.1.2. *(cf. [38], Theorem 7) Let G be a combinatorial graph. For any pair of vertices, there is a circuit visiting both. [Note the nonstandard definition of graph.]*

Proof. View G as a metric graph by assigning 1 to each edge length. Suppose there is a counterexample and choose p, q of minimal distance so that there is no circuit visiting both. Since G is path-connected, there is a vertex r such that $d(p,r) = d(p,q) - 1$ and $d(r,q) = 1$. Choose a circuit C visiting p and r and an edge e joining r to q. Since there are no separating edges, there is a path P from q to p that does not traverse e. Contrary to assumption, a circuit containing p, q is obtained: follow P from q until reaching a vertex of C; then follow C via p to r; finally traverse e to q. This contradiction establishes the lemma. □

In the context of metric graphs, the definitions of Kotani-Sunada's[21] Albanese and Jacbobian tori for graphs become:

Albanese and Jacobian Tori ([8]) Let G be a graph. Its *Albanese torus* $\mathrm{Alb}(G)$ is $\mathrm{Alb}(G) = H_1(G,\mathbb{R})/H_1(G,\mathbb{Z})$, with the flat metric induced by $\langle,\rangle_G$. The *Jacobian torus* of G is $\mathrm{Jac}(G) = H^1(G,\mathbb{R})/H^1(G,\mathbb{Z})$ with the flat metric induced by the dual inner product.

(The *dual inner product* sends a pair (f,g) of functionals $f, g \in C^1(C,\mathbb{R})$ to $\sum_{e\in E(G)} f(e)g(e)$ where the edges e are oriented arbitrarily.)

3.2 Symmetric Space, Outer Space and the Jacobian Map

In this section, the inner product $\langle , \rangle_G$ is used to define a map, the *Jacobian map*, from Culler-Vogtmann Outer space X_n to the homogeneous space $Y_n = \mathrm{SO}_n(\mathbb{R})\backslash \mathrm{SL}_n(\mathbb{R})$ of projectivized positive definite quadratic forms. Before defining the Jacobian map, basic properties of its domain and codomain are reviewed.

Homogeneous Space Y_n is the projectivized space of real symmetric positive definite $n \times n$ matrices.

There are various ways to think of such matrices, and these will be conflated when convenient. A real symmetric positive definite matrix M defines a positive definite biliear form $B : \mathbb{R}^n \times \mathbb{R}^n \to \mathbb{R}$ via $B(v, w) = {}^T vMw$ and a positive definite quadratic form $q : \mathbb{R}^n \to \mathbb{R}$ via $q(v) = B(v, v)$. Conversely, one passes from q to B via

$$B(v, w) = \frac{1}{2}\left(q(v + w) - q(v) - q(w)\right)$$

and from B to M via

$$M_{ij} = B(x_i, x_j)$$

where $x_1, \ldots, x_n$ is the standard basis for $\mathbb{R}^n$.

Some basic facts about Y_n are needed:

Proposition 3.2.1. *Y_n is a contractible space admitting a right action of $GL_n(\mathbb{Z})$ with finite point stabilizers.*

Proof. A weighted average of two positive definite quadratic forms is again a positive definite quadratic form. If q_0 is your favorite quadratic form, then $q \mapsto$

$(1-t)q + tq_0$ gives a homotopy from the identity map on Y_n to a constant map. Therefore Y_n is contractible.

The right action of $A \in \mathrm{GL}_n(\mathbb{Z})$ on the matrix $M \in Y_n$ is by $M \cdot A = {}^TAMA$. Using the bilinear form description, this action defines a bilinear form $(B \cdot A)$ given by $(B \cdot A)(v, w) = B(Av, Aw)$. Likewise $(q \cdot A)(v) = q(Av)$. Perhaps the easiest way to see that the stabilizer of q is finite is to observe that if $q = q \cdot A$, then A can't send any standard basis vectors $e_i \in \mathbb{R}^n$ too far from the origin: if the Euclidean distance from 0 to Ae_i is greater than the maximum value of q attained on the (compact) unit circle, then $q(e_i) \lneqq (qA)(e_i)$. □

Theorem 3.2.2 (Soulé [30] 1976)**.** *Y_3 has a $GL_3(\mathbb{Z})$-invariant deformation retract, the* well-rounded retract *Z_3, on which the action is compact.*

Soulé used this retract to compute the homology of $\mathrm{SL}_3(\mathbb{Z})$ and $\mathrm{GL}_3(\mathbb{Z})$[30]. This retract is described in the next chapter. Ash generalized this construction to form well-rounded retracts for other groups, including $\mathrm{GL}_n(\mathbb{Z})$[2].

Outer space gets its name from its use in studying $\mathrm{Out}(F_n)$, the outer automorphism group of a rank n free group. The following theorem shows it plays an analogous role to $\mathrm{Out}(F_n)$ as Y_n (with its well-rounded retract) does to $\mathrm{GL}_n(\mathbb{Z})$:

Theorem 3.2.3 (Culler-Vogtmann[11] 1986)**.** *X_n is a contractible space admitting a simplicial right action by $\mathrm{Out}(F_n)$ with finite point stabilizers. There is an $\mathrm{Out}(F_n)$-invariant deformation retract, the* spine*, on which the action is cocompact.*

Outer space was first defined in [11]. Its constructions requires some ancillary definitions.

Markings A *marking* on a rank n combinatorial or metric graph G is a homotopy equivalence $\rho : R_n \to G$ from the rose with n petals to G. A graph together with a marking is a *marked graph*.

Collapses If ρ is a marking of a combinatorial or metric graph G of rank n and $E' \subset E(G)$ is a set of edges spanning a forest (a disjoint union of trees) in G then the quotient graph G/E' is obtained by collapsing each constituent tree to a vertex. The induced marking $\overline{\rho}$ on the quotient graph G/E' is the composition of ρ followed by the quotient map $G \to G/E'$.

Homothety A *homothety* between two metric spaces G and G' is a composition of an isometry and a scaling. In other words, it is a bijection $\varphi : G \to G'$ such that there exists a positive real number c so that for all $x, y \in G$, $d_{G'}(\varphi(x), \varphi(y)) = c \cdot d_G(x, y)$.

Equivalent Markings Two marked graphs $(G, \rho), (G', \rho')$ of rank n are *equivalent* if there exists a homothety $\varphi : G \to G'$ such that $\varphi \circ \rho \simeq \varphi'$. In other words, $\begin{array}{ccc} R_n & \xrightarrow{\rho} & G \\ & \searrow^{\rho'} & \downarrow \exists\varphi \\ & & G' \end{array}$ commutes up to free homotopy. Two marked combinatorial graphs are *equivalent* if they are equivalent as metric graphs with the length function assigning 1 to each edge.

Outer Space Culler-Vogtmann Outer space X_n is the space of rank n marked graphs up to equivalence. The topology on Outer space is obtained from viewing X_n as a subspace of a simplicial complex. For each rank n combinatorial graph G and each marking equivalence class (G, ρ), let $\sigma_{(G,\rho)}$ be a simplex with vertex set in bijection with $E(G)$. If $E' \subset E(G)$ spans a forest in G, then $\sigma_{(G/E',\overline{\rho})}$

is identified with the sub-simplex in $\sigma_{(G,\rho)}$ spanned by $E(G) \setminus E'$. The interior of $\sigma_{(G,\rho)}$ is identified with the subset of X_n obtained by varying the length function on G: the graph (G, l) marked by ρ corresponds to the point in $\sigma_{(G,\rho)}$ with barycentric coordinates

$$\left(\frac{l(e)}{\sum_{e' \in E(G)} l(e')} : e \in E(G) \right).$$

In this way X_n is identified with a union of open simplices within a simplicial complex, and is endowed with the subspace topology.

Note: the points of $X_n \cap \sigma_{(G,\rho)}$ that are not in the interior of $\sigma_{(G,\rho)}$ can be thought of (in terms of their barycentric coordinates) assigning a length of 0 to the edges that were collapsed. Some sub-simplices of $\sigma_{(G,\rho)}$ are "missing" from X_n since they correspond to collapsing a subgraph containing a cycle, thereby reducing the rank of the graph.

The action of $\mathrm{Out}(F_n)$ on X_n is defined using the following well-known lemma.

Lemma 3.2.4 ((Nielsen) Automorphisms Realized)**.** *Any automorphism $\varphi \in Aut(F_n)$ of the free group is represented by a homotopy equivalence $f_\varphi : R_n \simeq R_n$.*

Proof. The fundamental group $\pi_1(R_n)$ of the rose with n petals $a_1, \ldots, a_n$ is the rank n free group $F_n = \langle x_1, \ldots, x_n \rangle$, with the petal a_i (arbitrarily oriented) representing x_i. Any automorphism φ of F_n can be realized by a map $f_\varphi : R_n \to R_n$ sending the vertex to itself and a_i to the edge-path corresponding to the word $\varphi(a_i)$ (say, traversed at constant speed). Then $f_{\varphi^{-1}} \circ f_\varphi$ sends a_i to an edgepath corresponding to a word freely reducing to x_i. As such, $f_{\varphi^{-1}} \circ f_\varphi \simeq \mathrm{id}_{R_n}$. Thus f_φ is a homotopy equivalence representing φ. □

The right action of $\varphi \in \text{Aut}(F_n)$ on $(G, \rho) \in X_n$ is given by $(G, \rho) \cdot A = (G, \rho \circ f_\varphi)$. If φ is an inner automorphism, conjugation by a word in F_n, then $f_\varphi \simeq \text{id}_{R_n}$ via a free homotopy moving the basepoint around the corresponding path in R_n. So the inner automorphisms $\text{Inn}(G)$ act trivially on X_n, and the action descends to an action of $\text{Out}(F_n) = \text{Inn}(F_n)\backslash\text{Aut}(F_n)$.

The Jacobian Map The Jacobian map $J : X_n \to Y_n$ is given by $J(G, \rho) = \rho^*(\langle , \rangle_G)$, the pullback of the inner product on G to an inner product on $H_1(R_n) = \mathbb{R}^n$. (This is the inner product sending $(x, y) \in H_1(G) \times H_1(G)$ to $\langle \rho_*(x), \rho_*(y) \rangle_G$.)

There is a natural map $\pi : \text{Out}(F_n) \to \text{GL}_n(\mathbb{Z})$. (Indeed, there is a natural map from the outer automorphism group of any group to the automorphism group of its abelianization, since commutator subgroups are characteristic.)

Proposition 3.2.5 (Jacobian Respects Actions)**.** *The Jacobian map respects the actions of Out(F_n) and GL$_n(\mathbb{Z})$: $J(G \cdot \varphi) = J(G) \cdot \pi(\varphi)$.*

Proof.

$$J((G, \rho)\cdot\varphi) = J(G, \rho\circ\varphi) = (\rho\circ\varphi)^*\langle , \rangle_G = \varphi^*(\rho^*\langle , \rangle_G) = \varphi^*(J(G, \rho)) = J(G, \rho)\cdot\pi(\varphi)$$

□

The map π is surjective (the Nielsen generators for $\text{Out}(F_n)$ map to the elementary matrices generating $\text{GL}_n(\mathbb{Z})$) and the kernel was studied by Magnus.

IA group The group IA_n (Identity on Abelianization) is the kernel

$$1 \to \text{IA}_n \to \text{Aut}(F_n) \to \text{GL}_n(\mathbb{Z}) \to 1.$$

The group IO_n is the kernel

$$1 \to \mathrm{IO}_n \to \mathrm{Out}(F_n) \to \mathrm{GL}_n(\mathbb{Z}) \to 1.$$

IA_n has also been called the *Induced Automorphism* group.

Bestvina, Bux and Margalit studied the group homology of IO_n by viewing the quotient of Outer space by IO_n as the space of *homology-marked graphs*[4]. (They called this group the *Torelli subgroup* of $\mathrm{Out}(F_n)$, in analogy with the eponymous subgroup of the mapping class group of a surface S that acts trivially on $H_1(S, \mathbb{Z})$.)

Homology Marked Graphs A *homology marking* on a rank n graph G is an isomorphism $\rho : \mathbb{Z}^n \cong H_1(G, \mathbb{Z})$. A graph together with a homology marking is called a *homology marked graph*. A marked graph (G, ρ) induces a homology marking via the identification $\mathbb{Z}^n = H_1(R_n, \mathbb{Z})$. The *space of homology marked graphs* is therefore the quotient X_n/IO_n of Outer space, with the quotient topology.

J factors through the quotient map $X_n \to X_n/IO_n$. The map $X_n/IO_n \to Y_n$ will also be denoted J.

3.3 Computation of Fibers in Rank 3

In this section, the fibers of the rank 3 Jacobian map ($J_3 : X_3/IO_3 \to Y_3$) are computed. In particular, they are shown to be nonempty – J_3 is surjective. The fiber computation will be used in Chapter 5 to induce a cell structure on the complex K constructed there. For this section, J means J_3.

There are 8 combinatorial graphs of rank 3. 5 of them are collapses of the 1-skeleton ☮ of a tetrahedron (including ☮ itself). The remaining 3 have pairs of separating edges; collapsing either of these edges results in a collapse of ☮. The computation of the fibers of J will use Minkowski reduction, a tool Soulé

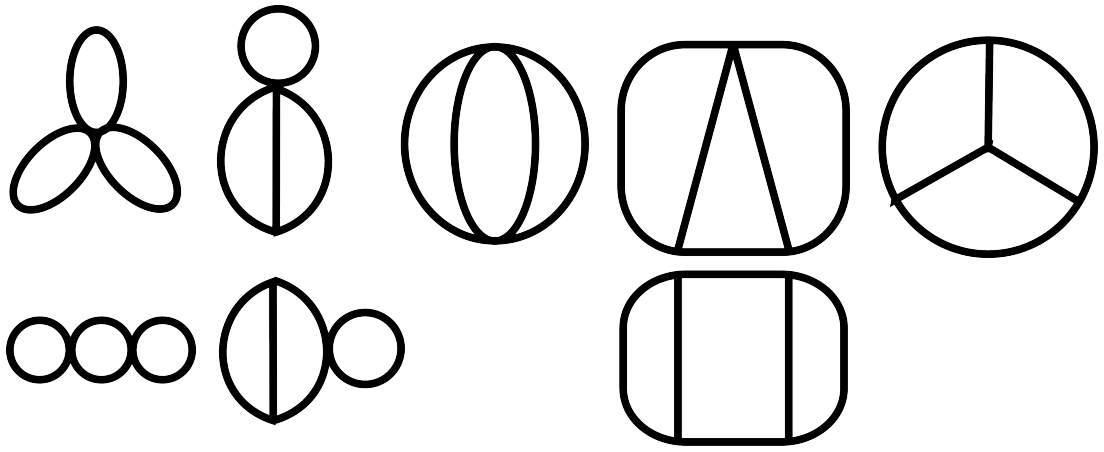

Figure 3.2: The 8 graphs of rank 3

The top row shows the collapses of ☮, the 1-skeleton of a tetrahedron. The bottom row shows the graphs with separating edge pairs. The graph above is obtained by collapsing (either) edge of the one below.

used in defining his well-rounded retract[30].

Minkowski-reduced Basis A basis $e_1, \ldots, e_n$ for $\mathbb{Z}^n$ is *Minkowski-reduced* with respect to an inner product if for every $1 \leq i \leq n$, e_i has minimal length among all $e_i' \in \mathbb{Z}$ for which there exists a basis $e_1, \ldots, e_{i-1}, e_i', \ldots, e_n'$ for $\mathbb{Z}^n$ extending $e_1, \ldots, e_{i-1}$. An inner product on $\mathbb{R}^n$ is *Minkowski-reduced* if the standard basis for $\mathbb{Z}^n$ is Minkowski-reduced with respect to it.

There is always a Minkowski basis for each inner product, but it is not unique.

Theorem 3.3.1 (Minkowski, see e.g.[10]). *A positive definite symmetric 3x3 matrix*

$$M = \begin{pmatrix} m_{11} & m_{12} & m_{13} \\ m_{12} & m_{22} & m_{23} \\ m_{13} & m_{23} & m_{33} \end{pmatrix}$$

is Minkowski-reduced if and only if the following inequalities hold:

$$m_{11} \leq m_{22} \leq m_{33}, \tag{3.1}$$

$$2|m_{12}| \leq m_{11}, \qquad 2|m_{13}| \leq m_{11}, \qquad 2|m_{23}| \leq m_{22}, \tag{3.2}$$

$$\max \left\{ \begin{array}{ll} -m_{12} + m_{13} + m_{23}, & m_{12} - m_{13} + m_{23}, \\ m_{12} + m_{13} - m_{23}, & -m_{12} - m_{13} - m_{23} \end{array} \right\} \leq \frac{m_{11} + m_{22}}{2}. \tag{3.3}$$

Associated diagonal entry Given two distinct entries m_{ij}, m_{kl} above the main diagonal in a 3x3 matrix, the *associated diagonal entry* is the unique diagonal entry $m_{\alpha\alpha}$ such that $\alpha \in \{i, j\} \cap \{k, l\}$. In other words, each of m_{ij}, m_{kl} shares a row or column with their associated diagonal entry. For example, the associated diagonal entry to m_{12} and m_{23} is m_{22}.

The aim of this section is to prove the following:

Theorem 3.3.2. *If $M \in Y_3$, then $J^{-1}(M) \subset X_3/IO_3$ is homeomorphic to one of the following:*

- *a rose on 3 petals, if M is in the $GL_3(\mathbb{Z})$-orbit of a diagonal Minkowski-reduced matrix;*
- *a theta graph, if M is in the $GL_3(\mathbb{Z})$-orbit of a Minkowski-reduced matrix with exactly two zeros above the diagonal;*

- *one point, if M is in the $GL_3(\mathbb{Z})$-orbit of a Minkowski-reduced matrix with equal positive values off the diagonal;*
- *a closed interval, if M is in the $GL_3(\mathbb{Z})$-orbit of a Minkowski-reduced matrix with either (i) a unique zero above the diagonal, the absolute values of the other two entries adding to less than their associated diagonal entry, or (ii) two equal positive values above the diagonal, strictly smaller than the third;*
- *two points, otherwise.*

Remark Given any Minkowski-reduced matrix in the orbit of M with m_{13} and m_{23} non-negative, one can determine which of the above cases corresponds to $J^{-1}(M)$ using Proposition 3.3.3 below.

The theorem follows from Proposition 3.3.3 below, which is proved at the end of this section.

Proposition 3.3.3. *Let M be a Minkowski-reduced matrix, with $m_{13}, m_{23} \geq 0$. There is a graph G_M and a homology marking ρ_M such that $J(G_M, \rho_M) = M$ and G_M is:*

- *A rose, if M is diagonal;*
- *A theta graph with a loop added to a vertex, if exactly two of m_{12}, m_{13}, m_{23} are zero;*
- *A 4-cage, if $m_{12} = m_{13} = m_{23} > 0$ or if exactly one of m_{12}, m_{13}, m_{23} is zero and the other two have absolute values equal to half their associated diagonal entry;*
- *$\mathbin{\text{☮}}$/edge, if exactly one of m_{12}, m_{13}, m_{23} is zero and the other two have absolute values adding to strictly less than their associated diagonal entry, or if the smallest two of $\{m_{12}, m_{13}, m_{23}\}$ are positive and equal and strictly smaller than the third, or if $-m_{12} = m_{13} = m_{11}/2$;*

- ☮, *in all other cases.*

Moreover, if (G, ρ) *is any other homology-marked graph homeomorphic to a collapse of* ☮ *with* $J(G, \rho) = M$*, then* $(G, \rho) = (G_M, \rho_M) \cdot \pm I$*.*

Assuming the truth of the above Proposition for now, Theorem 3.3.2 can be proved.

Proof of Theorem 3.3.2. Proposition 3.3.3 determines which homology-marked graphs that are collapses of ☮ are in the fiber $J^{-1}(M)$. The remaining graphs G have separating edge pairs $\{E_1, E_2\}$. But $J(G, \rho) = J(G/E_1, \overline{\rho})$ where $\overline{\rho}$ is the induced marking and where E_2 in G/E_1 is given the new length $l(E_1) + l(E_2)$. Visually, one can imagine one component of $G \setminus \{E_1, E_2\}$ sliding along $E_1 \cup E_2$ with the other component fixed in place.

Since no graph has a pair of separating edges for which collapsing one leads to a 4-cage, the fibers of J containing a 4-cage graph contain nothing else. They are therefore single points (mapped to themselves by $-I$.) Likewise, fibers containing ☮ graphs are pairs of points.

The fibers $J^{-1}(M)$ containing graphs homeomorphic to ☮ with an edge collapsed are larger, as they contain trivalent rank 3 graphs with separating edge pairs. The fiber is a closed interval parameterized by the relative lengths of the separating pair (with endpoints $G_M \cdot \pm I$ if M is Minkowski-reduced).

The fibers $J^{-1}(M)$ containing a theta graph with a loop attached to one vertex are larger still, as they contain the graphs obtained by moving the basepoint of the loop to anywhere on the theta graph. These fibers are therefore homeomorphic to a theta graph. (The vertices are $G_M \cdot \pm I$ if M is Minkowski-reduced).

The fibers $J^{-1}(M)$ containing a 3-rose R as a point (for example, $R = G_M$ if M is diagonal) are themselves homeomorphic to a 3-rose, with R serving as $(-I)$-invariant basepoint. The quotient map collapsing one edge of a separating pair induces a correspondence between the petals of $J^{-1}(M)$ and those of R.

As noted in the proof of the proposition, the two classes of matrices described in the statement of the proposition that are "missing" from the statement of the theorem are actually in the same $\mathrm{GL}_3(\mathbb{Z})$-orbit as other Minkowski-reduced matrices mentioned explicitly. □

Caution: recall that a *cycle* in G is a $H_1(G)$ element represented by an embedded circle. To distinguish this notion from the standard usage in homology theory, $H_1(G)$ *element* will be used to mean the latter.

The proof of Proposition 3.3.3 will need a few lemmas.

Embedded homology-markings Say that a homology marking $\rho : \mathbb{R}^n \to G$ is *embedded* if $\rho(x_i)$ is a cycle for each standard generator x_i of $\mathbb{R}^n$.

Lemma 3.3.4. *Every element of $H_1(G, \mathbb{Z})$ is a sum of cycles without cancellation (i.e., no edge is oriented differently in two of the cycles).*

Proof. This follows by induction on the sum of the absolute values of the coefficients in a $C_1(G, \mathbb{Z})$ representative. □

Lemma 3.3.5. *Any cycle or pair of (homology-)independent cycles in a rank 3 combinatorial graph can be extended to a basis of cycles for $H_1(G)$. Three independent cycles always form a basis, except in the case where G is the 1-skeleton of a tetrahedron and the cycles are the three 4-cycles of this graph.*

Note: it is not true that $n-1$ independent cycles in a rank n graph can always be extended to a basis for the homology. For instance, consider the graph G formed by identifying the inner and outer circles, with opposite orientation, in a "target" G_0 consisting of five concentric circles with five spokes (see Figure 3.3). Then rk $(G) =$ rk $(G_0) = 21$ since the Euler characteristic of a circle is 0. If each edge has length 1, G has 21 sytoles: the 20 planar quadrilaterals of G_0 and one of its spokes – the unique spoke with identified endpoints. These systoles are independent, but are not a basis since the sum of the 20 planar quadrilaterals is twice the inner/outer circle.

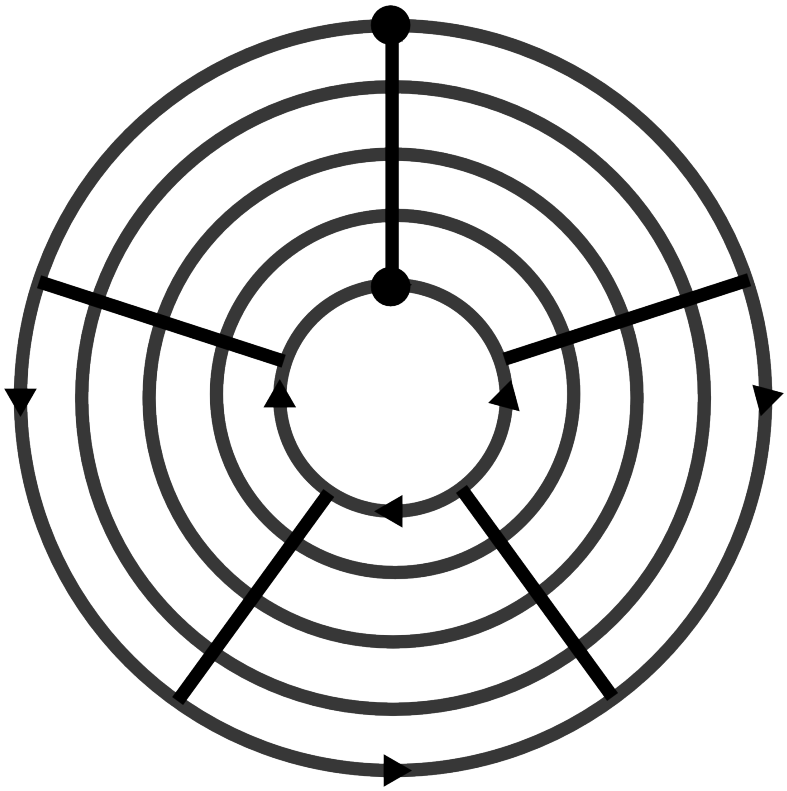

Figure 3.3: Lemma 3.3.5 does not hold for all n

Proof. Observe that collapsing an edge E from a separating pair in a graph G induces a bijection between the sets of cyles of G and those of G/E. So it suffices

to consider only the 5 collapses of the tetrahedral graph ☮. In all cases, except perhaps two, the claim is immediate. For ☮, the appropriate signed sum of any 4-cycle and any 3-cycle is a 3-cycle (and independent 3-cycles form a basis by tetrahedral symmetry). For the graph obtained by collapsing a single edge of ☮, the claim follows from the fact that given any three 3-cycles, two of them must share two edges in common; the appropriate signed sum is a 2-cycle. □

Note: The above proof used *cyclic equivalence* to reduce the number of cases. Cyclic equivalence is studied in the context of the Jacobian map on graphs in [8] based on work of Whitney[39].

Lemma 3.3.6. *If (G, ρ) is a rank 3 homology-marked graph and $J(G, \rho)$ is Minkowski-reduced, then ρ is embedded.*

Proof. Suppose $J(G, \rho)$ is Minkowski-reduced but ρ is not embedded. Take $1 \leq i \leq 3$ minimal so that $\rho(x_i)$ is not represented by a cycle. One of the summand cycles for $\rho(x_i)$ furnished by Lemma 3.3.4 is independent from the cycles $\rho(x_j), j < i$. By Lemma 3.3.5, the summand together with the $\rho(x_j), j < i$ can be extended to a basis for $H_1(G)$ producing a strictly smaller basis in the sense of Minkowski, except possibly in the case where $i = 3$, G is homeomorphic to the 1-skeleton of a tetrahedron, and $\rho(x_1), \rho(x_2)$ are 4-cycles. This case cannot occur: the graph would contain a 3-cycle σ of length stricly smaller than the average length of $\rho(x_1), \rho(x_2)$, and Lemma 3.3.5 would promote $\rho(x_1), \sigma$ to a Minkowski-smaller basis for $H_1(G)$. □

Proof of 3.3.3. Let M be Minkowski-reduced with $m_{13}, m_{23} \geq 0$. Then (G_M, ρ_M) can be defined as in Figure 3.4. (If $m_{12} \leq 0$ use figure (i). If $0 < m_{12} \leq m_{13}, m_{23}$ use figure (ii). If $0 \leq m_{23} < m_{12}, m_{13}$ use figure (iii). Otherwise use figure (iv).)

Theorem 3.3.1 guarantees the edgelengths are nonnegative (indeed, equations 3.1 and 3.2 suffice). A length of zero indicates a contracted edge. Now suppose

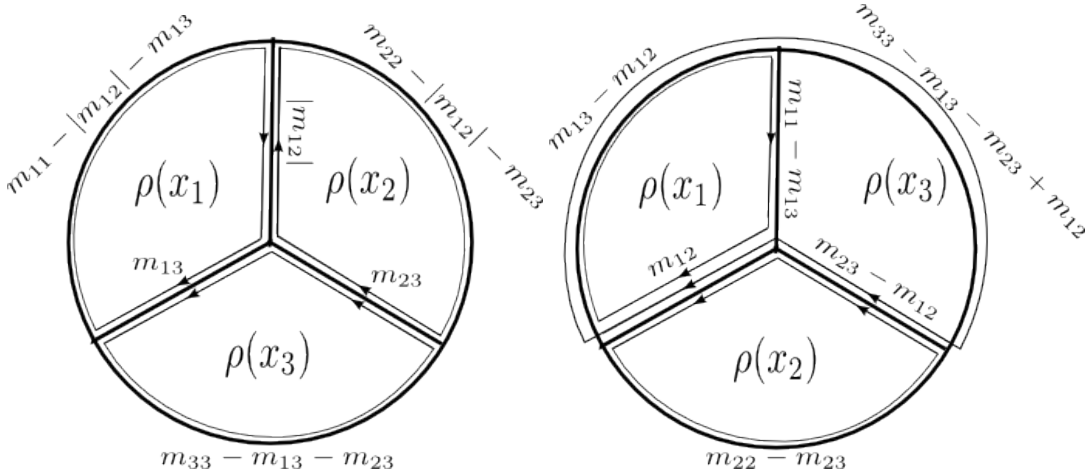

(i) G_M if $m_{12} \leq 0$

(ii) G_M if $0 < m_{12} \leq m_{13}, m_{23}$

(iii) G_M if $0 \leq m_{23} < m_{12}, m_{13}$

(iv) G_M otherwise

Figure 3.4: G_M of Proposition 3.3.3

(G, ρ) is a graph with $J(G, \rho) = M$. By Lemma 3.3.6, ρ is embedded. There are 5 combinatorial graphs to consider, one at a time.

- G is a rose with 3 petals. Then $\alpha_1, \alpha_2, \alpha_3$ must be the three petals in non-decreasing order of length. Choices of orientation and the permuting of petals of the same length make no difference up to graph equivalence. M

is diagonal and $G = G_M, \rho = \rho_M$.

- G is a theta graph with a loop added at one vertex. Then $\alpha_1, \alpha_2, \alpha_3$ are (in some order) the loop and two cycles of the theta graph. M therefore has exactly one nonzero entry above the diagonal. If this entry is m_{13} or m_{23}, then figure (i) defines G_M, which is the same graph as G. Under ρ, the shared edge over the overlapping cycles may be oriented towards or away from the loop, so $(G, \rho) = (G_M, \rho_M) \cdot \pm I$. If the nonzero entry is instead m_{12}, then figure (iv) applies and again $(G, \rho) = (G_M, \rho_M) \cdot \pm I$.

- G is the *4-cage*: the graph with 2 vertices joined by 4 edges. Either $\alpha_1, \alpha_2, \alpha_3$ all share a single edge in common, or one of these cycles shares one of its edges with another, the other with a third. In the first case, the common edge is oriented the same way on all three and $m_{12} = m_{13} = m_{23} > 0$. Then figure (ii) defines G_M and $(G, \rho) = (G_M, \rho_M)$. In the second case, the cycle bordering the other two must have minimal length, and its two edges must have equal length. So M has precisely two nonzero entries above the diagonal and they have absolute values equal to half the associated diagonal entry. Figure (i), (iii), or (iv) defines $(G_M, \rho_M) = (G, \rho)$. [Note: in this second case, M is in the orbit of a matrix of the form of the first 4-cage case.]

- G is ☮ with an edge collapsed. The α_i are either 2-cycles or 3-cycles, and there numerous straightforward cases. Suppose first that two are 2-cycles and one is a 3-cycle. If α_1 is the 3-cycle, then figure (i) or (iii) defines (G_M, ρ_M). If α_2 is the 3-cycle, then figure (i) or (iv) defines it. If α_3 is the 3-cycle, then figure (i) defines it. In all of these cases, the dot product of the disjoint 2-cycles is zero, while their dot products with the 3-cycle add up to less than the 3-cycle's length. Again, $(G_M, \rho_M) = (G, \rho) \cdot \pm I$.

If instead there are exactly two 3-cycles, with two edges in common, the 2-cycle has the same positive overlap with each of them, which is strictly less than their (positive) overlap with each other. Again, $(G_M, \rho_M) = (G, \rho) \cdot \pm I$.

If there are exactly two 3-cycles, overlapping in a single edge, then any two edges connecting the same two vertices must have the same length. Therefore the 2-cycle must be α_1, so $m_{12} = \alpha_1 \cdot \alpha_2 = -m_{11}/2$ and $m_{13} = \alpha_1 \cdot \alpha_3 = m_{11}/2$. Figure (i) defines $(G_M, \rho_M) = (G, \rho) \cdot \pm I$. [Note: M is therefore in the orbit of a matrix corresponding to the previous subcase (3-cycles overlapping in two edges).]

(It cannot be the case that α_1,α_2,α_3 are all 3-cycles, for again any two edges connecting the same two vertices would have the same length. Then one of the 3-cycles could be replaced by a stricly shorter 2-cycle.)

- $G = \mathbin{\text{☮}}$. Here the four subcases correspond to figures (i)-(iv). If $\alpha_1, \alpha_2, \alpha_3$ are 3-cycles, then figure (i) defines $(G_M, \rho_M) = (G, \rho) \cdot \pm I$. Likewise, if α_3, α_1, or α_2, respectively, is a 4-cycle then figure (ii), (iii), or (iv) respectively defines $(G_M, \rho_M) = (G, \rho) \cdot \pm I$.

  There can't be two or more 4-cycles. Indeed, suppose α_i and α_j are 4-cycles with α_k a 3-cycle. Then α_k has two edges in common with α_i; its remaining edge is the (strictly) longest side of α_k or else it could be substituted for the two edges to form a 3-cycle shorter than α_i. The same reasoning with α_j in place of α_i shows a different edge of α_k is longest, a contradiction. (The same argument works for three 4-cycles by using your favorite 3-cycle in place of α_k.)

□

Corollary 3.3.7. *The Jacobian map $J : X_3 \to Y_3$ is surjective.*

CHAPTER 4

THE SCHOTTKY PROBLEM

4.1 The Schottky Problem and Tropical Geometry

Both the classical and the Outer space Jacobian maps assign lattices (or tori or quadratic forms, depending on the point of view) to geometric objects. In both cases, they give the integral homology of the algebraic curve or graph sitting inside its real homology. The analogy can be made stronger since graphs can be viewed as *tropical curves*.

For an introduction to tropical geometry see [28]. Tropical geometry is algebraic geometry over $\mathbb{R}$ under the operations of *tropical addition* $a \oplus b := \min\{a, b\}$ and *tropical multiplication* $a \odot b = a + b$. A real polynomial in n variables defines, under these tropical operations, a function $\mathbb{R}^n \to \mathbb{R}$. The *tropical projective plane* is $\mathbb{T}^2 := \mathbb{R}^3/\mathbb{R}(1,1,1)$. A *tropical curve* in $\mathbb{T}^2$ is the image of the set of points in $\mathbb{R}^3$ at which a given real homogeneous polynomial in x, y, z fails to be linear (i.e., where the minimum value among the constituent monomials is realized at least twice.) A tropical curve is the union of finitely many line segments and rays in $\mathbb{T}^2$, each parallel to the image of some coordinate axis of $\mathbb{R}^3$. Dual to this subdivision of the plane $\mathbb{T}^2$ is a finite graph[28]. Curves are *tropically equivalent* if their graphs so associated are isomorphic[8]. One is therefore tempted to convert questions about the Jacobians of algebraic curves into corresponding questions about the Jacobians of graphs, as in [8].

The classical Schottky problem asks which symmetric matrices Ω with positive definite imaginary part arise as the period matrices (Equation 2.1) of com-

plex curves[9]. The problem remains open, though progress has been made on numerous fronts (see [12] for a survey). If Ω is any symmetric matrix with positive definite imaginary part, the *Theta functions* are holomorphic functions defined on $\mathbb{C}^g$ by:

$$\theta\begin{bmatrix}\delta\\ \epsilon\end{bmatrix}(u;\Omega) := \sum_{m\in\mathbb{Z}^g} \exp\{\pi i[^T(m+\delta/2)\Omega(m+\delta/2) + 2^T(m+\delta/2)(u+\epsilon/2)\},$$

in analogy with the classical (1-dimensional) theta functions $\theta\left[\begin{smallmatrix}\delta\\ \epsilon\end{smallmatrix}\right](u;\tau)$ from complex analysis. There is one for each choice of column vectors $\delta, \epsilon \in \{0,1\}^g$. The values of these functions at $u = 0$ are called the *theta-nulls* of Ω. Various relations have been found among the theta-nulls satisfied by period matrices, beginning with Schottky(1888 [29]; see e.g. [9] for a modern treatment). The *Riemann* Θ *function* is the theta function $\Theta = \theta\left[\begin{smallmatrix}0\\ 0\end{smallmatrix}\right]$. When Ω is a period matrix, a good deal is known about the zero set of Θ, including a lower bound on the dimension of its singular set and the geometry of its intersection with its translates[12].

The Schottky Problem for Graphs The Schottky Problem for graphs is to determine the image of $J : X_n \to Y_n$.

For instance, Corollary 3.3.7 answers the Schottky problem for $n = 3$: every inner product on $\mathbb{R}^3$ comes from a (metric) graph. On the other hand, the Jacobian map cannot be surjective for $n \geq 4$ for dimensional reasons. Outer space X_n has dimension $3n - 4$ (its spine has dimension $2n - 3$), while the symmetric space Y_n has dimension $\frac{n(n+1)}{2} - 1$ (and its well-rounded retract has dimension $\frac{n(n-1)}{2}$).

An explicit example of an element $M_n \in Y_n \setminus J(X_n)$ for each $n \geq 4$ is now constructed. This requires a lemma. A *systole* of a finite metric graph G is any

nontrivial element of $H_1(G;\mathbb{Z})$ that has minimal norm. Every systole is a cycle in the sense of Chapter 3. Sytoles will be intentionally confused with the corresponding subset of G when useful.

Lemma 4.1.1. *Any two distinct systoles γ_1, γ_2 of length L in a graph G have as intersection either:*

- *one point or a segment of length at most $L/2$;*
- *two points separated by distance exactly $L/2$; or*
- *the empty set*

Proof. If the intersection were a single component of length more than $L/2$, then the complements of this component in γ_1 and γ_2 would together form an embedded loop of length smaller than L, contradicting the definition of systole.

Suppose two components of the intersections are a and b of lengths $l(a), l(b)$. Then $\gamma_1 \setminus (a \cup b)$ and $\gamma_2 \setminus (a \cup b)$ each consist of two segments. The sum of lengths of these four segments is $2(L - l(a) - l(b))$. Depending on orientation, it is either the case that these four segments can be arranged into two pairs that together form loops, or that they can be arranged into two pairs that each together with b form loops. In any case, one of the loops has length at most $(L - l(a) - l(b)) + l(b) = L - l(a)$. Since γ_1 is a systole, it follows that $l(a) = 0$, so a is a point. By symmetry, b is a point. Then the lengths of the four segments mentioned above are each $L/2$, or else a minimal length segment of $\gamma_1 \setminus (a \cup b)$ together with the minimal length segment of $\gamma_2 \setminus (a \cup b)$ would form a loop of length strictly less than L.

There cannot be more than two components in the intersection, or else there

would be two that are not points exactly a distance $L/2$ apart, contradicting the previous paragraph. □

In particular, "cancellation" cannot occur when taking the dot product of two systoles: if two systoles have dot product 0, then their intersection contains no interval. This implies:

Lemma 4.1.2. *For $n \geq 4$,*

$$M_n := \begin{pmatrix} 4 & 0 & \cdots & 0 & 2 \\ 0 & 4 & \cdots & 0 & 2 \\ \vdots & \vdots & \ddots & \vdots & \vdots \\ 0 & 0 & \cdots & 4 & 2 \\ 2 & 2 & \cdots & 2 & n \end{pmatrix}$$

is not in the image of J.

Proof. Pettet-Souto showed that M_n induces a positive definite quadratic form on $\mathbb{Z}^n$, and that 4 is the minimum (nonzero) value achieved[27].

Indeed, the associated quadratic form is

$$4(x_1^2+\cdots+x_{n-1}^2)+4(x_1+\cdots+x_{n-1})x_n+nx_n^2 = (2x_1+x_n)^2+\cdots+(2x_{n-1}+x_n)^2+x_n^2,$$

which is positive definite. If $x_n = 0$, then any nonzero term on the right hand side is at least 4. If $x_n = \pm 1$, each term on the right hand side is at least 1, so the sum is at least 4. For any other value of x_n, the term $x_n^2 \geq 4$. So in any case, the quadratic form is bounded below by 4 on nonzero integer points. The minimum is achieved at each of the first $n-1$ standard basis vectors.

Now suppose $J(G) = M_n$. So 4 is the length of a systole. Let $\gamma_1, \ldots, \gamma_n$ be the

generators of $H_1(G;\mathbb{Z})$ given by the marking of G. Then $\gamma_1, \ldots, \gamma_{n-1}$ are systoles. By Lemma 4.1.1, these systoles pairwise intersect in finite sets of points.

Let S_i denote the set of edges for which both γ_i and γ_n have nonzero coefficients. The previous paragraph implies the S_i are disjoint. Write $\gamma_n = \sum_{e \in E(G)} c_e e$, $c_e \in \mathbb{Z}$. Then

$$\sum_{e \in S_i} c_e^2 l(e) \geq \gamma_i \cdot \gamma_n = 2.$$

Since the S_i are disjoint, $\gamma_n \cdot \gamma_n \geq 2(n-1) > n$. Contradiction. □

The notion of systoles and the matrix M_n will reappear in Section 5.1.

4.2 Voronoi Cells, Vonorms, Conorms

Building on the work of Voronoi, Selling, Stogrin, and Delone, Conway discusses a method of classifying positive definite quadratic forms in terms of the shapes of their *Voronoi cells*[10]. This classification and its relation to the Schottky Problem are discussed in this section and the next.

Voronoi Cells An n-ary positive definite quadratic form q induces a metric on $\mathbb{R}^n$: $d(v,w) = q(v-w)^{1/2}$. Given an integer lattice vector $a \in \mathbb{Z}^n$, its *Vornoi cell* with respect to q is the set of points (nonstrictly) closer to it than to any other integer lattice vector:

$$\{v \in \mathbb{R}^n : q(v-a) \leq q(v-b) \forall b \in \mathbb{Z}^n\}. \tag{4.1}$$

The Voronoi cells of q are translates of each other, and give a tessellation of $\mathbb{Z}^n$. Note: studying arbitrary positive definite quadratic forms on a fixed lattice

$\mathbb{Z}^n$ is isomorphic to studying a fixed quadratic form (say, corresponding to the standard inner product) on an arbitrary lattice in $\mathbb{R}^n$, so one often speaks of the Voronoi cells of a lattice.

For example, the Voronoi cells for the quadratic form x^2+y^2 (which corresponds to the standard inner product on $\mathbb{R}^2$) are squares of sidelength one centered about the integer lattice points. "Most" quadratic forms on $\mathbb{R}^2$ (i.e., those for which $\mathbb{Z}^2$ does not have an orthogonal basis) have hexagonal Voronoi cells instead. Conway uses *vonorms* and *conorms* to study the shape of Voronoi cells as combinatorial (e.g., rectangle vs. hexagon if $n = 2$) and metric objects. When the quadratic form is given as the Jacobian of a point in Outer space, it will be shown that these invariants can be read from the (metric) graph.

Note: The appearance of the lattice $2L$ in the following definition comes from a theorem of Voronoi – when defining the Voronoi cell about $0 \in L$, it suffices to include only those inequalities (4.1) for which b is minimal in its $2L$-coset[10].

Vonorms, Characters, and Conorms ([10]) Given a quadratic form q on a lattice L, the vectors in L that achieve the minimal norm on their $2L$-coset are called *Voroni vectors*. This minimal norm is called a *Vornoi norm* or *vonorm* of q. The function vo : $L/2L \to \mathbb{R}$ sending a coset to its vonorm is called the vonorm function. Note that vo$(0) = 0$. The remaining $2^n - 1$ vonorms are called *proper vonorms*.

A *character* on a lattice L is a group homomorphism $\chi : L \to \{\pm 1\}$. A character is *proper* if it is not the trivial (constant) group homomorphism.

A *conorm* (conjugate norm) is a character-weighted sum of vonorms. If χ is

a proper character, define

$$\mathrm{co}(\chi) = -\frac{1}{2^{n-1}} \sum_{\gamma \in L/2L} \chi(\gamma)\mathrm{vo}(\gamma).$$

Suppose now that $q = J(G, \rho)$, which is an inner product on $H_1(R_n, \mathbb{R})$ with integer lattice $H_1(R_n, \mathbb{Z})$. It is the pullback under ρ^* of the inner product $\cdot_G$ on $H_1(G, \mathbb{R})$ with lattice $H_1(G, \mathbb{Z})$. Therefore vo can be viewed as a function vo : $H_1(G, \mathbb{Z})/2H_1(G, \mathbb{Z}) \to \mathbb{R}$. The domain here is $H_1(G, \mathbb{Z}) \otimes \mathbb{Z}/2\mathbb{Z} = H_1(G; \mathbb{Z}/2\mathbb{Z}) = Z_1(G; \mathbb{Z}/2\mathbb{Z})$. This vonorm function on a graph admits a simple description:

Proposition 4.2.1 (Vonorm Function on a Graph)**.** *Let $\gamma \in Z_1(G; \mathbb{Z}/2\mathbb{Z})$. Write $e \in \gamma$ to mean the edge e has nonzero coefficient in γ. The vonorm function vo : $H_1(G; \mathbb{Z}/2\mathbb{Z}) \to \mathbb{R}$ is then given by:*

$$vo(\gamma) = \sum_{e \in \gamma} l(e).$$

Proof. This follows by essentially the same proof as for Lemma 3.3.4: the subgraph of G spanned by the edges with nonzero coefficients can be written as a union of cycles (in the terminology of Chapter 3), intersecting only in vertices. Arbitrarily orienting these cycles gives an element $\gamma \in H_1(G; \mathbb{Z})$ of the desired norm. γ has minimal norm on its $2H_1(G; \mathbb{Z})$-coset, since any other coset representative necessarily traverses each of the edges of γ at least once. □

Similarly, the conorms of G admit a nice description. Recall that graphs are not allowed to contain separating edges. The following proposition would still hold with separating edges, except that these edges would not contribute to any conorms.

Proposition 4.2.2. *Each nonzero conorm of $J(G)$ is a sum of edge lengths of G. Each edge e contributes to precisely one conorm: χ_e. Thus*

$$co(\chi) = \sum_{\{e:\chi=\chi_e\}} l(e).$$

Moreover, the following are equivalent for edges e, e' of G:

(i) $\chi_e = \chi_{e'}$.

(ii) Every cycle containing e contains e'.

(iii) The union of the interiors of e and e' disconnects G.

This proposition bears a striking resemblance to ([8] Lemma 2.3.2), though the latter does not involve conorms.

Proof. Given a nonseparating edge e in G, choose a maximal tree T *not* containing it. This tree gives a basis $v_1, \ldots v_n$ for $H_1(G; \mathbb{Z}/2\mathbb{Z})$. Reorder the basis if necessary so that $e \in v_1, e \notin v_i, i > 1$. The contribution from e in co(χ) is:

$$-\frac{1}{2^{n-1}} \sum_{\epsilon_2,\ldots,\epsilon_n \in \{0,1\}} \chi(v_1 + \epsilon_2 v_2 + \ldots + \epsilon_n v_n) l(e)$$

$$= -\frac{l(e)}{2^{n-1}} \chi(v_1) \sum_{\epsilon_2 \in \{0,1\}} \chi(v_2)^{\epsilon_2} \cdots \sum_{\epsilon_n \in \{0,1\}} \chi(v_n)^{\epsilon_n}.$$

If $\chi(v_i) = -1$ for some $2 \leq i \leq n$, then $\sum_{\epsilon_i \in \{0,1\}} \chi(v_i)^{\epsilon_i} = (-1)^0 + (-1)^1 = 0$, and the whole contribution from e vanishes. The only nontrivial character to whose conorm e contributes is thus the character χ_e. Now, $\chi_e(v_1) = -1, \chi_e(v_i) = 1$, $i \leq 2 \leq n$. Here each $\sum_{\epsilon_i \in \{0,1\}} \chi_e(v_i)^{\epsilon_i} = 1^0 + 1^1 = 2$, and so the contribution of e is

$$-\frac{l(e)}{2^{n-1}} \chi_e(v_1) \sum_{\epsilon_2 \in \{0,1\}} \chi_e(v_2)^{\epsilon_2} \cdots \sum_{\epsilon_n \in \{0,1\}} \chi_e(v_n)^{\epsilon_n} = -\frac{l(e)}{2^{n-1}} \cdot (-1) \cdot 2^{n-1} = l(e).$$

Now, (i) implies (ii) by the definition of χ_e. (ii) implies (iii) since otherwise there would be a path in $G \setminus e \cup e'$ joining the endpoints of e, which gives rise to a cycle in G containing e but not e'. Finally, (iii) implies both (ii) and its converse, which together imply (i). □

For $n \geq 4$, there are elements of Y_n with some conorms negative. The above proposition, however, shows

Corollary 4.2.3. *For any graph G of any rank, the conorms of $J(G)$ are all nonnegative.*

Since a graph G of rank n has at most $3n-3$ edges (realized precisely in the trivalent case), there are at least $2^n - 1 - (3n-3) = 2^n - 3n + 2$ conorms equal to zero. When $n = 3$, therefore, $J(G)$ has at least one conorm equal to zero. Since J is surjective for $n = 3$ (Corollary 3.3.7), this verifies the fact that every ternary quadratic form has a zero conorm, which Conway shows using superbases in [10]. When $n = 4$, there are at least 6 conorms equal to zero.

The situation is particularly nice when G (or more precisely, $H_1(G;\mathbb{Z})$) has an *obtuse superbase*.

Obtuse Superbase ([10]) A *superbase* for a lattice L is a tuple $(e_1, \ldots, e_n, e_{n+1})$ such that $\{e_1, \ldots, e_n\}$ is a basis and $e_1 + \cdots + e_{n+1} = 0$. A superbase is *obtuse* if $e_i \cdot e_j \leq 0$ for all $1 \leq i, j \leq n+1, i \neq j$.

Lemma 4.2.4. *If G is a planar graph, then $J(G)$ has an obtuse superbase.*

Proof. Embed the graph in an oriented sphere S^2. Take for a superbase the boundaries of the connected components of $S^2 \setminus G$, oriented compatibly with the sphere. □

The Selling parameters of a superbase $(v_1, \ldots, v_{n+1})$ are the numbers $p_{ij} := -v_i \cdot v_j$, $i \neq j$. The positive Selling parameters of the obtuse superbase given by embedding a graph in the sphere are the sums of the edgelengths between adjacent regions on the sphere. Proposition 4.2.2 shows that the nonzero Selling parameters are therefore the same as the nonzero conorms, so that the multiset of conorms is the multiset of Selling parameters padded by zeros. Conway shows that this relationship between Selling parameters and conorms holds for any lattice with an obtuse superbase, not just those of the form $J(G)$ ([10] pp.70-71). Indeed, his proof shows:

Proposition 4.2.5 (Selling parameters (Conway))**.** *Suppose $v_0, v_1, \ldots, v_n$ is an obtuse superbase. Let χ_i denote the character $\chi_i(v_j) = -\delta_{ij}$, $i, j > 0$ (the Kronecker δ_{ij}). Let χ_0 denote the character $\chi_0(v_j) = -1$ for $j > 0$. Then co$(\chi_i) = 0$ and co$(\chi_i\chi_j) = p_{ij}$ for all i, j. All other characters have conorm 0.*

4.3 The Case $n = 4$

Conway gives a complete classification of the shapes of the Voronoi cells for $n \leq 4$ in [10]. For n = 2 there are two combinatorial shapes the Voronoi cells may take: hexagon or rectangle. For n = 3 there are five shapes. For n = 4, there are 52 shapes (found by Delaunay[13] and corrected by Stogrin[32]). Conway classifies them in terms of vonorms and conorms. His list itself is corrected by Vallentin([34], p.60). The goal of this section is to explain that the image of J consists of precisely those quadratic forms for which the shape is one of 16 particular varieties.

Conway describes 17 "graphical cases" for Voronoi cell shape, each corre-

sponding to a different graph (see below). The remaining 35 Voronoi cell shapes represent lattices with negative conorms, so no such lattices are in the image of J. Conway parametrizes 16 of his "graphical cases" by subgraphs of K_5, the complete graph on 5 vertices. The vertices represent 5 nontrivial characters, each having conorm 0, that multiply to the trivial character. There is an edge connecting two such vertices if and only if the product of their characters has nonzero conorm.

Given a planar rank 4 graph G, Proposition 4.2.5 says that the obtuse superbase v_0, v_1, v_2, v_3, v_4 coming from the embedding of G in S^2 yields 5 such nontrivial characters $\chi_0, \chi_1, \chi_2, \chi_3, \chi_4$ multiplying to the trivial character, and that $\mathrm{co}(\chi_i\chi_j) = p_{ij}$. By Proposition 4.2.2, $J(G)$ fits the Voronoi graphical case whose graph parameter is a certain subgraph of K_5: the vertices correspond to faces of G embedded in S^2 and the edges correspond to adjacent faces (faces sharing at least one edge). Given any planar graph G realizing such a Voronoi graphical case, modifying the edge lengths of G can produce any other Voronoi cell shape with the same underlying combinatorial shape.

There are four trivalent rank 4 planar graphs (shown as the first graphs in the right-hand column of rows 1,2,4,7 of Table 4.1), and from these the lemma below assists in finding the planar rank 4 graphs. These are shown in the right-hand columns of Tables 4.1 and 4.2. The corresponding Conway parameter graphs are shown in the left columns. 15 of Conway's 16 "graphical cases" are realized in this way, all except K_5.

Lemma 4.3.1. *Every planar graph can be obtained from a planar trivalent graph by collapsing a sequence of edges. [Remember:* graphs *have no separating edges.]*

Proof. Suppose a vertex p in a planar graph G has valence at least 4. Let e be a

half-edge incident to p. Since the edge containing e does not separate G, there is another half-edge e' incident to p lying in the same connected component of $G \backslash p$ as e. Since p has valence at least 4, the incident half-edges can be partitioned into two sets S_1, S_2 each of cardinality at least 2, each set consisting of cyclicly consecutive half-edges under the adjacency relation given by the embedding of G in the plane. Then p can be replaced by a new edge f whose vertices v_1, v_2 are also incident to the half-edges of S_1 and S_2, respectively. f is not a separating edge since e and e' are in the same component. The other edges remain non-separating, and the resulting graph remains planar. The result follows by induction. □

By Kuratowksi's Theorem, the only nonplanar rank 4 graph is the complete bipartite graph $K_{3,3}$. Its Jacobian $J(K_{3,3})$ yields Conway's 17th graphical type, which he also calls $K_{3,3}$.

In summary:

Proposition 4.3.2. *A quadratic form $q \in Y_4$ is in the image of $J : X_4 \to Y_4$ if and only if its Voronoi cell has shape one of Conway's graphical cases, except K_5.*

Note: Vallentin ([34]) calls Conway's "graphical cases" *zonotopal* and breaks them into two overlapping categories: *graphical* (Jacobians of graphs, though he does not use this terminology) and *cographical*. The cographical lattices are dual to graphical lattices. In Vallentin's terminology, the combinatorial Voronoi cell shapes parametrized by subgraphs of K_5 are actually cographical lattices on their parametrizing graph, while $K_{3,3}$ is instead the graphical lattice on $K_{3,3}$[34]. This explains why all the 16 graphical cases parametrized by subgraphs of K_5 were dual to planar graphs except for K_5 itself.

Table 4.1: Conway's Graphical Lattices

Name	Positive Conorms	Graphs with Indicated Positive Conorms
$K_5 - 1$	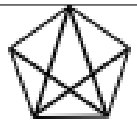	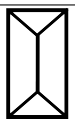
$K_5 - 2$		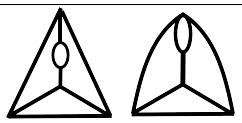
$K_5 - 1 - 1$	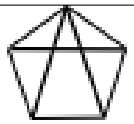	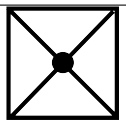
$K_5 - 3$	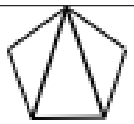	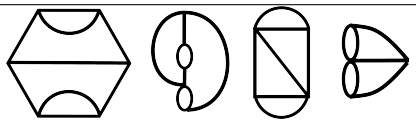
$K_5 - 2 - 1$		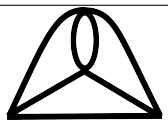
$K_4 + 1$		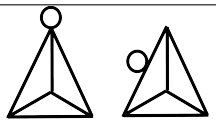
C_{2221}		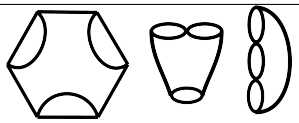
$C_{221} + 1$		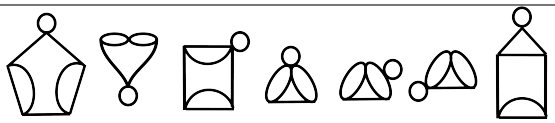
C_{321}	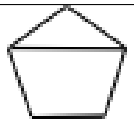	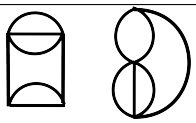
C_{222}		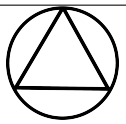

Table 4.2: Conway's Graphical Lattices (Continued)

Name	Positive Conorms	Graphs with Indicated Positive Conorms
$C_3 + C_3$	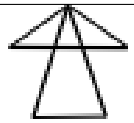	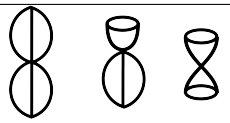
C_5	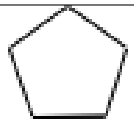	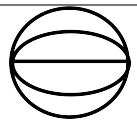
$C_4 + 1$	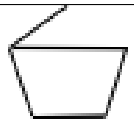	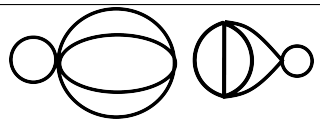
$C_3 + 1 + 1$	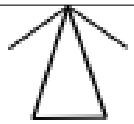	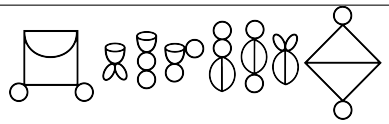
$1 + 1 + 1 + 1$	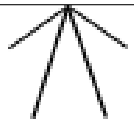	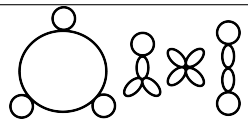

4.4 Higher Rank

After the author determined how rank 4 graph Jacobians fit into Conway's classification, he learned that Vallentin has developed a much more general theory translating between lattices with *zonotopal* Voronoi cells and *regular oriented matroids*[34]. This allowed Vallentin to cast Tutte's excluded minor characterizations of graphical matroids ([33]) in terms of lattices. In this section, the author will point out that Vallentin's results give an answer to the Schottky problem in higher rank.

Zonotopal Lattices (Vallentin, [34]) The *support* of a vector v in $\mathbb{Z}^n$ is the set of standard basis vectors with nonzero coefficient in v. An *elementary vector* of a subgroup L of $\mathbb{Z}^n$ is a vector $v \in L \cap \{1, 0, -1\}^n$ with minimal (nonempty)

support. Two vectors are *conformal* if they lie in the same closed orthant. A *zonotopal lattice* in $\mathbb{R}^d$ is a subgroup $L \subseteq \mathbb{Z}^d$ such that every element of L is a form of pairwise conformal elementary vectors. $\mathbb{R}^d$ is equipped with an inner product making the standard basis orthogonal, but not necessarily orthonormal.

Some notational caution for this section: A graphical lattice is a lattice in the image of the Jacobian map – graphical in the sense of Vallentin, a narrower sense than Conway's. *Circuit* in the sense of matroid theory corresponds to the more restricted notion of cycle of Chapter 3.

The argument of Lemma 3.3.4 shows:

Proposition 4.4.1 (Vallentin, [34] p.43)**.** *Graphical lattices are zonotopal.*

A zonotopal lattice is essentially the same object as a *regular oriented matroid*. A matroid specifies which subsets of a ground set E, or equivalently which vectors in $\{0,1\}^E$, are independent sets, bases, circuits, etc. Matroids are notorious for having many equivalent definitions – each special class of subset has its own axiomatization. Likewise, an *oriented matroid* over E specifies which vectors in $\{-1,0,1\}^E$ have various dependence properties. One such axiomatization is that the *circuits* $\mathcal{C} \subset \{-1,0,1\}^E$ satisfy the axioms[5]:

- $0^E \notin \mathcal{C}$;
- $C \in \mathcal{C}$ implies $-C \in \mathcal{C}$;
- If $C, D \in \mathcal{C}$ and the support of C is contained in that of D, then $C = \pm D$;
- If $C, D \in \mathcal{C}$ and $C \neq -D$ and C, D have opposite signs in coordinate e, then there exists $Z \in \mathcal{C}$ with support excluding e such that each nonzero coordinate of Z matches the corresponding coordinate of C or D.

The elementary vectors of a zonotopal lattice in $\mathbb{R}^d$ satisfy these axioms (for the last axiom, take Z to be any vector from a pairwise conformal set of elementary vectors summing to $C + D$). Let $\mathcal{M}(L)$ denote the oriented matroid corresponding to L. The supports of the vectors in $\mathcal{C}$ are the circuits of a matroid over E, called the underlying matroid of $\mathcal{M}(L)$.

Vallentin points out that a set of vectors in $\{-1, 0, 1\}^E$ is the set of elementary vectors of a zonotopal lattice precisely if they form the circuits of a *regular* oriented matroid ([34], p.40). (Recall that a matroid is regular if it is representable over a totally unimodular matrix: its circuits are the minimal sets of dependent column vectors in such a matrix. For the case of oriented matroids, this is equivalent to being representable over a matrix with entries in $\mathbb{Z}/2\mathbb{Z}$[26].)

Tutte showed that a regular matroid is graphic – its circuits are the cycles of some graph – precisely if it has no minor isomorphic to the dual of graphic matroids corresponding to the graphs $K_{3,3}$ or K_5. The matroid notions of duals and minors extend to regular oriented matroids, or equivalently to zonotopal lattices. The dual L^* of a zonotopal lattice $L \subseteq \mathbb{Z}^n$ is the lattice of vectors in $\mathbb{Z}^n$ orthogonal to all those in L, orthogonality given by the standard inner product on $\mathbb{Z}^n$. The deletion $L \setminus S$ of a set $S \subset E$ from L is the image of the projection of L to $\mathbb{R}^{E-S}$. The contraction L/S is the image of the projection to $\mathbb{R}^{E-S}$ of the vectors in L with supports disjoint from S. A minor of a matroid or lattice is the result of performing a sequence of deletions and contractions[34].

Theorem 4.4.2 (Tutte[33],Vallentin[34])**.** *A zonotopal lattice $L \subseteq \mathbb{Z}^E$ is of the form $L = H_1(G; \mathbb{Z}) \subseteq \mathbb{Z}^E$ for some graph G with edge set E if and only if L has no minor that is combinatorially isomorphic to the lattice $H_1(K_5; \mathbb{Z})^*$ or $H_1(K_{3,3})^*$.*

Corollary 4.4.3. *A positive definite quadratic form is in the image of J if and only if*

its corresponding lattice is equivalent to a zonotopal lattice containing no $J(K_5)^*$ or $J(K_{3,3})^*$ minor.

CHAPTER 5

AN EILENBERG-MACLANE SPACE FOR IO_3

As mentioned in the previous chapter, Soulé showed that the symmetric space Y_3 deformation retracts onto an invariant subspace, the well-rounded retract Z_3. In this chapter, $J^{-1}(Z_3)$ is shown to be an invariant deformation retract of X_3, so that $K = J^{-1}(Z_3)/\mathrm{IO}_3$ is an Eilenberg-MacLane space for IO_3. Then the CW-structure K inherits from the fiber calculation of section 3.3 is described.

5.1 The Well-Rounded Retract and its Preimage

The well-rounded retract consists of inner products generated by *systoles*.

Systoles A *systole* of a positive definite quadratic form q is a nonzero vector $v \in \mathbb{Z}^n$ for which $q(n)$ is minimal. A *systole* of a graph G is a nonzero element $\gamma \in H_1(G, \mathbb{Z})$ minimizing $\gamma \cdot_G \gamma$. Such a systole is represented by a cycle in G, also called a *systole*.

It is easy to see that three linearly independent systoles for a quadratic form $q \in Y_3$ form a basis for $\mathbb{Z}^3$. (For instance, the proof of 3.3.6 shows that cycles representing the systoles in 3.3.5 form a basis for $H_1(G_M, \mathbb{Z})$, where M is a Minkowski-reduced matrix in the $\mathrm{GL}_3(\mathbb{Z})$-orbit of q.) An example of a quadratic n-ary form with n independent systoles, $n \geq 5$, but no basis consisting of systoles is given by Pettet and Souto[27]. In fact, their example is the matrix M_n of Lemma 4.1.1.

Well-Rounded Retract[30] $Z_3 \subset Y_3$ is the subspace of quadratic forms generated by their systoles. Equivalently, this *well-rounded retract* is the space $D \cdot \mathrm{GL}_3(\mathbb{Z}) \subset Y_3$ where D is the subspace of Minkowski-reduced diagonal matrices.

Soulé constructed his (strong) deformation retract in two stages. Let Z_i, $1 \leq i \leq 3$ denote the subspace of Y_3 consisting of quadratic forms that have bases containing at least i systoles. So $Z_1 = Y_3$ and Z_3 agrees with the previous notation. The deformation proceeds from Z_1 to Z_2, and then to Z_3.

Theorem 5.1.1. *There is a (strong) equivariant deformation retraction from rank 3 Outer space X_3 to the Out(F_3)-invariant subspace $J^{-1}(Z_3)$. It is obtained as a deformation retraction A_1 from $X_3 = J^{-1}(Z_1)$ to $J^{-1}(Z_2)$ followed by a deformation retraction A_2 from $J^{-1}(Z_2)$ to $J^{-1}(Z_3)$.*

Proof. To describe the deformation $A_i : J^{-1}(Z_i) \times [0,1] \to J^{-1}(Z_{i+1})$, both a graph and a marking comprising $A_i((G,\rho),t)$ must be specified. This graph will always be combinatorially either G or a collapse of G, but with a modified metric. The marking will always be either ρ or the marking $\overline{\rho}$ induced by a collapse, so notation can be simplified by disregarding the marking. As a consequence, Out(F_3)-equivariance of A_i is automatic and continuity of A_i will follow immediately from the construction.

Suppose $G \in J^{-1}(Z_i)$, $i \in \{1,2\}$. Let $\mathcal{A}(G)$ denote the set of systoles in G, viewed as cycles (and thereby as 1-subcomplexes). If $G \in J^{-1}(Z_{i+1})$, let $A_i(G,t) = G$ (with the same metric) for all $t \in [0,1]$. Otherwise, shrink the complement of the subcomplex $\cup\mathcal{A}(G)$ at a constant rate until a graph in $J^{-1}(Z_{i+1})$ is obtained.

Formally, define G_λ ($\lambda \geq 0$) to be the metric graph obtained from G by changing the edgelength of $e \in G$ to

$$l_{G_\lambda}(e) := \begin{cases} l_G(e) & \text{if } e \in \cup\mathcal{A}(G) \\ \lambda l_G(e) & \text{if } e \notin \cup\mathcal{A}(G) \end{cases}$$

Any edge assigned a length of zero in G_λ is understood to have been collapsed.

Claim: for $G \in J^{-1}(Z_i)$ ($i \in \{1,2\}$), the set $S_{G,i} := \{s \in [0,1] : G_s \in J^{-1}(Z_{i+1})\}$ is nonempty. The theorem follows from the claim, using the retraction $A_i(G,t) = G_{1-t+t\lambda(G,i)}$ where

$$\lambda(G,i) = \sup\{s \in [0,1] : G_s \in J^{-1}(Z_{i+1})\}.$$

(It is also necessary to show that $A_i(G,1)$ is a rank 3 graph.)

It remains only to establish the claim for $i \in \{1,2\}$. First, consider the case $i = 1$. If $G \in J^{-1}(Z_2)$, then $1 \in S_{G,1}$. Otherwise, if $\alpha^{\pm 1}$ is the unique systole in G, then every other cycle in G gets length strictly less than $l(\alpha)$ in G_0. By continuity of the length of a fixed cycles under $s \mapsto G_s$, $S_{G,1} \neq \emptyset$. In fact, $A_1(G,1)$ has no collapsed edge.

Next, consider the case $i = 2$. Suppose $G \in J^{-1}(Z_2)$. As usual, it suffices to consider the five graph collapses of the tetrahedral graph ☮ in turn. Let α denote a systole.

- For the 3-rose, the claim is immediate, and $A_2(G,1)$ is also a 3-rose.
- For the theta graph with a loop added at a vertex, assume (in the harder case) the systoles consist of the loop and a 2-cycle in the theta graph. The remaining edge together with a minimal length edge of the theta graph

forms a 2-cycle whose length in G_0 is at most $l(\alpha)/2$. No edge is collapsed in $A_2(G, 1)$.

- The same reasoning works in the case of a 4-cage, unless there are two systoles with disjoint edge sets. But then all edges have the same length and $G \in J^{-1}(Z_3)$.
- Consider the case where G is $\clubsuit$ with an edge collapsed. If $\cup\mathcal{A}(G) = G$, then $G \in J^{-1}(Z_3)$. (Indeed, as in the proof of 3.3.3 two 3-cycles overlapping in a single edge cannot both be systoles.) If $e \in G \setminus \cup\mathcal{A}(G)$ is an edge connecting a valence 3 to the valence 4 vertex, then the 2-cycle formed by it and the other edge connecting the same vertices has length in G_0 stricly smaller than $l(\alpha)$. Alternatively, if e connects the two valence 3 vertices then a minimal length 3-cycle in G involving e gets length at most $l(\alpha)$ in G_0. Collapsing e results in a rank 3 graph: the 4-cage.
- Lastly, suppose $G = \clubsuit$. If $\cup\mathcal{A}(G) = G$, then $G \in J^{-1}(Z_3)$. (Indeed, as in the proof of 3.3.3 two independent 4-cycles cannot both be systoles.) If $G \notin J^{-1}(Z_3)$, let e be the edge not contained in any systole. Then e is contained in two 3-cycles of G. The average length of these two in G_0 is $l(\alpha)/2$ if G contains a systolic 4-cycle, and is strictly less than $l(\alpha)$ if G contains two independent systolic 3-cycles. In either case, $A_2(G, 1)$ has no collapsed edge.

□

Remark Ash constructed a well-rounded retract of the symmetric space for general n and an explicit deformation retraction to it[2]. In the case $n = 3$, his example and even the deformation retraction coincides precisely with Soulé's.

The deformation retraction of the preceding example can be used to recover the result that Y_3 deformation retracts onto Z_3, albeit using a different deformation retraction.

Theorem 5.1.2 (Soulé, [30]). *Y_3 deformation retracts onto Z_3.*

Proof. Define deformation retractions $\overline{A}_i : Z_i \times [0,1] \to Z_{i+1}$, for $i = 1, 2$, as follows. Given an element of Z_i, write it as $L \cdot g$ with L Minkowski reduced and $g \in \mathrm{GL}_3(\mathbb{Z})$. Define $\overline{A}_i(L \cdot g, t) = J(A_i(G_L \cdot \pm g, t))$. Although the marked graph $G_L \cdot g$ is only determined by the matrix $L \cdot g$ up to right-multiplication by $\pm I$, the equivariance of the construction of A_i (and the fact that $-I$ sends each fiber to itself) makes $\overline{A}_i$ well-defined. □

Remark The definition of the deformation A_i does not carry over to give a well-defined deformation in higher rank. For example, the rank 4 graph G consisting of three vertices each pair of which are joined by two edges assigned a length of unity has three independent systoles (the 2-cycles) whose union is the whole graph G. So $G_\lambda = G$ for all $\lambda \in [0,1]$, and the construction of Theorem 5.1.1 fails to produce a graph with a new systole.

Corollary 5.1.3. *The subspace $K := J^{-1}(Z_3)/IO_3 \subset X_3/IO_3$ is an Eilenberg-MacLane space for IO_3.*

Proof. $J^{-1}(Z_3)$ is contractible since it is a deformation retract of X_3, which is contractible[11]. Baumslag and Taylor showed IO_3 is torsion-free([3], [23] p.26). The stabilizer of a marked graph in Outer space is isomorphic to the group of isometries of the graph, and is therefore finite. Therefore the action of IO_3 on $J^{-1}(Z_3)$ is free and properly discontinuous. $J^{-1}(Z_3) \to K$ is thus a covering space and K is a $K(\mathrm{IO}_3, 1)$.(see e.g. [16]). □

5.2 K as a CW-complex

Soulé gave a simplicial structure to his well-rounded retract[30]. This section describes a CW-structure induced on K by Soulé's simplicial structure together with the fiber computation of Theorem 3.3.2.

Let $D \subset Y_3$ denote the subset of the symmetric space represented by Minkowski-reduced matrices. So $Z_3 = D \cdot \mathrm{GL}_3(\mathbb{Z})$. Any matrix in D has all of its diagonal entries equal. Soulé normalized this equal value to be 2, and wrote

$$h(x_1, x_2, x_3) := \begin{pmatrix} 2 & x_3 & x_2 \\ x_3 & 2 & x_1 \\ x_2 & x_1 & 2 \end{pmatrix},$$

thereby identifying D with the "truncated cube" (see Figure 5.1)

$$\{(x_1, x_2, x_3) \in \mathbb{R}^3 : h(x_1, x_2, x_3) \in D\}.$$

By the inequalities (3.1)-(3.3), D is the subset of $[-1, 1]^3$ satisfying

$$\max\{-x_1 + x_2 + x_3, x_1 - x_2 + x_3, x_1 + x_2 - x_3, -x_1 - x_2 - x_3\} \leq 2.$$

Soulé named certain points of D and computed their stabilizers. These points are shown in Figure 5.1.

Special Points, [30] $O = h(0, 0, 0)$. $Q = h(1, 0, 0)$. $M = h(1, 1, 1)$.
$N = h(1, 1, 1/2)$. $M' = h(1, 1, 0)$. $N' = h(1, 1/2, -1/2)$. $P = h(2/3, 2/3, -2/3)$.

Soulé showed that D is a union of 24 copies of a fundamental domain for the $\mathrm{GL}_3(\mathbb{Z})$ action on Z_3, 24 being the cardinality of the signed symmetric group (the

stabilizer of O consisting of the matrices in $\mathrm{GL}_3(\mathbb{Z})$ with a single nonzero entry in each row and each column.) In the sequel, D will be called *Soulé's domain*.

Corners, Hexagons, Boundary, Radii, Cones A *hexagon* in D is one of the six hexagonal faces of the truncated cube. An edge of a hexagon is a *hexagonal edge* A *truncated face* in D is one of the four remaining triangular faces of the truncated cube. The *corners* of D are the points of D in the $\mathrm{GL}_3(\mathbb{Z})$-orbit of M. A *radius* of a hexagon is a straight line segment joining the center of the hexagon (i.e. a point in the $\mathrm{GL}_3(\mathbb{Z})$-orbit of Q) to a corner of the hexagon. The *boundary* ∂D of D is the union of the six hexagons of D and the four truncated faces. In other words,

$$\partial D = D \cap \bigcup_{\substack{g \in \mathrm{GL}_3(\mathbb{Z}) \\ D \cdot g \neq D}} D \cdot g.$$

The *cone* on a subset $S \subseteq \partial D$ of the boundary is the set

$$CS := \{ts : t \in [0,1], s \in S\} \subseteq D.$$

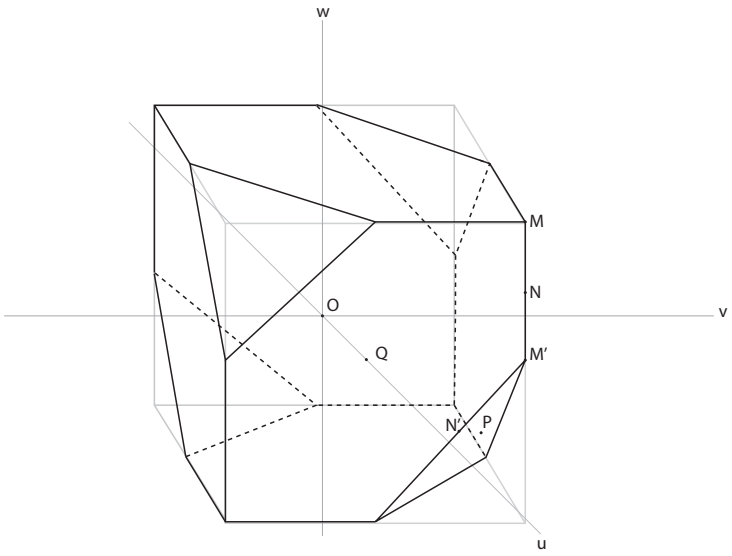

Figure 5.1: Soulé's Domain and Special Points

This same terminology (hexagons, cones, etc.) is used for the corresponding subsets of $\mathrm{GL}_3(\mathbb{Z})$-translates of D.

Thus the coordinate axes intersect D in the cones on the centers of pairs of opposite hexagons, and D is the convex hull of its corners.

In the present context, Theorem 3.3.2 becomes:

Proposition 5.2.1. *The fibers of J over the points of D are as follows:*

- *The fiber over O is a rose.*
- *The fibers over the remaining points on the coordinate axes are theta graphs.*
- *The fibers over the corners of D are single points, as are those of*

$$C\{(1,1,1),(1,-1,-1),(-1,1,-1),(-1,-1,1)\} \setminus O.$$

- *The remaining fibers over points in the cones of the radii of the hexagons are segments.*
- *All remaining fibers are pairs of points.*

The most interesting points of D are those with rose or theta graph fibers, since they form together to make "tubes" within K. Imagine a point E moving from Q to O along the positive x_1-axis of D. The fiber $J^{-1}(E)$ ($E \neq O$) can be identified with the theta subgraph of the graph G_E constructed in 3.3.3 (as in 3.3.2, a point of this theta graph corresponds to the graph obtained by adding a loop there). As E moves towards O, one of the edges of this subgraph shrinks until it collapses, while the other two grow into two petals of the rose $J^{-1}(O)$, forming a pair of "tubes" glued along a triangle (as in the bottom half of Figure

5.2(ii)). The fibers from two $\mathrm{GL}_3(\mathbb{Z})$-translates of D intersecting in a hexagon thus form *tubes* and *pinched tubes* in K joining the two rose fibers at the centers of the adjacent translates. These tubes (i) and pinched tubes (ii) are shown in Figure 5.2.

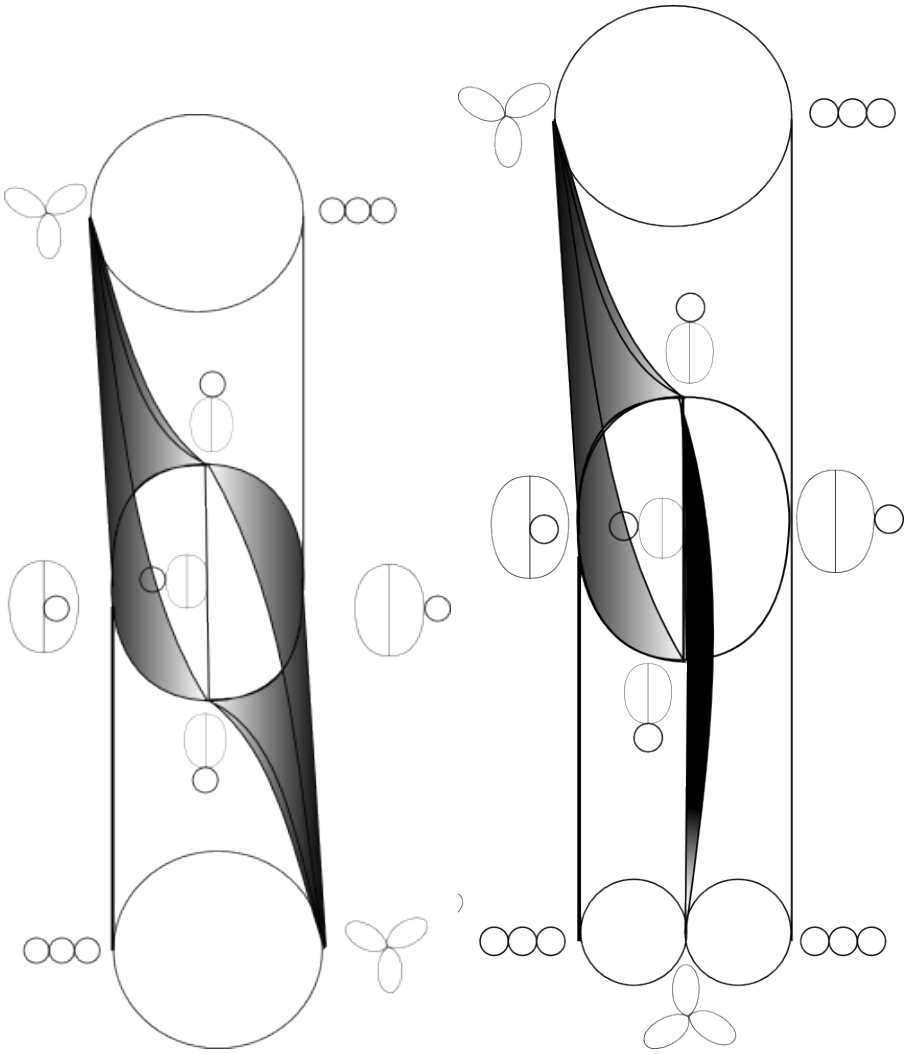

(i) Tube (ii) Pinched Tube

Figure 5.2: Tubes formed from Rose and Theta fibers

Subsets A and B Let $A \subset Z_3$ denote the subset of points with rose or theta graph fibers. B denotes the set of points whose fibers are roses, theta graphs,

segments, or single points. Denote their preimages in K by $\widetilde{A} = J^{-1}(A)$, $\widetilde{B} = J^{-1}(B)$.

It will be shown (Theorem 7.2.2) that every element of $H_*(\mathrm{IO}_3, \mathbb{Z})$ is represented by an element of $H_*(\widetilde{A}, \mathbb{Z})$ (i.e., that $H_*(\widetilde{A}, \mathbb{Z}) \to H_*(K, \mathbb{Z})$ is surjective.)

Adjacency Two hexagons are *adjacent* if they intersect. Two M-orbit vertices of D are *adjacent* if they lie on the same hexagonal edge (i.e., if some element of $\mathrm{GL}_3(\mathbb{Z})$ sends them to $\{M, M'\}$). An M-orbit vertex is *adjacent* to a Q-orbit vertex if they lie on the same radius (i.e., if some element of $\mathrm{GL}_3(\mathbb{Z})$ sends them to $\{M, Q\}$). Two O-orbit vertices (and by extension the D-orbits they are contained in) are adjacent if the corresponding D-orbits intersect in a hexagon.

Proposition 5.2.2. *K has a 3-dimensional CW-structure such that $\mathrm{GL}_3(\mathbb{Z})$ acts by cellular automorphisms. The fibers $J^{-1}(O)$, $J^{-1}(M)$, and $J^{-1}(Q)$ are subcomplexes, as is $J^{-1}(D)$, the preimage of Soulé's domain.*

Proof. $J^{-1}(D)$ consists of the following cells. The zero-cells are (G_O, ρ_O), (G_Q, ρ_Q), (G_M, ρ_M) and their $\mathrm{GL}_3(\mathbb{Z})$-translates within D. (Thus the 29 zero-cells are: the basepoint of the rose in the fiber of O; the 16 single point fibers of the translates of M; the two vertices each of the fibers of the 6 translates of Q.)

The 181 one-cells are: the three loops in the rose fiber of O; the three edges in the theta graph fibers of each of the 6 translates of Q; the two edges forming each of the preimages of the 24 hexagon edges; the two edges each lying over the 36 radii (swept by the two endpoints of the edge fibers); the pairs of edges swept by the vertices of theta graph fibers above the six coordinate half-axes (cones on hexagon centers); the preimages of the cones $C(1, 1, 1)$, $C(1, -1, -1)$,

$C(-1,1,-1)$, $C(-1,-1,1)$; and the pairs of edges above the cones of each of the remaining 24 M-orbit vertices swept by vertices of segment fibers.

The 266 two-cells are: one triangle comprising the preimage of each of the 36 radii; two quadrilaterals and one triangle comprising the preimage of each of the six coordinate half-axes as described in the paragraph following Proposition 5.2.1; one triangle each over 12 of the cones of corners (the cones whose fibers are intervals); two triangles over each of the 36 cones of radii (swept out by the endpoints of the interval fibers); four pairs of triangles over the truncated faces of the cube (i.e., convex hulls of pairwise adjacent triples of M-orbit points); two pairs of triangles over each of the 6 components of each hexagon minus its radii (accounting for 72 2-cells); and a pair of triangles over each of the cones of the 24 hexagonal edges.

The 116 three-cells are: simplices that are the preimages of 12 of the cones of radii (the ones involving $(1,1,1)$,$(1,-1,-1)$,$(-1,1,-1)$, and $(-1,-1,1)$); quadrilateral pyramids that are the preimages of the remaining 24 radii; two simplices each comprising the preimages for the cones on each of the 6 components of each hexagon upon deleting the radii (72 3-cells); and two simplices comprising the preimages of each of the cones on the four truncated faces. □

The Euler characteristic of $J^{-1}(D)$ is $\chi(J^{-1}(D)) = 29 - 181 + 266 - 116 = -2 = \chi(J^{-1}(O))$. Indeed,

Corollary 5.2.3. *$J^{-1}(D)$ deformation retracts onto the rose fiber $J^{-1}(O)$.*

Proof. All 3-cells have free faces contained in $J^{-1}(\partial D)$. Collapsing them yields a cell complex without 3-cells and with no 2-cells in $J^{-1}(\partial D)$. Every 1-cell in $J^{-1}(\partial D)$ is a free face of a 2-cell in the resulting complex; collapse these. Do the

same with all 0-cells in $J^{-1}(\partial D)$ that are free faces of 1-cells. All that remains is the preimage of the cone of 12 of the corners. The cone of each of these corners has preimage a "triangle" with base a petal of $J^{-1}(O)$. Collapsing these "triangles" to their bases completes the deformation retraction to the rose. $\square$

CHAPTER 6

$H_1(\mathbf{IO}_3)$

Magnus found a generating set for IA_n[24]. Andreadakis showed using purely algebraic methods that $H_1(\mathrm{IA}_n, \mathbb{Z})$ is free abelian of rank $n^2(n-1)/2$, with the Magnus generators as basis[1]. Kawazumi recovered this result and also showed $H_1(\mathrm{IO}_n, \mathbb{Z})$ is free abelian of rank $(n+1)n(n-2)/2$ by studying the Johnson homomorphism[20]. In this chapter, the result $H_1(\mathrm{IO}_3, \mathbb{Z}) = \mathbb{Z}^6$ is recovered using a topological approach: by computing $H_1(K, \mathbb{Z})$.

6.1 Roseboxes and their Ordering

Bestvina-Bux-Margalit defined an ordering on roses in the quotient of the spine of Outer space by IA_n, a subspace of X_n/IA_n[4]. The same idea can be used to order the set of rose fibers in $K \subset X_3/\mathrm{IA}_3$, so that K may be viewed as being built up inductively from preimages of Soulé domains.

Labeling a Homology-Marked Graph ([4]) A homology-marked graph (G, ρ) is represented by G with oriented-edge labels. The edge e is labelled by a row vector, an element of $\mathbb{Z}^n$, $n = \text{rk } (G)$. The ith coordinate of the label is the coefficient of the oriented edge in $\rho(x_i)$.

The labeling on $(G, \rho) \cdot A$ is obtained from that of (G, ρ) by right multiplying each label by A.

Corollary 5.2.3 motivates the definition:

Rosebox Let $\widetilde{D} = J^{-1}(D)$. A *rosebox* is any $\mathrm{GL}_3(\mathbb{Z})$-translate of $\widetilde{D}$ in K. Identify a rosebox with its rose fiber and thereby with a coset of $\mathrm{Stab}(O)$ in $GL_3(\mathbb{Z})$ via $\widetilde{D} \cdot A \leftrightarrow \mathrm{Stab}(O)A$. (In order to alleviate any potential confusion between the positive definite symmetric matrix ${}^TA(2I)A \in Y_3$ and the coset representative A, the former is written using round brackets and the coset class using square brackets.)

In other words, the $\mathrm{Stab}(O)$-coset corresponding to a rosebox is represented by any matrix whose row vectors are the labels in any homology-marked graph in its rose fiber (with any orientation). The first homology of a rosebox is generated by the three petals of its rose fiber. (Compare with the proof of Theorem 3.3.2.) These closed paths deserve names:

Rosebox Homology Generators $[v_1|v_2|v_3]$ denotes the closed path in the rose fiber of the rosebox $\begin{bmatrix} v_1 \\ v_2 \\ v_3 \end{bmatrix}$ obtained by rotating the (basepoint of the) loop labeled v_2 around the loop labeled v_1 (in the direction of its orientation), parameterized proportional to arclength. (Note: $[v_1|v_2|v_3]$ should be viewed as a 3x3 matrix with row vectors v_i since it then serves as a $\mathrm{Stab}(O)$-coset representative for its rosebox. Moreover, $[v_1|v_2|v_3]\, A = [v_1A|v_2A|v_3A]$ as paths. The notation $[v_1|v_2|v_3]$ is used for compactness of notation.)

There is redundancy in the naming of these oriented petals. Rotating v_2 around v_1 in one direction is the same as rotating v_3 about v_1 in the reverse direction, and the only edge whose orientation matters up to graph equivalence is that labeled v_1. Therefore:

Lemma 6.1.1. *At the level of closed paths:*

(i) $[v_1|v_2|v_3] = -[v_1|v_3|v_2]$

(ii) $[-v_1|v_2|v_3] = -[v_1|v_2|v_3]$

(iii) $[v_1| \pm v_2| \pm v_3] = [v_1|v_2|v_3]$

where the negation of a path is the path traversed with the reverse orientation.

Norm on Roseboxes, Ordering ([4]) The *norm* of a vector $v = (a, b, c) \in \mathbb{Z}^3$ is the vector $|v| = (|a|, |b|, |c|) \in \mathbb{N}^3_{\geq 0}$, so that vectors are partially ordered by a lexicographical ordering on their norms. The *norm* of a 3x3 matrix with rows v_1, v_2, v_3 is the triple $(|v_3|, |v_2|, |v_1|)$, so that matrices are partially ordered by a lexicographical ordering on their norms. Finally, the norm of a right Stab(O)-coset is the minimal norm among its representatives. Fix any total ordering extending $<$ by "arbitrarily breaking ties."

This ordering was chosen by Bestvina-Bux-Margalit so that $\begin{bmatrix} 1 & 0 & 0 \\ 0 & 1 & 0 \\ 0 & 0 & 1 \end{bmatrix}$ would be the (unique) smallest Stab(O)-coset. The ordering is useful in the current setting because that coset corresponds to the rosebox $\widetilde{D}$.

6.2 Connectedness of the Descending Links

The goal of this section is to show that as K is inductively built by gluing on roseboxes, each new rosebox is glued along a connected set, the *descending link*. It will follow from Mayer-Vietoris sequences that $H_1(K, \mathbb{Z})$ is generated by the petals of the rose fibers. In the coming sections, the number of petals needed

to generate $H_1(K, \mathbb{Z})$ is pared down to six. There will be no relations between these six, so $H_1(K, \mathbb{Z}) = \mathbb{Z}^6$. Knowledge of the structure of descending links will be useful in computing homology. Refer to section 5.2 for terminology of adjacency.

Descending Link, Inductive Complex Let ρ be a rosebox. Then define

$$K_{<\rho} := \bigcup_{\rho' < \rho} \rho' \qquad K_{\leq \rho} := \bigcup_{\rho' \leq \rho} \rho' \qquad \mathrm{Lk}_<(\rho) := \rho \cap K_{<\rho}.$$

$\mathrm{Lk}_<(\rho)$ is called the *descending link* of ρ.

Proposition 6.2.1 (Structure of Descending Link)**.** *Let $\rho \neq \widetilde{D}$ be a rosebox. Then $Lk_<(\rho)$ is homotopy equivalent to a wedge of circles and at most one 2-sphere. In particular, $Lk_<(\rho)$ is connected. Each of these circles is homologous in $Lk_<(\rho)$ to either the preimage of an edge of a Soulé domain or to one of the embedded circles in a theta fiber.*

The proof of this proposition will occupy the remainder of this section. A number of lemmas are needed.

Lemma 6.2.2. *The descending link $Lk_<(\rho)$ is the preimage of a subcomplex of the boundary of Soulé's truncated cube, given its natural CW-structure as a Euclidean polytope (see Figure 5.1). In particular, the entire preimage of a hexagon (resp. truncated face, resp. edge) is contained in $Lk_<(\rho)$ iff the Q-orbit (resp. P-orbit, resp. N-orbit) fiber it contains is.*

Proof. Soulé essentially proves this in [30] by computing stabilizers. Alternatively, the lemma follows from the observation that a translate of the preimage of a face of Soulé's truncated cube can be reconstructed knowing only a marked graph in its Q, P, or N-orbit fiber. □

Lemma 6.2.3 is a summary of [Proposition 5.2 and Lemma 6.3 of [4]].

Lemma 6.2.3. *The descending link of any rosebox except $\widetilde{D}$ contains a fiber over the orbit of Q. In particular, $Lk_<(\rho) \neq \emptyset$. Moreover, no two opposite Q-orbit vertices are contained in $Lk_<(\rho)$.*

Recall $M = h(1,1,1), M' = h(1,1,0), N = h(1,1,1/2), N' = h(1,1/2,-1/2)$. Let $M'' = h(1,0,-1)$. See [30] for the computations of stabilizers of these points.

Let $A = \begin{pmatrix} v_1 \\ v_2 \\ v_3 \end{pmatrix} \in \mathrm{GL}_3(\mathbb{Z})$. For which $B \in \mathrm{GL}_3(\mathbb{Z})$ does $D_3 \cdot B$ contain $M \cdot A$? Since every M-orbit point in D_3 is in the $\mathrm{Stab}(O)$-orbit of M or M', this amounts to finding all B such that for some $\pi \in \mathrm{Stab}(O)$, $M \cdot A = M \cdot \pi B$ or $M \cdot A = M' \cdot \pi B$. The solutions of the first equation are the matrices in $\mathrm{Stab}(O)\mathrm{Stab}(M)A$. These $[\mathrm{Stab}(M) : \mathrm{Stab}(OM)] = 4$ right cosets of $\mathrm{Stab}(O)$, give rise to the following roseboxes:

$$\begin{bmatrix} v_1 \\ v_2 \\ v_3 \end{bmatrix}, \begin{bmatrix} v_1+v_2+v_3 \\ v_1 \\ v_2 \end{bmatrix}, \begin{bmatrix} v_1+v_2+v_3 \\ v_1 \\ v_3 \end{bmatrix}, \text{ and } \begin{bmatrix} v_1+v_2+v_3 \\ v_2 \\ v_3 \end{bmatrix}.$$

Since $q_1 := \begin{pmatrix} 1 & 0 & 0 \\ 0 & 0 & -1 \\ 0 & 1 & 1 \end{pmatrix}$ satisfies $M = M' \cdot q_1$, the solutions to the second equation are $\mathrm{Stab}(O)q_1\mathrm{Stab}(M) = \mathrm{Stab}(O)\mathrm{Stab}(M')q_1$. This gives rise to

$[\text{Stab}(O) : \text{Stab}(OM')] = 12$ translates:

$$\begin{bmatrix} v_1+v_2 \\ v_1 \\ v_3 \end{bmatrix}, \begin{bmatrix} v_1+v_2 \\ v_2 \\ v_3 \end{bmatrix}, \begin{bmatrix} v_1+v_3 \\ v_1 \\ v_2 \end{bmatrix}, \begin{bmatrix} v_1+v_3 \\ v_2 \\ v_3 \end{bmatrix}, \begin{bmatrix} v_2+v_3 \\ v_1 \\ v_2 \end{bmatrix},$$
$$\begin{bmatrix} v_2+v_3 \\ v_1 \\ v_3 \end{bmatrix}, \begin{bmatrix} v_1+v_2+v_3 \\ v_1+v_2 \\ v_1 \end{bmatrix}, \begin{bmatrix} v_1+v_2+v_3 \\ v_1+v_2 \\ v_2 \end{bmatrix}, \begin{bmatrix} v_1+v_2+v_3 \\ v_1+v_3 \\ v_1 \end{bmatrix},$$
$$\begin{bmatrix} v_1+v_2+v_3 \\ v_1+v_3 \\ v_3 \end{bmatrix}, \begin{bmatrix} v_1+v_2+v_3 \\ v_2+v_3 \\ v_2 \end{bmatrix}, \begin{bmatrix} v_1+v_2+v_3 \\ v_2+v_3 \\ v_3 \end{bmatrix}.$$

Say that each of the 16 roseboxes in the previous two lists is *adjacent to A through M*. Analogously, define the concept of adjacent to A through M',M'',N, or N'. This notion of adjacency depends on the matrix A, and not just its $\text{Stab}(O)$ coset.

Since $N = N' \cdot q_1$, the above argument holds mutatis mutandis with N (resp N') in place of M (resp M'), yielding the $[\text{Stab}(N) : \text{Stab}(ON)] + [\text{Stab}(N') : \text{Stab}(ON')] = 4 + 4 = 8$ roseboxes adjacent to A through N:

$$\begin{bmatrix} v_1 \\ v_2 \\ v_3 \end{bmatrix}, \begin{bmatrix} v_1+v_3 \\ v_1 \\ v_2 \end{bmatrix}, \begin{bmatrix} v_1+v_3 \\ v_2 \\ v_3 \end{bmatrix}, \begin{bmatrix} v_2+v_3 \\ v_1 \\ v_2 \end{bmatrix}, \begin{bmatrix} v_2+v_3 \\ v_1 \\ v_3 \end{bmatrix},$$
$$\begin{bmatrix} v_1+v_2+v_3 \\ v_1 \\ v_2 \end{bmatrix}, \begin{bmatrix} v_1+v_2+v_3 \\ v_1+v_3 \\ v_1 \end{bmatrix}, \begin{bmatrix} v_1+v_2+v_3 \\ v_2+v_3 \\ v_2 \end{bmatrix}.$$

Using the above computations, it is straightforward to compute the lists of roseboxes adjacent to A through the remaining points of interest. For instance,

replacing v_i with the ith row of $q_1^{-1}A$ (i.e. $v_1 \mapsto v_1, v_2 \mapsto v_2 + v_3, v_3 \mapsto -v_2$) in the list for M produces the list for M':

$$\begin{bmatrix} v_1 \\ v_2+v_3 \\ -v_2 \end{bmatrix}, \begin{bmatrix} v_1+v_3 \\ v_1 \\ v_2+v_3 \end{bmatrix}, \begin{bmatrix} v_1+v_3 \\ v_1 \\ -v_2 \end{bmatrix}, \begin{bmatrix} v_1+v_3 \\ v_2+v_3 \\ -v_2 \end{bmatrix},$$
$$\begin{bmatrix} v_1+v_2+v_3 \\ v_1 \\ -v_2 \end{bmatrix}, \begin{bmatrix} v_1+v_2+v_3 \\ v_2+v_3 \\ -v_2 \end{bmatrix}, \begin{bmatrix} v_1-v_2 \\ v_1 \\ v_2+v_3 \end{bmatrix}, \begin{bmatrix} v_1-v_2 \\ v_2+v_3 \\ -v_2 \end{bmatrix},$$
$$\begin{bmatrix} v_3 \\ v_1 \\ v_2+v_3 \end{bmatrix}, \begin{bmatrix} v_3 \\ v_1 \\ -v_2 \end{bmatrix}, \begin{bmatrix} v_1+v_3 \\ v_1+v_2+v_3 \\ v_1 \end{bmatrix}, \begin{bmatrix} v_1+v_3 \\ v_1+v_2+v_3 \\ v_2+v_3 \end{bmatrix}, \begin{bmatrix} v_1+v_3 \\ v_1-v_2 \\ v_1 \end{bmatrix},$$
$$\begin{bmatrix} v_1+v_3 \\ v_1-v_2 \\ -v_2 \end{bmatrix}, \begin{bmatrix} v_1+v_3 \\ v_3 \\ v_2+v_3 \end{bmatrix}, \begin{bmatrix} v_1+v_3 \\ v_3 \\ -v_2 \end{bmatrix}.$$

Note that the roseboxes adjacent through N are all adjacent through both M and M', as must be the case since two roseboxes contain a given translate of N iff they contain the corresponding translate of the whole edge MM'. Observe that the descending link does not depend on the choice of tie-breaking, as adjacent matrices (through any of these vertices) can never have rows (unequal up to multiplication by ± 1) of equal norm, for their difference would then be a multiple of 2 [cf [4] Lemma 4.1].

Lemma 6.2.4. *If $M \cdot A$ and $M' \cdot A$ are in the descending link of $\rho_0 \cdot A$, then $(MM') \cdot A \subseteq Lk_<(\rho_0 \cdot A)$.*

Proof. Suppose, for a contradiction, that none of the 8 roseboxes adjacent to A through N is descending, but that at least one of the 16 roseboxes ad-

jacent through M is descending, as is at least one of the sixteen adjacent through M'. Inspecting the roseboxes adjacent to M but not to N, one sees $v_1 + v_2 < \max\{v_1, v_2\}$ or $v_1 + v_2 + v_3 < \max\{v_1, v_2\}$. For instance, if $\begin{bmatrix} v_1+v_2+v_3 \\ v_2+v_3 \\ v_3 \end{bmatrix}$ is descending, then one of $v_1 + v_2 + v_3, v_2 + v_3$ is less than both v_1 and v_2. This one can not be $v_2 + v_3$, or else $\begin{bmatrix} v_2+v_3 \\ v_1 \\ v_3 \end{bmatrix}$ would be descending through N, so $v_1 + v_2 + v_3 < \min\{v_1, v_2\} < \max\{v_1, v_2\}$. The other cases are similar.

Likewise, inspecting the roseboxes adjacent to M' but not to N, one sees $v_1 - v_2 < v_3, \max\{v_1, v_2\}$. Without loss of generality, assume $v_1 > v_2$ ($M = h(1, 1, 1,)$ and $M' = h(1, 1, 0)$ are invariant under transposing the first two coordinates.) It cannot be that both $v_1 + v_2 < \max\{v_1, v_2\} = v_1$ and $v_1 - v_2 < v_1$. Indeed, if the first nonzero entry of v_2 has the same (resp. opposite) sign as the corresponding entry of v_1, then $v_1+v_2 > v_1$ (resp. $v_1-v_2 > v_1$) [cf Lemma 6.2.3]. So $v_1+v_2+v_3 < \max\{v_1, v_2\} = v_1$.

Also, $v_1 + v_2 + v_3 > v_3$ or else $\begin{bmatrix} v_1+v_2+v_3 \\ v_1 \\ v_2 \end{bmatrix}$ is descending through N, so $v_1 > v_1 + v_2 + v_3 > v_3$. Write $A = \begin{pmatrix} v_1 \\ v_2 \\ v_3 \end{pmatrix} = \begin{pmatrix} a & b & c \\ d & e & f \\ g & h & i \end{pmatrix}$ with $a \neq 0$. Since $v_1 + v_2, v_1 + v_3 > v_1$, no entry of the first column of A can have the opposite sign as a. But $v_1 > v_1 + v_2 + v_3$, so $d = g = 0$. Then $v_1 - v_2$ has $a \neq 0$ as first entry,

contradicting that $v_1 - v_2 < v_3$. $\square$

One might hope for an analogous result with M', M'', but it is not true. Indeed, $A = \begin{pmatrix} 1 & -1 & 1 \\ 1 & 0 & 0 \\ 0 & 0 & 1 \end{pmatrix}$ has descending link containing M', M'', but not N'.

Just as the roseboxes adjacent through M' were found from those adjacent through M by the substitution $v_1 \mapsto v_1, v_2 \mapsto v_2+v_3, v_3 \mapsto -v_2$, the same substitution yields the roseboxes adjacent to A through N' from those adjacent through N, namely:

$$\begin{bmatrix} v_1 \\ v_2+v_3 \\ -v_2 \end{bmatrix}, \begin{bmatrix} v_1-v_2 \\ v_1 \\ v_2+v_3 \end{bmatrix}, \begin{bmatrix} v_1-v_2 \\ v_2+v_3 \\ -v_2 \end{bmatrix}, \begin{bmatrix} v_3 \\ v_1 \\ v_2+v_3 \end{bmatrix}, \begin{bmatrix} v_3 \\ v_1 \\ -v_2 \end{bmatrix},$$

$$\begin{bmatrix} v_1+v_3 \\ v_1 \\ v_2+v_3 \end{bmatrix}, \begin{bmatrix} v_1+v_3 \\ v_1-v_2 \\ v_1 \end{bmatrix}, \begin{bmatrix} v_1+v_3 \\ v_3 \\ v_2+v_3 \end{bmatrix}.$$

Lemma 6.2.5. *If $M' \cdot A, M'' \cdot A \in Lk_<(\rho_0 \cdot A)$, then they lie in the same connected component of $Lk_<(\rho_0 \cdot A)$.*

Proof. Assume $N' \cdot A \notin \mathrm{Lk}_<(\rho_0 \cdot A)$, for otherwise the lemma follows as in Lemma 6.2.4. Then $v_1 + v_3 < \max\{v_1, v_3\}$ or $v_1 + v_2 + v_3 < v_3$, as is seen by inspecting the 8 roseboxes adjacent through M' but not through N'. Since N' is fixed and M', M'' are transposed by the substitution $v_1 \mapsto v_1, v_2 \mapsto -v_3, v_3 \mapsto -v_2$, it is also true that $v_1 - v_2 < \max\{v_1, v_2\}$ or $v_1 - v_2 - v_3 < v_2$.

Claim: in fact, $v_1 + v_3 < \max\{v_1, v_3\}$. This claim will occupy most of the remainder of this proof. Assume then for a contradiction that $v_1+v_3 > \max\{v_1, v_3\}$, so that also $v_1 + v_2 + v_3 < v_3$. Write $A = \begin{pmatrix} v_1 \\ v_2 \\ v_3 \end{pmatrix} = \begin{pmatrix} a & b & c \\ d & e & f \\ g & h & i \end{pmatrix}$.

Suppose first that $a \neq 0$. There are two subcases, depending on if $g = 0$ or $g \neq 0$. If $g \neq 0$, then a and g have the same sign, since $v_1 + v_3 > \max\{v_1, v_3\}$. But then it must be that d has sign opposite to a and g since $v_1+v_2+v_3 < v_3$. But then $v_2 + v_3 < \max\{v_2, v_3\}$, contradicting the fact that $N' \cdot A$ is not in the descending link. On the other hand, if $a \neq 0$ and $g = 0$, then since $v_1 + v_2 + v_3 < v_3$, it must be that $|a + d| \leq 0$, so that $d = -a$. Then $v_1 - v_2 > \max\{v_1, v_2\}$ and $v_1 - v_2 - v_3 > \max\{v_1, v_2\}$, contradicting the first paragraph of this proof.

It is thus established that $a = 0$. Next assume $d \neq 0$. Then d and g must have opposite signs, since $v_1 + v_2 + v_3 > v_3$. But then $v_2 + v_3 < \max\{v_2, v_3\}$, contradicting the fact that $N' \cdot A$ is not in the descending link. So $d = 0$. Since $v_1 - v_2 - v_3 > v_2$, as one sees by comparing first coordinates, it follows that $v_1 - v_2 < \max\{v_1, v_2\}$.

There are now several cases, depending on which of b, e are zero. First suppose b, e are both nonzero.Then $v_1 - v_2 < \max\{v_1, v_2\}$ implies that b and e have the same sign. Since $v_1 + v_2 + v_3 < v_3$, h has the opposite sign to b and e and $|b+e+h| \leq |h|$, so that $|b|+|e| \leq 2|h|$. On the other hand, since $v_1+v_3, v_2+v_3 > v_3$, one sees $|b|, |e| \geq 2|h|$. So $4|h| \leq |b| + |e| \leq 2|h|$, and therefore $h = 0$. Then $|b|, |e| \leq 2|h| = 0$, so that $b = e = 0$, a contradiction.

Next suppose $b = 0, e \neq 0$. Then $v_1 + v_2 + v_3 < v_3$, so $|e| \leq 2|h|$. And $v_2 + v_3 > v_3$, so $|e| \geq 2|h|$. Equality holds, and so e is even. But then $\det A$ is

even, a contradiction. The case $b \neq 0, e = 0$ is similar, since $v_1 + v_3 > v_3$.

Having eliminated all possibilities, it is therefore established that indeed $v_1 + v_3 < \max\{v_1, v_3\}$ as claimed. The substitution in the first paragraph of this proof immediately establishes $v_1 - v_2 < \max\{v_1, v_2\}$ as well. The hexagons containing $h(0,1,0) \cdot A$ and $h(0,0,-1) \cdot A$ are in the descending link. These hexagons intersect and contain $M' \cdot A$ and $M'' \cdot A$ respectively, which establishes the lemma. □

Lemma 6.2.6. *If $M \cdot A, M'' \cdot A \in Lk_<(\rho_0 \cdot A)$, then they are in the same connected component.*

Proof. Suppose $M \cdot A, M'' \cdot A \in \mathrm{Lk}_<(\rho_0 \cdot A)$. Assume $M' \notin \mathrm{Lk}_<(\rho_0 \cdot A)$, for otherwise the lemma follows immediately from Lemmas 6.2.4 and 6.2.5. As in the proof of Lemma 6.2.4, $v_1 + v_2 < \max\{v_1, v_2\}$ or $v_1 + v_2 + v_3 < \max\{v_1, v_2\}$. By the proof of Lemma 6.2.5, if there is a descending adjacent rosebox through M' but none through N', then $v_1 + v_3 < \max\{v_1, v_3\}$ or $v_1 + v_2 + v_3 < v_3$. Using the substitution that fixes N' and transposes M', M'', it follows that $v_1 - v_2 < \max\{v_1, v_2\}$ or $v_1 - v_2 - v_3 < v_2$. Moreover, since there is no descending rosebox adjacent through M', it must be that $v_2 + v_3 > \max\{v_2, v_3\}$ and $v_1 + v_3 > \max\{v_1, v_3\}$.

Proceed now by cases on the matrix $A = \begin{pmatrix} v_1 \\ v_2 \\ v_3 \end{pmatrix} = \begin{pmatrix} a & b & c \\ d & e & f \\ g & h & i \end{pmatrix}$. In this paragraph, suppose $g \neq 0$. Neither a nor d can have the sign opposite to g, since $v_2 + v_3 > \max\{v_2, v_3\}$ and $v_1 + v_3 > \max\{v_1, v_3\}$. But then $v_1 + v_2 + v_3 > \max\{v_1, v_2\}$, so $v_1 + v_2 < \max\{v_1, v_2\}$ (so at least one of a,d is zero). This means $v_1 - v_2 > \max\{v_1, v_2\}$, so $v_1 - v_2 - v_3 < v_2$. Then a cannot be 0, so $d = 0$. Since there is a vector of lesser norm than v_2, $e \neq 0$. Now, since $v_1 + v_2 < v_1$, it must be that

$|e| \leq 2|b|$ and b, e have opposite signs. Since $v_1 - v_2 - v_3 < v_2$, it follows that $a = g$ and $|b - e - h| \leq |e|$, so h and e have opposite signs and $|h| \geq |b|$. Since $v_2 + v_3 > v_3$, then $|e| \geq 2|h|$. The three inequalities $|e| \geq 2|h|, |h| \geq |b|, 2|b| \geq |e|$ must all be equalities. In particular, the first two entries of v_1 match the corresponding entries of v_3, so $\det(A) = ge(c - i)$. As $|e| = 2|b|$, the determinant is even. This is a contradiction.

Therefore $g = 0$. If both a and d are nonzero, then either they have the same sign, contradicting $\min\{v_1 + v_2, v_1 + v_2 + v_3\} < \max\{v_1, v_2\}$, or they have opposite signs, contradicting $\min\{v_1 - v_2, v_1 - v_2 - v_3\} < \max\{v_1, v_2\}$. So one of a and d is zero. Suppose for a contradiction that $d = 0$. Then $v_1 - v_2 - v_3 > v_2$, so $v_1 - v_2 < \max\{v_1, v_2\} = v_1$ and hence also $v_1 + v_2 + v_3 < v_1$. So $|b - e| \leq |b|$ and $|b + e + h| \leq |b|$. Then $e = 0$, for otherwise e and b would have the same sign, forcing h to have the opposite sign and contradicting $v_2 + v_3 \geq v_2, v_3$. Now $\det(A) = -afh$. Since $v_1 + v_2 + v_3 < v_1$ and $v_1 + v_3 > v_1$, it follows that $|b + h| = |b|$, making h and hence $\det(A)$ even. This is a contradiction, so $d \neq 0$ and $a = 0$.

Next, suppose for a contradiction that $b = 0$. Then $\det(A) = cdh$, so h is nonzero. Since $v_2 + v_3 > \max\{v_2, v_3\}$, e cannot have the sign opposite that of h. But then $v_1 + v_2 + v_3, v_1 - v_2 - v_3 > v_2$, so $v_1 + v_2, v_1 - v_2 < \max\{v_1, v_2\}$, a contradiction.

In summary, $a = g = 0, b \neq 0$. Now, h cannot have a sign opposite to b since $v_1 + v_3 > \max\{v_1, v_3\}$. Since $v_1 + v_2$ or $v_1 + v_2 + v_3$ is less than $\max\{v_1, v_2\} = v_2$, e and b have opposite signs. Then $v_1 - v_2 > \max\{v_1, v_2\}$, so $v_1 - v_2 - v_3 < v_2$. So $|b - e - h| \leq e$, and therefore $|h| \geq |b|$. In particular, $h \neq 0$. Since h, b have the same sign, $v_1 - v_3 < \max\{v_1, v_2\}$, so $h(0, -1, 0) \cdot A \in \mathrm{Lk}_<(\rho_0 \cdot A)$.

Since $v_2 + v_3 > v_2$, $|h| \geq 2|e|$. Therefore $|b + e + h| \geq |b| + |e| > |e|$, so $v_1 + v_2 + v_3 > v_2$. So $v_1 + v_2 < \max\{v_1, v_2\}$, and thus $h(0, 0, 1) \cdot A \in \text{Lk}_<(\rho_0 \cdot A)$. Since the hexagons containing $h(0, 0, 1)$ and $h(0, -1, 0)$ intersect, it follows that $M \cdot A$ and $h(1, -1, -1) \cdot A$ are in the same component of the descending link. But $h(1, -1, -1) \cdot A$ and $M'' \cdot A$ are in the same component by lemma 6.2.4. Therefore $M \cdot A$ and $M'' \cdot A$ lie in the same component. □

Note that the situation described in the previous lemma is not vacuous: the matrix $A = \begin{pmatrix} 0 & 1 & 0 \\ 1 & -1 & 0 \\ 0 & 2 & 1 \end{pmatrix}$ has just such a descending link, containing M and M'' but not M'.

Finally, there are enough tools to show that descending links are connected:

Proof of Proposition 6.2.1. Let ρ be a translate of D_3 in Y_3. By Lemmas 6.2.2 and 6.2.3, $\text{Lk}_<(\rho)$ contains a whole hexagon H. To show that $\text{Lk}_<(\rho)$ is connected, it suffices to show that every M-orbit point in the descending link lies in the same connected component of $\text{Lk}_<(\rho)$ as H. Any M-orbit point is contained in some hexagon whose intersection with H is a hexagonal edge. If the M-orbit point is adjacent in ρ to a vertex of this edge, apply Lemma 6.2.4 or 6.2.5 to the appropriate coset representative of $\text{Stab}(O)A$. Otherwise, apply Lemma 6.2.6. Thus $\text{Lk}_<(\rho)$ is connected.

Now, perform a sequence of deformation retractions of $\text{Lk}_<(\rho)$ to produce a homotopy equivalent subcomplex as follows. By Proposition 5.2.2, the preimage of a truncated face is formed by two triangles, with vertices identified in pairs. If the truncated face has a free edge in $J(\text{Lk}_<(\rho))$, then the preimage of

the truncated face can be deformed accordingly in $\text{Lk}_<(\rho)$ to the preimage of the other two edges. Similarly, if a hexagon has a free edge in $J(\text{Lk}_<(\rho))$, then the preimage of the triangular convex hull formed by it and the two incident radii of the hexagon can be deformed to the preimage of the two radii. Next, if the preimage of a radius has a free edge, deform this triangular preimage away from it. Finally, some of the triangular convex hulls mentioned above may now be deformed from radius preimages. At this stage, the only way 2-cells can remain in $\text{Lk}_<(\rho)$ is if they came from three hexagons and the surrounded truncated face. These 2-cells form a 2-sphere pinched at three points: the preimages of the vertices of the truncated face. □

6.3 An Equivalence Relation

In this section, the descending link computations of the previous section are used to show that $H_1(K, \mathbb{Z})$ is generated by the (infinitely many) rose fiber petals, subject to an equivalence relation. This relation $\sim$ is generated by the equalities of closed paths of Lemma 6.1.1 together with the equalities in homology coming from the tubes and pinched tubes of Figure 5.2. The next section uses a greedy algorithm to reduce the number of generators to 9, and a further reduction to reduce the number to 6. The final section will show $H_1(K; \mathbb{Z}) = \mathbb{Z}^6$.

Recall the compact notation $[v_1|v_2|v_3]$ for the 3x3 matrix with rows v_1, v_2, v_3, introduced in the definition of rosebox homology generators.

Proposition 6.3.1. *Let $\sim$ be the relation on the group ring $\mathbb{Z}[GL_3(\mathbb{Z})]$ generated by*

(i) $[v_1|v_2|v_3] \sim -[v_1|v_3|v_2]$

(ii) $[-v_1|v_2|v_3] \sim -[v_1|v_2|v_3]$

(iii) $[v_1| \pm v_2| \pm v_3] \sim [v_1|v_2|v_3]$

(a) $[v_1|v_2|v_3] \sim [v_1 + v_3|v_2|v_3]$

(b) $[v_1|v_2|v_3] \sim [v_1|v_2|v_1 + v_3] + [v_1 + v_3|v_2|v_1]$

Then the map $\mathbb{Z}[GL_3(\mathbb{Z})]/\sim \to H_1(K, \mathbb{Z})$ *(given by* $[v_1|v_2|v_3] \mapsto [v_1|v_2|v_3]$*) is a right* $GL_3(\mathbb{Z})$*-module isomorphism.*

The proof of the proposition will make use of some relations in $\sim$ derived from the generating relations. These "rules" will be applied by a greedy algorithm in the next section.

Lemma 6.3.2 (Rules in $\sim$)**.** *The following hold:*

(1a) $[u|v|w] \sim [u \pm v|v|w]$

(1b) $[u|v|w] \sim [u \pm w|v|w]$

(2) $[u|v|w] \sim [u \pm v \pm w|v|w]$

(3a) $[u|v|w] \sim [u \pm w|v|u] + [u|v|u \pm w]$

(3b) $[u|v|w] \sim [u \pm v|u|w] + [u|u \pm v|w]$

(4a) $[u|v|w] \sim [u \pm v \pm w|v|u \pm v] + [u \pm v|v|u \pm v \pm w]$

(4b) $[u|v|w] \sim [u \pm v \pm w|u \pm w|w] + [u \pm w|u \pm v \pm w|w]$

(5) $[u|v|w] \sim 2\,[u|v + w|w] - [u|v + 2w|w]$

Proof. Rules (1)-(3) are immediate from (i)-(iii),(a)-(b).

Rule (4a):

$$[u|v|w] \overset{(1a)}{\sim} [u \pm v|v|w] \overset{(3a)}{\sim} [u \pm v \pm w|v|u \pm v] + [u \pm v|v|u \pm v \pm w]$$

Rule (4b):

$$[u|v|w] \overset{(1b)}{\sim} [u \pm w|v|w] \overset{(3b)}{\sim} [u \pm w \pm v|u \pm w|w] + [u \pm w|u \pm w \pm v|w]$$

Rule (5):

$$\begin{aligned}
[u|v+w|w] &\overset{(4b)}{\sim} [u+v|u-w|w] + [u-w|u+v|w] \\
&\overset{(1b)}{\sim} [u+v+w|u-w|w] + [u|u+v|w] \\
&\overset{(3b)}{\sim} [[u+v+w|v+2w|w] + [v+2w|u+v+w|w]] \\
&\qquad + [[-v|u|w] + [u|v|w]] \\
&\overset{(2),(1b)}{\sim} [u|v+2w|w] + [[v+w|u+v+w|w] - [v+w|u|w]] + [u|v|w] \\
&\overset{(1a)}{\sim} [u|v+2w|w] + [-u|u+v+w|w] - [u+v+w|u|w] + [u|v|w] \\
&\overset{(3b)}{\sim} [u|v+2w|w] - [u|v+w|w] + [u|v|w]
\end{aligned}$$

□

Proof of 6.3.1. Let $\rho \neq \widetilde{D}$ be a rosebox. By Proposition 6.2.1, the descending link is connected: $\widetilde{H_0}(\mathrm{Lk}_<(\rho), \mathbb{Z}) = 0$. So in the Mayer-Vietoris sequence for $K_{\leq\rho} = K_{<\rho} \cup \rho$ contains the terms:

$$H_1(\mathrm{Lk}_<(\rho), \mathbb{Z}) \to H_1(K_{<\rho}, \mathbb{Z}) \oplus H_1(\rho, \mathbb{Z}) \to H_1(K_{\leq\rho}, \mathbb{Z}) \to 0.$$

Thus $H_1(K_{\leq\rho})$ is generated by $H_1(K_{<\rho}, \mathbb{Z})$ together with the homology generators for the rosebox ρ. By transfinite induction on the order $<$, $H_1(K, \mathbb{Z})$ is generated by the $[v_1|v_2|v_3]$ (the base case and limit ordinal steps are immediate.)

Proposition 6.2.1 shows $H_1(\mathrm{Lk}_<(\rho), \mathbb{Z})$ is generated by circles γ embedded in theta fibers of $\mathrm{Lk}_<(\rho)$ or over hexagon edges. It has already been observed that the generators of $\sim$ hold as equalities in $H_1(K, \mathbb{Z})$, so it suffices to show that the

relations obtained from these embedded circles lie in $\sim$. It will be convenient to ignore the ordering on the roseboxes and prove the stronger statement that $i_{\rho_1}(\gamma) \sim i_{\rho_2}(\gamma)$ for every pair ρ_1, ρ_2 of roseboxes containing γ.

If γ is embedded in a theta fiber, then it collapses to a rosebox generator in two of the roseboxes containing it, and to a sum of two generators in the third adjacent rosebox (see figure 5.2). Therefore, the relation such a circle induces between the generators of ρ_1 and ρ_2 is in $\sim$, since it is given by either rule(1) or rule(3).

If the circle instead lies above a non-truncated edge of ρ_1 and above a non-truncated edge of ρ_2, then the corresponding homology relation is a case of rule(1) or rule(2). If the circle lies above a non-truncated edge of one and above a truncated edge of the other, then the homology relation is rule(3) or rule(4). Finally, the case of two truncated edges is dealt with by passing through an intermediary rosebox where the edge is non-truncated. □

6.4 A Greedy Algorithm

The previous section showed that $H_1(K;\mathbb{Z}) \cong \mathbb{Z}[\mathrm{GL}_3(\mathbb{Z})]/\sim$. The goal is to show that $H_1(K;\mathbb{Z}) \cong \mathbb{Z}^6$; this is proved in the next section. In this section, a procedure reminiscent of Gaussian elimination to prove that 9 generators suffice (Lemma 6.4.1). Then Lemma 6.4.2 pares the number generators down to 6.

Lemma 6.4.1. *As a group, $\mathbb{Z}[GL_3(\mathbb{Z})]/\sim$ is generated by the nine matrices:*

$$\begin{bmatrix} 1 & 0 & 0 \\ 0 & 1 & 0 \\ 0 & 0 & 1 \end{bmatrix}, \begin{bmatrix} 0 & 1 & 0 \\ 1 & 0 & 0 \\ 0 & 0 & 1 \end{bmatrix}, \begin{bmatrix} 0 & 0 & 1 \\ 1 & 0 & 0 \\ 0 & 1 & 0 \end{bmatrix}, \begin{bmatrix} 1 & 0 & 0 \\ 0 & 1 & 1 \\ 0 & 0 & 1 \end{bmatrix}, \begin{bmatrix} 0 & 1 & 0 \\ 1 & 0 & 1 \\ 1 & 0 & 0 \end{bmatrix}, \begin{bmatrix} 0 & 0 & 1 \\ 1 & 1 & 0 \\ 0 & 1 & 0 \end{bmatrix},$$
$$\begin{bmatrix} 1 & 0 & 0 \\ 0 & 1 & 1 \\ 0 & 1 & 0 \end{bmatrix}, \begin{bmatrix} 0 & 1 & 0 \\ 1 & 0 & 1 \\ 0 & 0 & 1 \end{bmatrix}, \begin{bmatrix} 0 & 0 & 1 \\ 1 & 1 & 0 \\ 1 & 0 & 0 \end{bmatrix}.$$

Proof. It suffices to show a matrix M of determinant ± 1 can be written as a $\mathbb{Z}$-sum of the nine generators.

Claim: M is equivalent to a $\mathbb{Z}$-sum of matrices whose first columns are among $[100]^T, [010]^T, [011]^T$. Indeed, applying rules (1) and (3), decrease the set of absolute values of the entries of this column until $m_{11} = 0$ or $m_{21} = m_{31} = 0$. If $m_{11} = 0$, apply rule(5) until $m_{21} = m_{31}$ or one of m_{21}, m_{31} is 0. The claim then follows from the fact that $\det(M) = \pm 1$ using (i)-(iii).

The potential first columns $[100]^T, [010]^T, [011]^T$ are treated in sequence. Assume M has first column $[100]^T$. By the determinant condition, $\gcd(m_{22}, m_{32}) = 1$. Iteratively applying rule(5) reduces to the case $m_{22} = 1$ and $m_{32} \in \{0, 1\}$. Then rule(1a) reduces to the case that the middle column is $[011]^T$ or $[010]^T$. In the latter case, $\pm 1 = \det(M) = m_{33}$ so that rule (1) and rule(5) prove the claim. In the former, the determinant condition means (without loss of generality) $m_{23} = m_{33} + 1$. Applying rule(5) iteratively reduces to the case $m_{23} = 1$, since the case where the second column is $[010]^T$ has already been dealt with. Finally, iterating rule (2) reduces to the case $m_{13} = 0$, proving the lemma.

Next assume M has first column $[010]^T$. By the determinant condition, $\gcd(m_{12}, m_{32}) = 1$, so rules (1b) and (3a) reduce to the cases $m_{12} = 1, m_{32} = 0$

or $m_{12} = 0, m_{32} = 1$. In the former case, rule (3b) reduces to the case that the second column is $[100]^T$, as the case where the first column is $[100]^T$ was dealt with in the previous paragraph. Then $m_{33} = \pm 1$, so rule (1) and rule(5) complete the proof. In the latter case, rule(5) means the second column can be taken to be among $[011]^T, [010]^T$. Now $m_{13} = \pm 1$. Rule (3), together with the former case and the previous paragraph now prove the lemma.

Finally assume M has first column $[011]^T$. Using rule(3), it suffices to suppose $m_{12} = 0$ or else $0 \leq m_{22}, m_{32} < m_{12}$. Using rule(2) and the previous paragraph, one may further suppose $m_{22} = m_{32}$ or else $0 \leq m_{12} < |m_{22} - m_{32}|$. The determinant condition reduces to two cases: $m_{12} = 0, m_{22} = m_{32} + 1$, or else $m_{12} = 1, m_{22} = m_{32}$. In the former case, rule(5) reduces to the case that the middle column is $[010]^T$, and rule (3) with the previous paragraph reduces to the case that the last column is $[100]^T$. This is one of the generators. In the latter case, rule(3) and the previous paragraph reduce to the case that the middle column is $[100]^T$. Then $\pm 1 = \det(M) = m_{23} - m_{33}$, so rule (2) reduces to the case $m_{13} = 0$. Finally, rule(5) can be applied to reduce to the case the last column is $[010]^T$. This is in the generating set, proving the lemma. □

Lemma 6.4.2. *As a group, $\mathbb{Z}[GL_3(\mathbb{Z})]/\sim$ is generated by the six matrices*

$$\begin{bmatrix} 1 & 0 & 0 \\ 0 & 1 & 0 \\ 0 & 0 & 1 \end{bmatrix}, \begin{bmatrix} 0 & 1 & 0 \\ 1 & 0 & 0 \\ 0 & 0 & 1 \end{bmatrix}, \begin{bmatrix} 0 & 0 & 1 \\ 1 & 0 & 0 \\ 0 & 1 & 0 \end{bmatrix}, \begin{bmatrix} 1 & 0 & 0 \\ 0 & 1 & 1 \\ 0 & 0 & 1 \end{bmatrix}, \begin{bmatrix} 0 & 1 & 0 \\ 1 & 0 & 1 \\ 1 & 0 & 0 \end{bmatrix}, \begin{bmatrix} 0 & 0 & 1 \\ 1 & 1 & 0 \\ 0 & 1 & 0 \end{bmatrix}.$$

Proof. It suffices to show that three of the matrices in Lemma 6.4.1 are in the subgroup generated by the remaining six.

Observe:

$$\begin{bmatrix} 1 & 0 & 0 \\ 0 & 1 & 1 \\ 0 & 1 & 0 \end{bmatrix} \overset{(3b)}{\sim} \begin{bmatrix} 1 & 1 & 1 \\ 1 & 0 & 0 \\ 0 & 1 & 0 \end{bmatrix} + \begin{bmatrix} 1 & 0 & 0 \\ 1 & 1 & 1 \\ 0 & 1 & 0 \end{bmatrix} \overset{(2)}{\sim} \begin{bmatrix} 0 & 0 & 1 \\ 1 & 0 & 0 \\ 0 & 1 & 0 \end{bmatrix} - \begin{bmatrix} 0 & 0 & 1 \\ 1 & 1 & 1 \\ 0 & 1 & 0 \end{bmatrix}$$

$$\begin{bmatrix} 0 & 0 & 1 \\ 1 & 1 & 0 \\ 0 & 1 & 0 \end{bmatrix} \overset{(3b)}{\sim} \begin{bmatrix} 0 & 0 & 1 \\ 1 & 1 & 1 \\ 0 & 1 & 0 \end{bmatrix} + \begin{bmatrix} 1 & 1 & 1 \\ 0 & 0 & 1 \\ 0 & 1 & 0 \end{bmatrix} \overset{(2,iii)}{\sim} \begin{bmatrix} 0 & 0 & 1 \\ 1 & 1 & 1 \\ 0 & 1 & 0 \end{bmatrix} - \begin{bmatrix} 1 & 0 & 0 \\ 0 & 1 & 0 \\ 0 & 0 & 1 \end{bmatrix}$$

Adding the two proves

$$\begin{bmatrix} 0 & 0 & 1 \\ 1 & 0 & 0 \\ 0 & 1 & 0 \end{bmatrix} \sim \begin{bmatrix} 1 & 0 & 0 \\ 0 & 1 & 1 \\ 0 & 1 & 0 \end{bmatrix} + \begin{bmatrix} 0 & 0 & 1 \\ 1 & 1 & 0 \\ 0 & 1 & 0 \end{bmatrix} + \begin{bmatrix} 1 & 0 & 0 \\ 0 & 1 & 0 \\ 0 & 0 & 1 \end{bmatrix}. \tag{6.1}$$

Thus the first matrix on the bottom row of the statement of Lemma 6.4.1 is a sum of the stated generators. The other two matrices of the bottom row are obtained from it by permuting the columns, so correspond to right-multiplying by a permutation matrix. But $\sim$ is closed under right-multiplication, and the corresponding column permutations of (6.1) completes the lemma. □

6.5 Explicit Isomorphism to Magnus Generators

Recall the notation of the Magnus generators from Section 2.4. Using the vertex of the fiber of $O = h(0,0,0)$ as basepoint, the Magnus generators appear within Z_3 as follows. The $K_{i,j}$ are the loops of the fiber of O:

$$K_{2,1} = \begin{bmatrix} 1 & 0 & 0 \\ 0 & 1 & 0 \\ 0 & 0 & 1 \end{bmatrix}, K_{3,2} = \begin{bmatrix} 0 & 1 & 0 \\ 0 & 0 & 1 \\ 1 & 0 & 0 \end{bmatrix}, K_{1,3} = \begin{bmatrix} 0 & 0 & 1 \\ 1 & 0 & 0 \\ 0 & 1 & 0 \end{bmatrix}.$$

The $K_{i,j,k}$ can be understood as pushing down to K the path σ in X_3 described as follows. σ visits in succession the following marked roses with oriented loops A, B, C. All are marked $A_j \mapsto B, A_k \mapsto C$, and the roses in succession send A_i to $A, AC^{-1}, AB^{-1}C^{-1}, ACB^{-1}C^{-1}, ABCB^{-1}C^{-1}$. Thus the initial and terminal point of this path push to the basepoint of Z_3. Between a pair of adjacent roses, σ travels along marked graphs above translates of the sort shown in the two vertices of Figure 6.1.

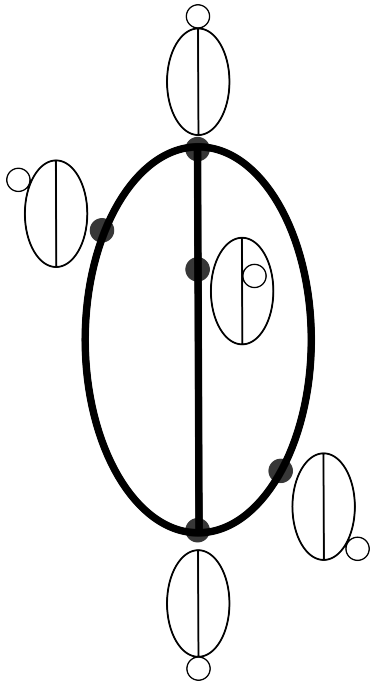

Figure 6.1: The Fiber over Q

Using the algorithm of Lemma 6.4.1 and applying Lemma 6.4.2:

$$K_{1,2,3} = \begin{bmatrix} 0 & 1 & 0 \\ 1 & 0 & 0 \\ 0 & 0 & 1 \end{bmatrix} + \begin{bmatrix} 0 & 1 & 0 \\ 1 & 0 & 1 \\ 1 & 0 & 0 \end{bmatrix},$$

$$K_{2,3,1} = \begin{bmatrix} 0 & 0 & 1 \\ 0 & 1 & 0 \\ 1 & 0 & 0 \end{bmatrix} + \begin{bmatrix} 0 & 0 & 1 \\ 1 & 1 & 0 \\ 0 & 1 & 0 \end{bmatrix},$$

$$K_{3,1,2} = \begin{bmatrix} 1 & 0 & 0 \\ 0 & 0 & 1 \\ 0 & 1 & 0 \end{bmatrix} + \begin{bmatrix} 1 & 0 & 0 \\ 0 & 1 & 1 \\ 0 & 0 & 1 \end{bmatrix}.$$

Thus $H_1(\mathrm{IO}_3;\mathbb{Z})$ is generated by the six Magnus generators $K_{1,2,3}$, $K_{2,3,1}$, $K_{3,1,2}$, $K_{2,1}$, $K_{3,2}$, and $K_{1,3}$. Moreover, the result $H_1(IO_3;\mathbb{Z}) \cong \mathbb{Z}^6$ is recovered with an explicit isomorphism:

Proposition 6.5.1. *$H_1(IO_3) \cong \mathbb{Z}^6$ via an isomorphism Φ sending*

$$A = \begin{bmatrix} a_{11} & a_{12} & a_{13} \\ a_{21} & a_{22} & a_{23} \\ a_{31} & a_{32} & a_{33} \end{bmatrix} \overset{\Phi}{\mapsto} \det(A) \begin{array}{c} (a_{21}a_{31}, a_{22}a_{32}, a_{23}a_{33}, a_{22}a_{33} + a_{23}a_{32}, \\ a_{21}a_{33} + a_{23}a_{31}, a_{21}a_{32} + a_{22}a_{31}). \end{array}$$

Moreover, $\Phi(z)$ give the coordinates of z with respect to the Magnus generators: $K_{1,2,3}, K_{2,3,1}, K_{3,1,2}, K_{2,1}, K_{3,2}, K_{1,3}$.

Proof. First, observe that Φ is invariant under the equalities and relations. Indeed, to see that (i), (ii), and (a) are respected, note that respectively switching the bottom two rows of A, changing the sign of the top row of A, or adding the third row to the top changes the sign of $\det(A)$ while preserving the homogeneous quadratics. Negating the second or third row negates both $\det(A)$ and the quadratics, verifying (iii). Relation (b) is also respected: for instance, checking the first coordinate, the right hand side of (b) is

$$\det(A)a_{2,1}(a_{1,1} + a_{3,1}) - \det(A)(a_{2,1}a_{1,1}) = \det(A)a_{2,1}a_{3,1},$$

equal to the left hand side of (b). Verifying the other coordinates is precisely analogous. Thus Φ is a well-defined homomorphism.

Next observe that Φ does send each Magnus generator to the appropriate coordinate vector, so Φ is surjective. Finally, since $H_1(\mathrm{IO}_3; \mathbb{Z})$ is an abelian group generated by 6 elements (Lemma 6.4.2), it must be $\mathbb{Z}^6$, and Φ must be an isomorphism. $\square$

CHAPTER 7

$H_2(\mathbf{IO}_3)$

In Section 5.2, subsets A and B of Z_3 were defined as the subsets with "interesting fibers". Since $\widetilde{A}$ contains the tubes and pinched tubes of Figure 5.2, it appears to be a good subset on which to find representatives of $H_2(\mathrm{IO}_3;\mathbb{Z})$ elements. Indeed, the maps $H_i(\widetilde{A};\mathbb{Z}) \to H_i(K;\mathbb{Z}) = H_i(\mathrm{IO}_3;\mathbb{Z})$ are shown to be surjective for all i. It is shown that $H_2(\mathrm{IO}_3;\mathbb{Z})$ is finitely generated as a module if and only if $H_2(\widetilde{A};\mathbb{Z})$ is.

7.1 The Components of $Z_3 \setminus B$

In this section, the homology $H_*(B;\mathbb{Z})$ is computed as a preliminary step in studying $H_*(\widetilde{A},\mathbb{Z}) \to H_*(K;\mathbb{Z})$.

Refer to Section 5.2 for the terminology used to describe subsets and special points (O, Q, M, M', N, N', P) of Soulé's domain D, the truncated cube (Figure 5.1). Recall that a *hexagon* is a hexagonal facet of D, a *truncated face* is a triangular facet of D, a *hexagonal edge* is an edge of D, a *radius* is a segment from the center of a hexagon to one of its vertices. This terminology applies as well to other Soulé domains (translates of D). A *triangular piece* will be one of the triangular components of a hexagon minus its radii (e.g. QMM' or $QM'M''$ – see Figure 7.1): each hexagon consists of six triangular pieces.

Recall that $A \subset Z_3$ consists of the points with rose and theta fibers. By Proposition 5.2.1, $A \cap D$ is the intersection of D with the coordinate axes. The preimage $\widetilde{A} \subset K$ of A consists of the tubes and pinched tubes that featured prominently in

the previous chapter. The subset $B \subset Z_3$ consists of the points with connected fibers. Only the fibers consisting of two points are excluded. A portion of B is shown in Figure 7.1. By Proposition 5.2.1, the excluded fibers are generic in the sense that $Z_3 \setminus B$ contains all the interior points of the 3-simplices of Soulé's triangulation of the polytope D (convex hulls of $OQMN$, $OQNM'$, $OQM'N'$, $OM'N'P$): $B \cap D$ is the cone on the union of all $6 \cdot 6 = 36$ radii of D. In other words, B is the union of all translates of OQM and OQM'.

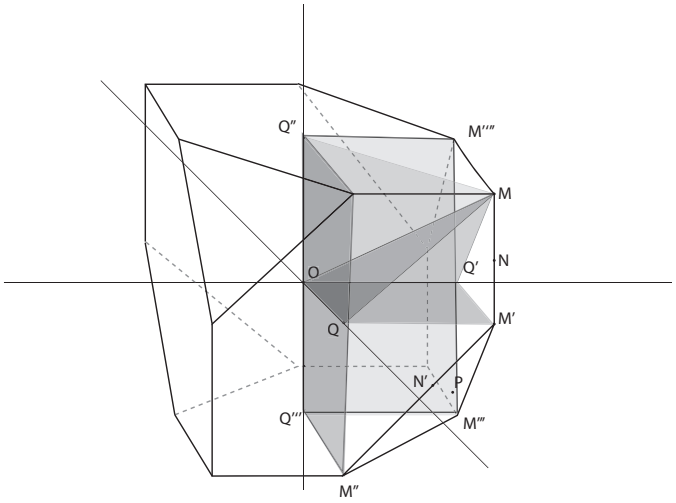

Figure 7.1: A portion of B inside Soulé's domain D

In order to compute the homology of B, it helps to understand the topology of $Z_3 \setminus B$. The components of $Z_3 \setminus B$ are described in Proposition 7.1.1, but first consider the components of $(Z_3 \setminus B) \cap D$. These are of two types:

- the intersection of D with an open orthant containing one of the truncated faces Δ. The image of such a component in Z_3/B, obtained by collapsing the boundary of the orthant to a point, is a 3-ball. The three hexagonal edges of Δ project to petals of a rose on the surface of the ball, and Δ projects to the exterior of the rose. See Figure 7.2.

- the cone on two triangular pieces (from adjacent hexagons) sharing a common hexagonal edge (e.g., the square pyramid $MOQM'Q'$ in Figure 7.1). The image of such a component in Z_3/B, obtained by collapsing the cone on the four radii to a point, is a 3-ball. The triangular pieces project to the hemispheres of the surface of the ball, and the shared hexagonal edge projects to its equator.

The following proposition describes how these components, from different Soulé domains, fit together to form components of $Z_3 \setminus B$.

Proposition 7.1.1. *Let C be a connected component of $Z_3 \setminus B$. Then C is contractible and intersects precisely 16 Soulé domains. Each intersection is one of the two types described immediately above. Let $\overline{C}$ be the closure of C in Z_3, and $L := \overline{C}/(\overline{C} \cap B)$ the result of collapsing $\overline{C} \cap B$ to a point. Then L has the homotopy type of a wedge of six 3-spheres.*

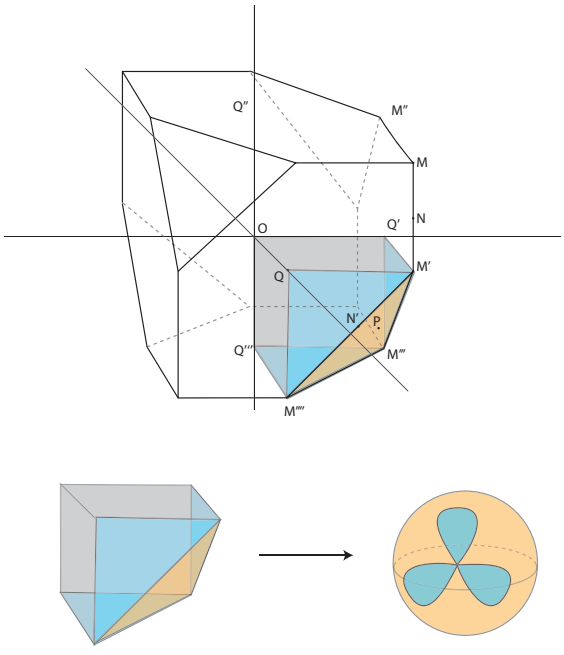

Figure 7.2: A portion of a component of $Z_3 \setminus B$ and its image in Z_3/B

Proof. Choose a Soulé domain D' intersecting C. Then C must contain one of the two types of components of $D' \setminus B$ listed before the statement of the proposition. In particular, C must contain (the interior of) some hexagonal edge e of D'. Replacing D' by another Soulé domain containing e if necessary, it follows that C contains (all but the vertices of) some truncated face Δ. Replacing C with a $\mathrm{GL}_3(\mathbb{Z})$-translate, it suffices to assume $D' = D$ and $P \in \Delta$.

Claim: there are precisely 4 Soulé domains containing Δ. This claim follows from Soulé's computation ([30], p.5) that the index of $\mathrm{Stab}(OP)$ in $\mathrm{Stab}(P)$ is equal to 4. Alternatively, the graph G_P of figure 3.4(i) shows that the set of Soulé domains containing P is in bijection with the set of 3-cycles of the tetrahedral graph (the 1-skeleton of a tetrahedron), of which there are four.

Any component of the intersection of a Soulé domain and $Z_3 \setminus B$ that contains an edge of Δ contains no hexagonal edges except those of Δ (see Figure 7.1). Since $[\mathrm{Stab}(N') : \mathrm{Stab}(ON')] = 4$, each of these three edges is contained in 4 Soulé domains besides those containing all of Δ, for a total of $4 + 3 \cdot 4 = 16$ Soulé domains. None of these domains D'' contain two hexagonal edges of Δ in separate components of $D'' \setminus B$, so C intersects each of the 16 Soulé domains D'' in precisely one component of $D'' \setminus B$. To see that C is contractible, it suffices to give a deformation retraction from C to Δ. This can be achieved by deforming the portion of C inside each Soulé domain to its intersection with Δ.

If D''' is one of the four Soulé domains containing Δ, then the component of $D''' \setminus B$ containing Δ is of the first type mentioned in the list above the statement of the proposition, so $D''' \cap C$ contains exactly three triangular pieces, one from each hexagon incident in D''' to the truncated face Δ. Figure 7.2 shows that the image of $D''' \cap \overline{C}$ in $\overline{C}/(\overline{C} \cap B)$ is a solid ball, on whose surface we draw a rose

with three petals, the images of the three edges of Δ. The interior of each petal is the image of the triangular piece adjacent to the corresponding edge. The exterior of the rose in the boundary sphere is the image of Δ.

Considering all four Soulé domains together, the image in $\overline{C}/(\overline{C} \cap B)$ is a cellular complex L_0 consisting of four solid balls glued together along the complements of the roses painted on their respective boundary spheres. The 12 intersections of the remaining Soulé domains with $\overline{C}$ – each of the second type described before the proposition – project to solid 3-balls in L. Let I denote one of these 12 intersections and $\overline{I}$ its projection in L. Since I contains a hexagonal edge of Δ, the equator of $\overline{I}$ is one of the three rose petals of L_0. Each triangular piece of I is shared by exactly three Soulé domains (one of which contains I). Since all hexagonal pieces of Z_3 are in the same $\mathrm{GL}_3(\mathbb{Z})$-orbit, one of these three Soulé domains D'''' contains a truncated face adjacent to the triangular piece. This truncated face must be Δ, so D'''' is one of the 4 Soulé domains contributing to L_0. The two hemispheres of $\overline{I}$ are therefore the interiors of the same petal in two of the four balls comprising L_0.

Form a graph (simplicial, no restrictions on valence) on the abstract set of 4 petal interiors in L_0 for a fixed petal. Connect two vertices by an edge if the corresponding petal interiors form the hemispheres for one of the 4 balls described in the preceding paragraph, with the given petal as equator. Call this the *petal graph* corresponding to the petal. Since every vertex has valence 2 (there are three Soulé domains containing a given triangular piece, but the one contributing to L_0 does not yield an edge), the graph is a 4-cycle. The 4 balls therefore glue together to form a 3-sphere in L.

Now, L has one 0-cell, three 1-cells (the petals), 13 2-cells (the image of Δ and

the $4 \cdot 3$ petal interiors), and 16 3-cells (corresponding to the Soulé domains). So $\chi(L) = 1 - 3 + 13 - 16 = -5 = 6\chi(S^3) - 5$, consistent with the claim on the homotopy type of L. Indeed, the desired homotopy equivalence is obtained by collapsing a certain contractible subset: starting with one of the 3-balls comprising L_0, glue on, for each petal, three of the four balls having that petal as equator. The subspace being collapsed is contractible by Van Kampen's Theorem, since it is inductively built by gluing along disks. The remaining six 3-balls – three of which were in L_0 and one for each of the petals – project to 3-spheres upon this collapse.

For later reference, here is a more detailed description of how the 12 balls are glued to L_0 to produce L. Let B_a, B_b, B_c, B_d denote the rose-painted balls that are the images of the four Soulé domains containing Δ. The center of Δ has fiber containing an equilateral tetrahedral graph, and as observed above there is a bijection between the 3-cycles of the graph and the Soulé domains containing Δ. Fix one of these 3-cycles, with edges labeled v_1, v_2, v_3. The other edges of the graph are labeled $v_2 - v_3, v_3 - v_1, v_1 - v_2$ up to sign (under the homology-marked graph convention of Section 6.1). The midpoints of the three edges of Δ have fiber containing the same combinatorial graph, but where v_i and $v_j - v_k$ have length 1 and the other edges have length $1/2$, for some cyclic permutation i, j, k of $1, 2, 3$. Let i denote 1-cell in L that contains this midpoint. Write T to denote the image of Δ in L. For $i \in \{1, 2, 3\}, x \in \{a, b, c, d\}$, write ix to denote the interior of petal i in B_x. (If the ball in Figure 7.2 is B_c, say, then T is shown in peach, petals $1, 2, 3$ – common to all four balls – in grey, and disks $1c, 2c, 3c$ in blue.)

Observe that each of the triangular pieces in C is shared by precisely 3 Soulé

domains, precisely one of which contains Δ. There is a ball whose hemispheres are the regions i in two of the four balls of L_0 if and only if those two regions correspond to two 3-cycles, one involving the edge labeled v_i and the other involving the edge labeled $v_j - v_k$. The assignment of a petal graph on the abstract vertex set $\{a, b, c, d\}$ to a petal, therefore, runs through all 3 possible such 4-cycle graphs as the petal varies.

Write B_{ixy}, $i \in \{1, 2, 3\}$, $x, y \in \{a, b, c, d\}$ to mean the 3-ball whose equators are ix and iy if such a 3-ball exists (i.e., if there is an edge from x to y in the petal graph for i). After permuting the labels B_a, B_b, B_c, B_d if necessary, the 12 such 3-balls are thus:

$$B_{1ab}, B_{1bc}, B_{1cd}, B_{1da}, \quad B_{2ab}, B_{2bd}, B_{2dc}, B_{2ca}, \quad B_{3ac}, B_{3cb}, B_{3bd}, B_{3da}.$$

Then $H_3(L; \mathbb{Z}) \cong \mathbb{Z}^6$, with generators

$$B_{1ab} + B_{1bc} + B_{1cd} + B_{1da}, \tag{7.1}$$

$$B_{2ab} + B_{2bd} + B_{2dc} + B_{2ca}, \tag{7.2}$$

$$B_{3ac} + B_{3cb} + B_{3bd} + B_{3da}, \tag{7.3}$$

$$B_a - B_b + B_{1ab} + B_{2ab} + B_{3cb} + B_{3ac}, \tag{7.4}$$

$$B_a - B_c + B_{1bc} + B_{1ab} + B_{2ac} + B_{3ac}, \tag{7.5}$$

$$B_a - B_d - B_{1da} + B_{2cd} + B_{2ac} - B_{3da} \tag{7.6}$$

□

Corollary 7.1.2. *For $m \geq 0$, $\widetilde{H}_m(B; \mathbb{Z}) \cong H_{m+1}(Z_3/B; \mathbb{Z})$. In particular, $\widetilde{H}_m(B; \mathbb{Z}) = 0$ for $m \neq 2$.*

Proof. Since Z_3 is contractible, the isomorphism follows from the homology long exact sequence for the pair (Z_3, B). The corollary then follows from the fact that

Z_3/B has homology only in dimension 3:

$$Z_3/B \cong \bigvee_C \overline{C}/(\overline{C} \cap B) \simeq \bigvee_C \bigvee_{i=1}^{6} S^3,$$

where C ranges over the connected components of $Z_3 \setminus B$. □

7.2 The Intermediate Space $\overline{K}$

In this section, it is shown that $H_*(\widetilde{A}; \mathbb{Z}) \to H_*(K; \mathbb{Z})$ is surjective. To this end, it is useful to study the effect of collapsing the fibers in $\widetilde{A}$ to points. The resulting space $\overline{K}$ is then homotopy equivalent to the space obtained by collapsing the remaining contractible fibers to points. Up to homotopy equivalence, then, $\overline{K}$ is obtained by collapsing the fibers of B to points. In the previous section, the homology of B was computed. This section propagates the information about the homology of B to information about the homology of $\widetilde{A}$.

The intermediate space $J : K \to Z_3$ factors as a projection $\pi : K \to \overline{K}$ followed by a map $\overline{J} : \overline{K} \to Z_3$, where $\overline{K}$ is obtained from K by collapsing each connected fiber to a point. Let $\overline{A} = \pi(\widetilde{A})$.

Proposition 7.2.1. *For all $m \geq 0$, $H_{m+1}(\overline{K}; \mathbb{Z}) \cong \widetilde{H}_m(B; \mathbb{Z})$. In particular, $H_2(\overline{K}; \mathbb{Z}) = H_1(\overline{K}; \mathbb{Z}) = 0$.*

Proof. Over each component C of $Z_3 \setminus B$, there is a fiber bundle $\pi : \pi^{-1}(C) \to C$. The fibers are each two points. Since C is contractible, the fiber bundle is trivial. Therefore $\overline{K}$ is obtained from two disjoint copies of Z_3 by identifying their respective copies of B. The Mayer-Vietoris sequence for $(Z_3 \sqcup_B Z_3, B)$ then

establishes the proposition, since B is connected and Z_3 is contractible. The last sentence of the proposition follows from Corollary 7.1.2. □

Theorem 7.2.2. *The maps $i_* : H_i(\widetilde{A};\mathbb{Z}) \to H_i(K;\mathbb{Z})$ induced by inclusion are surjective for all i.*

Proof. The naturality of the homology Long Exact Sequences means the map $\pi : (K, \widetilde{A}) \to (\overline{K}, \overline{A})$ induces a commutative diagram:

$$\begin{array}{ccccccccc}
H_2(\widetilde{A}) & \xrightarrow{i_*} & H_2(K) & \xrightarrow{0} & H_2(K/\widetilde{A}) & \longrightarrow & H_1(\widetilde{A}) & \longrightarrow & H_1(K) \\
\downarrow & & \downarrow & & \downarrow\cong & & \downarrow & & \downarrow \\
H_2(\overline{A}) = 0 & \longrightarrow & H_2(\overline{K}) = 0 & \longrightarrow & H_2(\overline{K}/\overline{A}) & \xrightarrow[\cong]{} & H_1(\overline{A}) & \longrightarrow & H_1(\overline{K}) = 0
\end{array}$$

Proposition 7.2.1 shows that $H_2(\overline{K};\mathbb{Z}) = H_1(\overline{K};\mathbb{Z}) = 0$, so that the map $H_2(\overline{K}/\overline{A}) \to H_1(\overline{A})$ on the bottom row is an isomorphism. The map $\pi : K/\widetilde{A} \to \overline{K}/\overline{A}$ is a homotopy equivalence, as it merely collapses segment fibers to points, so the vertical map $H_2(K/\widetilde{A}) \to H_2(\overline{K}/\overline{A})$ is an isomorphism. By commutativity of the diagram, it follows that $H_2(K/\widetilde{A}) \to H_1(\widetilde{A})$ is injective. Exactness of the top row then shows $H_2(K) \to H_2(K/\widetilde{A})$ is the zero map, and $i_* : H_2(\widetilde{A};\mathbb{Z}) \to H_2(K;\mathbb{Z})$ is surjective.

The same argument applies to show $H_i(\widetilde{A};\mathbb{Z}) \to H_i(K;\mathbb{Z})$ is surjective for $i = 1$. The case $i = 3$ follows from the Bestvina-Bux-Margalit calculation ([4]) that $H_3(K;\mathbb{Z}) = 0$. All other cases are trivial. □

Corollary 7.2.3. *There is a canonical splitting $H_1(\widetilde{A};\mathbb{Z}) \cong H_1(A;\mathbb{Z}) \oplus H_1(IO_3;\mathbb{Z})$.*

Proof. This follows from the splitting of the exact sequence:

$$\begin{array}{ccccccccc}
0 & \longrightarrow & H_2(K/\widetilde{A}) & \longrightarrow & H_1(\widetilde{A}) & \longrightarrow & H_1(K) & \longrightarrow & 0 \\
 & & \downarrow\cong & & \downarrow & & & & \\
 & & H_2(\overline{K}/\overline{A}) & \xrightarrow{\cong} & H_1(\overline{A}) & & & &
\end{array}$$

since $H_1(K) = H_1(\mathrm{IO}_3)$ and $H_1(\overline{A}) = H_1(A)$. □

7.3 Steinberg Relations and the Kernel

Recall that $\mathrm{SL}(n, \mathbb{Z})$ is generated by the *elementary matrices*.

Elementary Matrices The matrix e_{ij}, $i \neq j$ has 1 in entry (i, j) and in the diagonal entries, and 0 in all other entries. All such matrices are called *elementary matrices*.

In Section 5.2, two Soulé domains were defined to be *adjacent* if they share a hexagonal face. Equivalently, they are adjacent precisely if one is obtained from the other by multiplication by an elementary matrix.

Theorem 7.3.1 (Steinberg ([31],p.96-97)). *$SL_3(\mathbb{Z})$ has a presentation with generators $e_{ij}, i \neq j$ and relations:*

1. $[e_{ij}, e_{ik}] = 1$, *if* $\{i, j, k\} = \{1, 2, 3\}$;
2. $[e_{ij}, e_{kj}] = 1$, *if* $\{i, j, k\} = \{1, 2, 3\}$;
3. $[e_{ij}, e_{jk}] = e_{ik}$, *if* $\{i, j, k\} = \{1, 2, 3\}$;
4. $(e_{12}e_{21}^{-1}e_{12})^4 = 1$.

Relations (1)-(3) are called *Steinberg relations*.

If D is the Soulé domain of Minkowski-reduced matrices, then $A \cap D$ consists of the coordinate axes (Proposition 5.2.1). Thus a Steinberg relation determines a closed path in A based at O. (If $w_1 \cdots w_{k-1} w_k$ is a word of length k in the

elementary matrices and their inverses, then the corresponding path visits in turn O, $O \cdot w_k$, $O \cdot w_{k-1}w_k$, $\ldots$, $O \cdot w_1 \cdots w_k$.)

α and β Let α be the closed path corresponding to the type (1) Steinberg relation

$$e_{13}^{-1}e_{12}^{-1}e_{13}e_{12}.$$

Let β be obtained by gluing together the paths corresponding to relations

$$e_{13}e_{23}e_{13}^{-1}e_{23}^{-1} \quad \text{and} \quad e_{12}e_{23}e_{12}^{-1}e_{13}^{-1}e_{23}^{-1},$$

of type (2) and (3), respectively, along the common segment $e_{13}^{-1}e_{23}^{-1}$.

Lemma 7.3.2. *Let α, β as above. Then $J^{-1}(\alpha)$ and $J^{-1}(\beta)$ each contain unique embedded 2-cycles (up to orientation).*

Call these cycles (arbitrarily oriented) $\widetilde{\alpha}$ and $\widetilde{\beta}$, respectively.

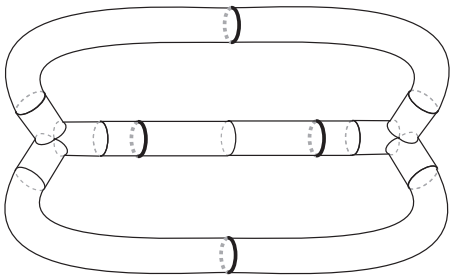

Figure 7.3: The cycle $\widetilde{\beta}$ is a genus two surface, pinched twice

Proof. Consider α first. $J^{-1}(\alpha)$ contains an embedded torus $\widetilde{\alpha}$, made up of four of the tubes shown in 5.2(i) glued along the meridianal loops

$$\begin{bmatrix} 1 & 0 & 0 \\ 0 & 1 & 0 \\ 0 & 0 & 1 \end{bmatrix}, \begin{bmatrix} 1 & 1 & 0 \\ 0 & 1 & 0 \\ 0 & 0 & 1 \end{bmatrix}, \begin{bmatrix} 1 & 1 & 1 \\ 0 & 1 & 0 \\ 0 & 0 & 1 \end{bmatrix}, \begin{bmatrix} 1 & 0 & 1 \\ 0 & 1 & 0 \\ 0 & 0 & 1 \end{bmatrix}$$

in the rose fibers of the respective roseboxes. There are additional loops in the rose fibers that do not contribute to the torus, but these are free edges that can be collapsed in $J^{-1}(\alpha)$. The Q-orbit fibers in the middle of these four tubes each contains an additional edge to $J^{-1}(\alpha)$ that does not contribute to the torus. Together with the torus, these edges form a space homotopy equivalent to the wedge of a torus and four circles. Thus $\widetilde{\alpha}$ is unique.

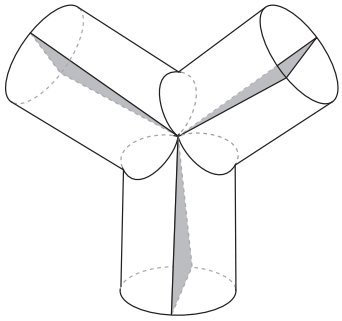

Figure 7.4: A pinched pair of pants inside a rosebox

For β, observe that the bottom halves of three pinched tubes (5.2(ii)), corresponding to three faces of a Soulé domain adjacent to a common truncated face, fit together to form a pair of pants with two interior points identified. Call the resulting shape a *pinched pair of pants* (Figure 7.4). The cycle $\widetilde{\beta}$ will involve two pinched pairs of pants, contained in $\widetilde{D}$ and $\widetilde{D} \cdot e_{13}^{-1} e_{23}^{-1}$. The following homology equivalences show how to connect the three boundary components of one pinched pair of pants to the homologous boundary components of the other, along cylindrical tubes within the remaining four roseboxes:

$$\begin{bmatrix} 1 & 0 & 0 \\ 0 & 1 & 0 \\ 0 & 0 & 1 \end{bmatrix} + \begin{bmatrix} 0 & 0 & 1 \\ 0 & 1 & 0 \\ 1 & 0 & 0 \end{bmatrix} \sim \begin{bmatrix} 0 & 0 & 1 \\ 0 & 1 & 0 \\ 1 & 0 & -1 \end{bmatrix} \sim \begin{bmatrix} 0 & 1 & -1 \\ 1 & 0 & -1 \\ 0 & 0 & 1 \end{bmatrix} + \begin{bmatrix} 0 & 0 & 1 \\ 0 & 1 & -1 \\ 1 & 0 & -1 \end{bmatrix}.$$

$$\begin{bmatrix} 0 & 1 & 0 \\ 1 & 0 & 0 \\ 0 & 0 & 1 \end{bmatrix} + \begin{bmatrix} 0 & 0 & 1 \\ 1 & 0 & 0 \\ 0 & 1 & 0 \end{bmatrix} \sim \begin{bmatrix} 0 & 0 & 1 \\ 1 & 0 & 0 \\ 0 & 1 & -1 \end{bmatrix} \sim \begin{bmatrix} 0 & 0 & 1 \\ 1 & 0 & -1 \\ 0 & 1 & -1 \end{bmatrix} + \begin{bmatrix} 1 & 0 & -1 \\ 0 & 1 & -1 \\ 0 & 0 & 1 \end{bmatrix}.$$

$$\begin{bmatrix} 0 & 1 & 0 \\ 0 & 0 & 1 \\ 1 & 0 & 0 \end{bmatrix} + \begin{bmatrix} 1 & 0 & 0 \\ 0 & 0 & 1 \\ 0 & 1 & 0 \end{bmatrix} \sim \begin{bmatrix} 0 & 1 & 0 \\ 0 & 0 & 1 \\ 1 & -1 & 0 \end{bmatrix} \sim \begin{bmatrix} 0 & 1 & -1 \\ 0 & 0 & 1 \\ 1 & -1 & 0 \end{bmatrix}$$

$$\sim \begin{bmatrix} 0 & 1 & -1 \\ 0 & 0 & 1 \\ 1 & 0 & -1 \end{bmatrix} + \begin{bmatrix} 1 & 0 & -1 \\ 0 & 0 & 1 \\ 0 & 1 & -1 \end{bmatrix}.$$

The resulting cycle $\widetilde{\beta}$ is a genus two surface, pinched twice (Figure 7.3). Now, $J^{-1}(\beta)$ is a 2-complex that has some 1-dimensional free faces (contained in the rose fibers of the four roseboxes that do not contribute pinched pairs of pants.) Collapsing these free faces yields another 2-complex with one free face in each of six of the Q-orbit fibers: edges not involved in the tubes and pinched tubes comprising $\widetilde{\beta}$. These edges can be collapsed to the pinch points of the pinched pairs of pants. The resulting complex consists of $\widetilde{\beta}$ and one other edge e (in the Q-orbit fiber in the middle of the longer of the three cylinders joining the pinched pairs of pants). Therefore, $J^{-1}(\beta)$ is homotopy equivalent to the wedge of a genus 2 surface with three circles. The circles correspond to e and the two pinch points. So $\widetilde{\beta}$ is unique. □

Theorem 7.3.3. *The kernel of the map $H_2(\widetilde{A};\mathbb{Z}) \twoheadrightarrow H_2(K;\mathbb{Z})$ induced by inclusion is generated by $\widetilde{\alpha}, \widetilde{\beta}$ as a GL$(3,\mathbb{Z})$-module.*

Proof. In Proposition 7.1.1, it was shown that $H_3(L;\mathbb{Z}) = \mathbb{Z}^6$ where $L \subset Z_3/B$ is a subspace such that Z_3/B is a wedge of GL$(3,\mathbb{Z})$-translates of L. Explicit generators (7.1)–(7.6) were given for $H_3(L;\mathbb{Z})$.

Claim: the generators (7.1)–(7.3) map under the connecting homomorphism $H_3(Z_3/B) \cong H_2(B) \cong H_3(\overline{K}) \cong H_3(\overline{K}/\overline{A}) \cong H_3(K/\widetilde{A}) \to H_2(\widetilde{A})$ to translates of the cycle $\widetilde{\alpha}$; the other generators (7.4)–(7.6) map to translates of $\widetilde{\beta}$. Indeed, since no two 3-cells comprising any given $H_3(L)$ generator lie in the same rose-box (Proposition 7.1.1), the six generators map under the connecting homomorphism to embedded 2-cycles in $\widetilde{A}$. For (7.1)–(7.3), these cycles are translates of cycles lying over the fibers of a path corresponding to a Steinberg relation of type (1). All such paths are translates of each other by permutation matrices. But by the Lemma, there is only one such embedded 2-cycle over a given type (1) Steinberg relation, so it must agree with the appropriate translate of the generator. This establishes the claim for (7.1)–(7.3).

For the remaining generators (7.4)–(7.6), the cycles lie over the fibers of two Steinberg relations glued as in the Lemma. The same argument as above establishes the claim. The theorem then follows from the long exact sequence for the pair $(K, \widetilde{A})$. □

Corollary 7.3.4. *$H_2(IO_3; \mathbb{Z})$ is finitely generated as a right $GL_3(\mathbb{Z})$-module if and only if $H_2(\widetilde{A}; \mathbb{Z})$ is.*

The corollary reduces the problem of determining whether $H_2(\mathrm{IO}_3; \mathbb{Z})$ is finitely generated as a $\mathrm{GL}_3(\mathbb{Z})$-module to the problem of determining the top homology of an explicitly defined 2-complex. This should be a tractable problem.

BIBLIOGRAPHY

[1] S. Andreadakis. On the automorphisms of free groups and free nilpotent groups. *Proc. London Math. Soc.*, 15(3):239–268, 1965.

[2] Avner Ash. Small-dimensional classifying spaces for arithmetic subgroups of general linear groups. *Duke Math. J.*, 51(2):459–468, 1984.

[3] Gilbert Baumslag and Lewin T. Taylor. The centre of groups with one defining relator. *Math. Ann.*, 175:315–319, 1968.

[4] Mladen Bestvina, Kai-Uwe Bux, and Dan Margalit. Dimension of the Torelli group for Out(F_n). *Invent. Math.*, 170(1):1–32, 2007.

[5] Anders Björner, Michel Las Vergnas, Bernd Sturmfels, Neil White, and Gunter M. Ziegler. *Oriented Matroids*. Cambridge University Press, second edition, 2000.

[6] A. Borel and J.-P. Serre. Corners and arithmetic groups. *Comentarii Mathematici Helvetici*, 48(1):436–491.

[7] Kenneth Brown. *Cohomology of Groups*. Springer-Verlag, 1982.

[8] Lucia Camporaso and Fillippo Viviani. Torelli theorem for graphs and tropical curves. *Duke Math. J.*, 153(1):129–171, 2010.

[9] C. Herbert Clemens. *A Scrapbook of Complex Curve Theory*, volume 55 of *Graduate Studies in Mathematics*. American Mathematical Society, second edition, 2003.

[10] John H. Conway. *The sensual (quadratic) form*, volume 26 of *Carus Mathematical Monographs*. Mathematical Association of America, Washington, DC, 1997. With the assistance of Francis Y. C. Fung.

[11] Marc Culler and Karen Vogtmann. Moduli of graphs and automorphisms of free groups. *Invent. Math.*, 84(1):91–119, 1986.

[12] Olivier Debarre. *Current Topics in Complex Algebraic Geometry*, volume 28, chapter The Schottky Problem: An Update, pages 57–64. 1995.

[13] B. N. Delaunay. Sur la partition réguliere de l'espace à 4 dimensions. *Izv. Akad. Nauk. SSSR Otdel Fiz-Mat. Nauk*, 7(2):79–110, 147–164, 1929.

[14] Benson Farb and Dan Margalit. *A Primer on Mapping Class Groups*. Princeton University Press, preprint.

[15] Phillip Griffiths and Joseph Harris. *Principles of Algebraic Geometry*. John Wiley & Sons, Inc., 1978.

[16] Allen Hatcher. *Algebraic Topology*. Cambridge University Press, 2002.

[17] Dennis Johnson. An abelian quotient of the mapping class group $\mathcal{I}_g$. *Math. Ann.*, 249(3):225–242, 1980.

[18] Dennis Johnson. Quadratic forms and the Birman–Craggs homomorphisms. *Transactions of the AMS*, 261(1):235–254, 1980.

[19] Dennis Johnson. The structure of the Torelli group. i. a finite set of generators for $\mathcal{T}$. *Ann. of Math.*, 118(3):423–442, 1983.

[20] Nariya Kawazumi. Cohomological aspects of Magnus expansions. 2005.

[21] Motoko Kotani and Toshikazu Sunada. Jacobian tori associated with a finite graph and its abelian covering graphs. *Advances in Applied Mathematics*, 24:89–110, 2000.

[22] Sava Krstić and James McCool. The non-finite presentability of IA(F_3) and GL$_2(Z[t, t^{-1}])$. *Invent. Math.*, 129(3):595–606, 1997.

[23] Roger C. Lyndon and Paul E. Schupp. *Combinatorial Group Theory*. Springer, 1977.

[24] Wilhelm Magnus. Über n-dimensionale gittertransformationen. *Acta Math.*, 64:353–367, 1934.

[25] Tatiana Nagnibeda. Jacobian of a finite graph. In Adam Kornyi, editor, *Harmonic Functions on Trees and Buildings*, volume 206, pages 149–151. AMS, 1997.

[26] James G. Oxley. *Matroid Theory*. Oxford University Press, 1992.

[27] Alexandra Pettet and Juan Souto. The spine that was no spine. *LEnseignement Mathématique*, 54:273–285, 2008.

[28] Jürgen Richter-Gebert, Bernd Sturmfels, and Thorsten Theobald. First steps in tropical geometry. In G.L. Litvinov and V.P. Maslov, editors, *Idempotent Mathematics and Mathematical Physics*, volume 377, pages 289–317. AMS, 2005.

[29] F. Schottky. Zur theorie der abelschen funktionen von vier variabeln. *J. reine angew. Math.*, 102:304–352, 1888.

[30] Christophe Soulé. The cohomology of $\mathrm{SL}_3(\mathbb{Z})$. *Topology*, 17(1):1 – 22, 1978.

[31] Robert Steinberg. Lectures on Chevalley groups. Yale Notes, 1967.

[32] Mikhail I. Stogrin. Regular Dirichlet-Voronoi partitions for the second triclinic group. In *Proceedings of the Steklov Institute of Mathematics*, volume 123, 1973.

[33] William T. Tutte. Matroids and graphs. *Trans. Amer. Math. Soc.*, 90:527–552, 1959.

[34] Frank Vallentin. *Sphere Coverings, Lattices, and Tilings (in Low Dimensions)*. PhD thesis, Technische Universität München, 2003.

[35] Karen Vogtmann. Automorphisms of free groups and outer space. In *Proceedings of the Conference on Geometric and Combinatorial Group Theory, Part I*, volume 94, pages 1–31, 2002.

[36] Karen Vogtmann. The cohomology of automorphism groups of free groups. In Juan Luis Varona Marta Sanz-Sole, Javier Soria and Joan Verdera, editors, *Proceedings of the International Congress of Mathematicians, Madrid 2006*, volume II, pages 1101–1117. European Mathematical Society, 2007.

[37] Karen Vogtmann. What is…Outer Space? *Notices of the AMS*, 55(7):784–786, August 2008.

[38] Hassler Whitney. Non-separable and planar graphs. *Transactions of the American Mathematical Society*, 34(2), 1932.

[39] Hassler Whitney. 2-isomorphic graphs. *Amer. Journ. Math.*, 55:245–254, 1933.